NCHRP
REPORT 496

NATIONAL COOPERATIVE HIGHWAY RESEARCH PROGRAM

Prestress Losses in Pretensioned High-Strength Concrete Bridge Girders

TRANSPORTATION RESEARCH BOARD
OF THE NATIONAL ACADEMIES

NATIONAL COOPERATIVE HIGHWAY RESEARCH PROGRAM

NCHRP REPORT 496

Prestress Losses in Pretensioned High-Strength Concrete Bridge Girders

MAHER K. TADROS
NABIL AL-OMAISHI
University of Nebraska
Lincoln, NE

STEPHEN J. SEGUIRANT
Concrete Technology Corporation
Tacoma, WA

AND

JAMES G. GALLT
Palmer Engineering Company
Winchester, KY

SUBJECT AREAS
Bridges, Other Structures, and Hydraulics and Hydrology • Materials and Construction

Research Sponsored by the American Association of State Highway and Transportation Officials
in Cooperation with the Federal Highway Administration

TRANSPORTATION RESEARCH BOARD

WASHINGTON, D.C.
2003
www.TRB.org

NATIONAL COOPERATIVE HIGHWAY RESEARCH PROGRAM

Systematic, well-designed research provides the most effective approach to the solution of many problems facing highway administrators and engineers. Often, highway problems are of local interest and can best be studied by highway departments individually or in cooperation with their state universities and others. However, the accelerating growth of highway transportation develops increasingly complex problems of wide interest to highway authorities. These problems are best studied through a coordinated program of cooperative research.

In recognition of these needs, the highway administrators of the American Association of State Highway and Transportation Officials initiated in 1962 an objective national highway research program employing modern scientific techniques. This program is supported on a continuing basis by funds from participating member states of the Association and it receives the full cooperation and support of the Federal Highway Administration, United States Department of Transportation.

The Transportation Research Board of the National Academies was requested by the Association to administer the research program because of the Board's recognized objectivity and understanding of modern research practices. The Board is uniquely suited for this purpose as it maintains an extensive committee structure from which authorities on any highway transportation subject may be drawn; it possesses avenues of communications and cooperation with federal, state and local governmental agencies, universities, and industry; its relationship to the National Research Council is an insurance of objectivity; it maintains a full-time research correlation staff of specialists in highway transportation matters to bring the findings of research directly to those who are in a position to use them.

The program is developed on the basis of research needs identified by chief administrators of the highway and transportation departments and by committees of AASHTO. Each year, specific areas of research needs to be included in the program are proposed to the National Research Council and the Board by the American Association of State Highway and Transportation Officials. Research projects to fulfill these needs are defined by the Board, and qualified research agencies are selected from those that have submitted proposals. Administration and surveillance of research contracts are the responsibilities of the National Research Council and the Transportation Research Board.

The needs for highway research are many, and the National Cooperative Highway Research Program can make significant contributions to the solution of highway transportation problems of mutual concern to many responsible groups. The program, however, is intended to complement rather than to substitute for or duplicate other highway research programs.

Note: The Transportation Research Board of the National Academies, the National Research Council, the Federal Highway Administration, the American Association of State Highway and Transportation Officials, and the individual states participating in the National Cooperative Highway Research Program do not endorse products or manufacturers. Trade or manufacturers' names appear herein solely because they are considered essential to the object of this report.

NCHRP REPORT 496

Project D18-07 FY'99

ISSN 0077-5614

ISBN 0-309-08766-X

Library of Congress Control Number 2003110071

Price $19.00

NOTICE

The project that is the subject of this report was a part of the National Cooperative Highway Research Program conducted by the Transportation Research Board with the approval of the Governing Board of the National Research Council. Such approval reflects the Governing Board's judgment that the program concerned is of national importance and appropriate with respect to both the purposes and resources of the National Research Council.

The members of the technical committee selected to monitor this project and to review this report were chosen for recognized scholarly competence and with due consideration for the balance of disciplines appropriate to the project. The opinions and conclusions expressed or implied are those of the research agency that performed the research, and, while they have been accepted as appropriate by the technical committee, they are not necessarily those of the Transportation Research Board, the National Research Council, the American Association of State Highway and Transportation Officials, or the Federal Highway Administration, U.S. Department of Transportation.

Each report is reviewed and accepted for publication by the technical committee according to procedures established and monitored by the Transportation Research Board Executive Committee and the Governing Board of the National Research Council.

Published reports of the

NATIONAL COOPERATIVE HIGHWAY RESEARCH PROGRAM

are available from:

Transportation Research Board
Business Office
500 Fifth Street, NW
Washington, DC 20001

and can be ordered through the Internet at:

http://www.national-academies.org/trb/bookstore

Printed in the United States of America

THE NATIONAL ACADEMIES

Advisers to the Nation on Science, Engineering, and Medicine

The **National Academy of Sciences** is a private, nonprofit, self-perpetuating society of distinguished scholars engaged in scientific and engineering research, dedicated to the furtherance of science and technology and to their use for the general welfare. On the authority of the charter granted to it by the Congress in 1863, the Academy has a mandate that requires it to advise the federal government on scientific and technical matters. Dr. Bruce M. Alberts is president of the National Academy of Sciences.

The **National Academy of Engineering** was established in 1964, under the charter of the National Academy of Sciences, as a parallel organization of outstanding engineers. It is autonomous in its administration and in the selection of its members, sharing with the National Academy of Sciences the responsibility for advising the federal government. The National Academy of Engineering also sponsors engineering programs aimed at meeting national needs, encourages education and research, and recognizes the superior achievements of engineers. Dr. William A. Wulf is president of the National Academy of Engineering.

The **Institute of Medicine** was established in 1970 by the National Academy of Sciences to secure the services of eminent members of appropriate professions in the examination of policy matters pertaining to the health of the public. The Institute acts under the responsibility given to the National Academy of Sciences by its congressional charter to be an adviser to the federal government and, on its own initiative, to identify issues of medical care, research, and education. Dr. Harvey V. Fineberg is president of the Institute of Medicine.

The **National Research Council** was organized by the National Academy of Sciences in 1916 to associate the broad community of science and technology with the Academy's purposes of furthering knowledge and advising the federal government. Functioning in accordance with general policies determined by the Academy, the Council has become the principal operating agency of both the National Academy of Sciences and the National Academy of Engineering in providing services to the government, the public, and the scientific and engineering communities. The Council is administered jointly by both the Academies and the Institute of Medicine. Dr. Bruce M. Alberts and Dr. William A. Wulf are chair and vice chair, respectively, of the National Research Council.

The **Transportation Research Board** is a division of the National Research Council, which serves the National Academy of Sciences and the National Academy of Engineering. The Board's mission is to promote innovation and progress in transportation through research. In an objective and interdisciplinary setting, the Board facilitates the sharing of information on transportation practice and policy by researchers and practitioners; stimulates research and offers research management services that promote technical excellence; provides expert advice on transportation policy and programs; and disseminates research results broadly and encourages their implementation. The Board's varied activities annually engage more than 4,000 engineers, scientists, and other transportation researchers and practitioners from the public and private sectors and academia, all of whom contribute their expertise in the public interest. The program is supported by state transportation departments, federal agencies including the component administrations of the U.S. Department of Transportation, and other organizations and individuals interested in the development of transportation. **www.TRB.org**

www.national-academies.org

AUTHOR ACKNOWLEDGMENTS

The research reported herein was performed under NCHRP Project 18-07 by the University of Nebraska—Lincoln, the contractor for this study, jointly with Concrete Technology Corporation, Tacoma, Washington, and Palmer Engineering, Lexington, Kentucky. Maher K. Tadros, Cheryl Prewett Professor of Civil Engineering, was the principal investigator, and Nabil Al-Omaishi, Research Assistant Professor, was a prime participant in the research. Other major participants in the project were Stephen J. Seguirant of Concrete Technology Corporation and James G. Gallt of Palmer Engineering.

Sherif Yehia, Nick Meek, Kelvin Lein, and Wilast Amornrattanopong of the University of Nebraska provided assistance during the experimental phases of the project. David Scott of New Hampshire Department of Transportation, Bill Augustus of Northeast Concrete Products, Robert Steffen of the University of New Hampshire, Kevin Pruski of Texas Department of Transportation, Burson Patton of Texas Concrete Company, Arlen Clark of Clark County, Washington, Jim Parkins of Concrete Technology Corporation, and Mark Lafferty of Concrete Industries provided assistance in instrumentation and data acquisition of instrumented bridges in Nebraska, New Hampshire, Texas, and Washington. Karen Harris of the University of Nebraska contributed to the project administration. Audra Hansen, Nipon Jongpitaksseel, Ann Kulik, Chuanbing Sun, and Emil Tadros contributed to report preparation.

FOREWORD

By Amir N. Hanna
Staff Officer
Transportation Research Board

This report presents guidelines to help bridge designers obtain realistic estimates of prestress losses in high-strength pretensioned concrete bridge girders and thus achieve economical designs. These guidelines incorporate procedures that yield more accurate predictions of modulus of elasticity, shrinkage, and creep of concrete and more realistic estimates of prestress losses than those provided by the procedures contained in current specifications. This report will be of particular interest to engineers, researchers, and others concerned with the design of pretensioned concrete bridge structures.

The use of high-strength concrete for pretensioned concrete bridge girders has become accepted practice by many state highway agencies because of its engineering and economic benefits. High-strength concrete permits longer girders and increased girder spacing, thus reducing total bridge cost. Design of pretensioned concrete girders requires accurate estimates of prestress losses. These losses are affected by factors such as mix design, curing, concrete strength, and service exposure conditions.

Recent research has indicated that the current provisions used for calculating prestress losses in normal-strength concrete may not provide reliable estimates for high-strength concrete bridge girders. Thus, research was needed to evaluate the applicability of the current provisions for estimating prestress losses in high-strength concrete bridge girders and to develop guidelines for better estimating these losses in order to help bridge design engineers develop economic designs for such girders.

Under NCHRP Project 18-07, "Prestress Losses in Pretensioned High-Strength Concrete Bridge Girders," the University of Nebraska—Lincoln was assigned the task of developing design guidelines for estimating prestress losses in pretensioned high-strength concrete bridge girders. To accomplish this objective, the researchers reviewed relevant domestic and foreign literature; identified limitations on the methods currently used for estimating prestress losses; conducted laboratory tests for evaluating relevant properties of concrete; derived formulas for predicting modulus of elasticity, shrinkage, and creep of concrete; and developed a "detailed" method and an "approximate" method for estimating prestress losses in pretensioned high-strength concrete bridge girders.

The research also included (a) field measurements on seven full-scale bridge girders in four states selected to represent a wide range of geographic and construction practices and (b) analysis of data from earlier field measurements on 31 pretensioned girders in seven states. The report gives numerical examples that illustrate the use of these methods and demonstrate that the methods developed in this research yield better estimates of prestress losses than those obtained from the current methods.

The methods developed in this research can be used to obtain realistic estimates of prestress losses in pretensioned high-strength concrete bridge girders. These methods will be particularly useful to highway agencies and consulting firms involved in the design of pretensioned concrete bridge structures and are recommended for consideration and adoption by AASHTO as part of the LRFD Bridge Design Specifications.

CONTENTS

1 SUMMARY

3 CHAPTER 1 Introduction
- Problem Statement, 3
- Objectives and Scope of the Research, 3
- Research Approach, 3
- Organization of the Report, 4
- Applicability of Results to Highway Practice, 4

5 CHAPTER 2 Background and Literature Search
- Introduction, 5
- Definitions, 5
- Components of Prestress Losses in Pretensioned Girders, 6
- Factors Influencing Modulus of Elasticity, 6
- Factors Influencing Shrinkage, 8
- Factors Influencing Creep, 8
- Factors Influencing Relaxation of Strands, 9
- Time-Dependent Stress Analysis, 9
- Prestress Loss Calculation Methods, 10
- Time-Step Prestress Loss Methods, 10
- Refined Prestress Loss Methods, 11
- Lump-Sum Methods, 13

14 CHAPTER 3 Research Results
- Introduction, 14
- Experimental Program, 14
- Modulus of Elasticity, 17
- Experimental Shrinkage Results, 18
- Experimental Creep Results, 20
- Proposed Creep and Shrinkage Correction Factors, 21
- Proposed Shrinkage Formula, 27
- Proposed Creep Formula, 28
- Relaxation of Prestressing Strands, 28
- Proposed AASHTO-LRFD Revisions, 29
- Numerical Example of Material Properties Using Proposed Prediction Formulas, 29
- Prestress Loss, 30
- Experimental Program, 30
- Other Experimental Data, 35
- Proposed Detailed Prestress Loss Method, 38
- Proposed Approximate Prestress Loss Method, 45
- Comparison of Measured and Predicted Losses, 48
- Comparison with Previously Reported Experimental Results, 49
- Numerical Examples: Comparison of Proposed Prestress Loss Prediction Methods with AASHTO-LRFD Methods, 49

56 CHAPTER 4 Conclusions and Suggested Research
- Conclusions, 56
- Suggested Research, 57

58 SIGN CONVENTION AND NOTATION

61 REFERENCES

63 APPENDIX A Other Methods of Shrinkage Strain Prediction

63 APPENDIX B Other Methods of Creep Coefficient Prediction

63 APPENDIX C Other Methods of Prestress Losses Prediction

63 APPENDIX D Material Testing

63 APPENDIX E Modulus of Elasticity Data

63 APPENDIX F Shrinkage Data

63 APPENDIX G Creep Data

63 APPENDIX H Temperature Readings

63 APPENDIX I Strain Readings

63 APPENDIX J Specific Details of the Previous Measured Prestress Losses Experimental Data

63 APPENDIX K Prestress Loss Data

63 APPENDIX L Detailed Method Spreadsheet

63 APPENDIX M Proposed AASHTO-LRFD Revisions

PRESTRESS LOSSES IN PRETENSIONED HIGH-STRENGTH CONCRETE BRIDGE GIRDERS

SUMMARY

The objective of this research was to develop design guidelines for estimating prestress losses in high-strength pretensioned concrete girder bridges. The guidelines are intended to address limitations in the current AASHTO-LRFD Bridge Design Specifications. Two main areas were identified for improvement: (a) prediction of modulus of elasticity, shrinkage, and creep of concrete, especially as they relate to the high-strength concrete and (b) methods for estimating prestress losses that would account for the effects of differential creep and shrinkage between precast concrete girder and cast-in-place concrete deck and for relatively high prestress levels and low creep and shrinkage in high-strength concrete.

The research consisted of experimental and theoretical programs. The experimental program consisted of measurements of properties of materials and of prestress loss in seven full-scale bridge girders in four states, representing a range of geographic conditions and construction practices: Nebraska, New Hampshire, Texas, and Washington. In addition, test results previously reported for 31 pretensioned girders in seven states, Connecticut, Illinois, Nebraska, Ohio, Pennsylvania, Texas, and Washington, were included in the study. Additionally, relevant data reported by American Concrete Institute (ACI) Committee 363 and FHWA were considered.

Formulas for prediction of modulus of elasticity, shrinkage, and creep of concrete that were consistent in form with the AASHTO-LRFD formulas were developed. These formulas produced comparable results for conventional concrete with those of the AASHTO-LRFD formulas. It was concluded that local material properties significantly impacted the prediction of modulus of elasticity, shrinkage, and creep. The proposed formulas produce national averages; factors are given to adjust these averages for the four states covered in the project.

A “detailed method” based on pseudo-elastic analysis theory using modified “age-adjusted effective modulus” of elasticity of concrete is proposed for estimating prestress losses. The method considers the effects of composite action between the precast concrete girder and the cast-in-place concrete deck, material properties, environmental conditions, and construction schedule parameters available. An “approximate method” that produces reasonable estimates for commonly encountered conditions is also proposed.

Both methods produced better correlation with test results than current AASHTO-LRFD methods.

Numerical examples are given to demonstrate the proposed loss prediction methods and to explain the recommendation that no elastic shortening losses at prestress transfer or elastic elongation gains at application of additional load, be considered in the calculation of concrete stresses, if transformed section properties are used.

CHAPTER **1**

INTRODUCTION

PROBLEM STATEMENT

Use of high-strength concrete for pretensioned concrete bridge girders has become accepted practice by many state highway agencies because of its technical and economic benefits. High-strength concrete permits longer girders and increased girder spacing, thus reducing total bridge cost. The design of pretensioned concrete girders requires accurate estimates of prestress losses. These losses are affected by factors such as mix design, curing, concrete strength, and service exposure conditions.

Recent research has indicated that the current provisions developed for calculating prestress losses in normal-strength concrete may not provide reliable estimates for high-strength concrete bridge girders. Thus, research was needed to evaluate the applicability of the current provisions for estimating prestress losses in high-strength concrete bridge girders and to develop guidelines for estimating these losses. This information will help bridge design engineers to develop economical designs for such girders. This project was conducted to address this need.

If one underestimates prestress losses, there is a risk of cracking the girder bottom fibers under full service loads. On the other hand, if prestress losses are overestimated, a higher prestress force must be provided, which will result in larger amounts of camber and shortening than is necessary. It is, therefore, important to have a reasonably accurate estimate of prestress losses.

OBJECTIVE AND SCOPE OF THE RESEARCH

The objective of this research was to develop design guidelines for estimating prestress losses in pretensioned high-strength concrete bridge girders. The research was limited to the materials and practices currently used by state highway agencies in the design and production of prestressed concrete bridge girders and to assess their effects on prestress losses.

To accomplish this objective the following tasks were performed:

1. Relevant literature, design specifications, research findings, and current practices for estimating prestress losses in pretensioned concrete bridge girders were collected and reviewed. This information was assembled from published and unpublished reports, contacts with state transportation agencies, industry organizations, and other domestic and foreign sources.
2. Based on the information gathered in Task 1, the applicable range of concrete strengths for which the current AASHTO provisions for estimating prestress losses in pretensioned concrete bridge girders was determined.
3. Based on the information gathered in Task 1, the material properties and other factors such as curing, exposure, and loading conditions that affect prestress losses in pretensioned high-strength concrete girders were studied. The test methods used for determining these material properties were identified.
4. A detailed experimental research plan, which encompassed the investigation of full-scale girders and associated analysis, was developed for evaluating the effects of the material properties and other factors on the prestress losses in pretensioned concrete bridge girders. This plan addressed concrete strength levels that are currently used by state highway agencies and are beyond the applicability range of the current AASHTO Specifications.
5. The plan developed in Task 4 was executed. It included a material testing program for the field and laboratory and a full-scale testing of seven bridge girders in four states. Also, an implementation plan for putting the results of this research into practice was suggested.
6. Design guidelines for estimating prestress losses in pretensioned high-strength concrete bridge girders were developed based on the results of the entire research effort.

RESEARCH APPROACH

Time-dependent prestress loss is influenced by creep and shrinkage of concrete and stress relaxation of the prestressing strands. As concrete shrinks, the prestressing steel shortens and loses some of its tension. Consequently, concrete creeps less than in the case of sustained constant compression; so-called “creep recovery” takes place. Also, as concrete creeps and shrinks, the prestressing strands relax at a slower rate than they would if they were stressed and kept stretched between

two fixed points; thus, the "reduced" relaxation is less than the "intrinsic" relaxation that occurs in a constant-length laboratory test. This interaction between shrinkage and creep of concrete and relaxation of prestressing strands is partially taken into account in the current prediction formulas of the AASHTO-LRFD Specifications (*1*).

The effect of high compressive strength concrete on the prestress loss due to creep and shrinkage strain is not taken into account in the current AASHTO-LRFD Specifications (*1*). The use of high-strength concrete to improve the structural efficiency of pretensioned bridge girders has created the need for an accurate estimation of material properties that impact the time-dependent components of prestress losses.

Also, the current AASHTO-LRFD formulas do not consider the interaction between the precast pretensioned concrete girder and the precast or cast-in-place concrete deck. The concrete deck, if used, can induce significant shrinkage deformation that results in additional stresses, thus affecting the magnitude of the prestress losses and the tensile stress at the girder bottom.

ORGANIZATION OF THE REPORT

This report consists of four chapters. This chapter provides the introduction and research approach, describes the problem statement and research objective, and outlines the scope of the study. Chapter 2 describes the findings of the literature review, relevant material properties, and current loss prediction methods. The conditions for which the current AASHTO-LRFD loss prediction methods are applicable are indicated. Chapter 3 discusses the material properties that affect prestress losses. It also covers the experimental program for material properties and prestress loss measurements in seven full-scale girders located in Nebraska, New Hampshire, Texas, and Washington. The proposed formulas for prediction of modulus of elasticity, shrinkage, and creep of concrete and relaxation of prestressing strands are presented. A detailed method and an approximate method for estimating prestress losses in pretensioned bridge girders and numerical examples to demonstrate their use are presented in Chapter 3. Chapter 4 summarizes the significant conclusions of this project and presents suggestions for future research.

APPLICABILITY OF RESULTS TO HIGHWAY PRACTICE

The design and construction of precast prestressed concrete bridge girders is impacted by the amount of prestressing that could be applied to the girders and the effective prestress remaining after elastic and short-term losses have developed. The findings presented in Chapters 3 and 4 on the prediction of modulus of elasticity, shrinkage, and creep of concrete and on the estimation of prestress losses could be included in the AASHTO-LRFD Specifications to provide designers of prestressed concrete bridges with more realistic estimates of prestress losses. Realistic estimates of prestress losses, especially for high-strength concrete, would prevent specifying excessive prestress forces and should result in economical designs with realistic concrete stresses at service conditions and relatively moderate girder camber.

CHAPTER 2

BACKGROUND AND LITERATURE SEARCH

INTRODUCTION

There are two sources of possible inaccuracies in prestress losses calculations: (a) incorrect theory and (b) inaccurate estimate of material properties. The research team reviewed domestic and foreign literature, research findings, and experimental data. The literature search focused on experiments related to concrete material properties and prestress losses.

The prestress losses prediction formulas are used by current AASHTO-LRFD and AASHTO Standard Specifications (*2*) for considering the effects of variation in material properties, especially concrete strength. The range of conditions for which the current AASHTO-LRFD and the AASHTO Standard Specifications are applicable, was determined from three parametric studies. The first study assessed the variability of the prestress loss component attributed to concrete creep. The second study evaluated the shrinkage component with consideration to type of beam cross section, concrete compressive strength, relative humidity, and amounts of prestressing steel. The third study compared prestress losses for a number of designs using the AASHTO-LRFD methods.

DEFINITIONS

Definitions of the significant terms used in this study are given below because some of the terms, such as long-term prestress loss, have no universally accepted definitions. This makes comparing the results of some methods misleading.

Prestress Loss

The primary purpose of calculating the effective prestress force acting on a prestressed concrete section is to evaluate concrete stresses and deformations under service conditions. The most representative definition of prestress loss is the loss of compressive force acting on the concrete component of a prestressed concrete section. Creep and shrinkage cause member shortening and a loss of tension in the prestressing tendons as well as a compression force increment in nonprestressed reinforcement, if such reinforcement exists in a member. The sum of the reduction in tensile force in the tendons and compression force increment in the non-prestressed reinforcement is equal and opposite to the incremental loss of compression force in concrete. That force is the force needed for concrete stress analysis.

Since this project deals with pretensioned members, which are generally reinforced in flexure with prestressing strands only, loss of tension in the strands is equal and opposite to loss of compression in the concrete. Therefore, the more common, though less comprehensive, definition of prestress loss, that is, loss of tension in the prestressing strands is adopted. Prestress loss is considered a positive quantity, even though it is a compression increment in the strands.

Total Loss of Prestress

Theoretically, total loss of prestress is the reduction of tension from the time strands are tensioned until the end of service life of the prestressed concrete member. Only the part of that total loss that is of practical significance to bridge designers is considered in this project. Thus, the total loss of prestress is defined as the difference in the stress in the strands immediately before transfer to the concrete member and the stress at the end of service life of the member.

Elastic Loss (or Gain)

As the prestressing force is released from the bed and transferred to the concrete member, the member undergoes shortening and cambers upward between its two ends. The elastic loss at transfer is the tensile stress loss due to prestress combined with stress gain due to member weight. As an additional load, for example, the deck weight, is introduced to the member, the strands elongate, and thus undergo elastic gain. As will be shown in Chapters 3 and 4, the elastic losses and gains do not have to be calculated. They can be automatically accounted for when transformed section properties are used. When prestress loss prediction methods are compared, it is important to isolate elastic losses and gains and properly account for them in the comparison. Elastic gain is considered a negative quantity in the total loss value.

Long-Term Losses

Long-term prestress loss is the loss due to creep and shrinkage of concrete and relaxation of steel. In this study, the elastic losses or gains due to applied dead and live loads are not included in the long-term prestress loss. Because the current AASHTO Specifications do not include any terms for elastic

gain due to any of the loads applied after prestress transfer, the long-term losses given in these specifications implicitly include these elastic gain increments.

COMPONENTS OF PRESTRESS LOSSES IN PRETENSIONED GIRDERS

Components of prestress losses are illustrated in Figure 1 and described below.

(a) Loss due to prestressing bed anchorage seating, relaxation between initial tensioning and transfer, and temperature change from that of the bare strand to temperature of the strand embedded in concrete. This component is not considered in this project.
(b) Instantaneous prestress loss at transfer due to prestressing force and self weight.
(c) Prestress loss between transfer and deck placement due to shrinkage and creep of girder concrete and relaxation of prestressing strands.
(d) Instantaneous prestress gain due to deck weight on the noncomposite section and superimposed dead loads (SIDL) on the composite section.
(e) Long-term prestress losses after deck placement due to shrinkage and creep of girder concrete, relaxation of prestressing strands, and deck shrinkage.

Prestress losses in pretensioned high-strength concrete girders are influenced by material properties (internal factors) and environmental conditions (external factors). Accurate prediction of prestress losses requires accurate prediction of the long-term properties of concrete and prestressing strands, which is a very complex process because of the uncontrollable variables involved. The material properties that vary with time and affect prestress losses are compressive strength, modulus of elasticity, shrinkage (stress independent), and creep (stress dependent) of concrete, and relaxation of strands.

The rate at which concrete properties change with time depends on a number of factors, including type and strength of cement, type, quality, and stiffness (i.e., modulus of elasticity) of aggregates, and quantity of coarse aggregates; type and amount of admixtures; water/cement ratio; size and shape of the girder; stress level; and environmental conditions (humidity and temperature). Relaxation of strands is a long-term reduction of stress when strands are subjected to an imposed strain, and can be estimated with good accuracy.

FACTORS INFLUENCING MODULUS OF ELASTICITY

The factors that affect the determination of modulus of elasticity in the laboratory are the moisture content and the loading conditions, such as top and bottom bearing plate sizes, loading rate, and specimen shape and size. Stiffness of the cement paste, porosity and composition of the boundary zone between paste and aggregates, stiffness and porosity of the aggregates, and proportion of the concrete constituents are also factors. Both concrete strength and concrete unit weight are indirect factors in influencing the modulus of elasticity. They are dominantly used in prediction formulas as a way of capturing the fundamental underlying factors. This, in part, explains the inaccuracy in the current prediction of the modulus of elasticity of concrete, E_c. In early-age concrete, the strength of the cement paste is the primary contributor to the strength while the stiffness of the coarse aggregates is the primary contributor to the modulus of elasticity.

Accurately estimating the value of E_c allows for accurate prediction of the initial camber and initial elastic prestress loss and helps improve the accuracy of the prediction of creep loss. The modulus of elasticity increases approximately with the square root of the concrete compressive strength; empirical equations have been developed to estimate the modulus of elasticity based on the compressive strength of the concrete.

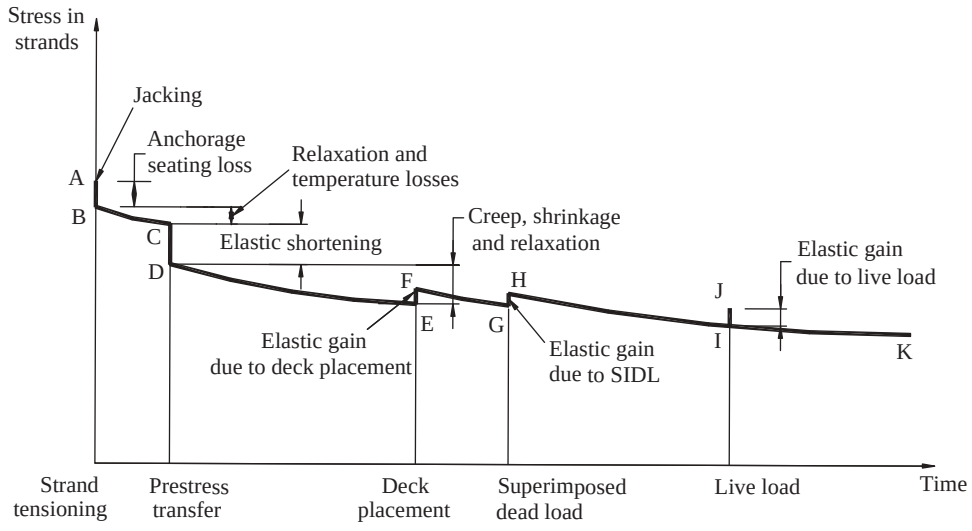

Figure 1. Stress versus time in the strands in a pretensioned concrete girder.

When the unit weight of concrete, w_c, is different from 0.145 kcf (assumed for the normal unit weight concrete in Section C5.4.2.4 of the AASHTO-LRFD Specifications), and in the absence of more laboratory data, the modulus of elasticity, according to the AASHTO-LRFD (*1*), the ACI-318 (*3*), and the Precast/Prestressed Concrete Institute Bridge Design Manual (PCI-BDM) (*4*), is based on the compressive strength and unit weight of concrete (AASHTO Equation 5.4.2.4-1 and ACI-318 Equation 8.5.1):

$$E_c = 33,000\, w_c^{1.5}\sqrt{f'_c} \qquad \text{(kcf and ksi)} \tag{1}$$

$$E_c = 0.043\, w_c^{1.5}\sqrt{f'_c} \qquad \left(\text{kg/m}^3 \text{ and MPa}\right)$$

The above formula is applicable to concretes with unit weights between 0.090 and 0.155 kip/ft^3 (1,442 and 2,483 kg/m^3). According to ACI-363 Committee Report (*5*), this formula tends to significantly overestimate the modulus of elasticity for concretes with compressive strengths over 6 ksi (41 MPa). Other equations were proposed, and the following formula was adopted by ACI Committee 363 (ACI-363 Equation 5-1):

$$E_c = (w_c/0.145)^{1.5}\left(1000 + 1265\sqrt{f'_c}\right) \qquad \text{(kcf and ksi)} \tag{2}$$

$$E_c = (w_c/86)^{1.5}\left(6900 + 3320\sqrt{f'_c}\right) \qquad \left(\text{kg/m}^3 \text{ and MPa}\right)$$

This formula does not account for factors other than the unit weight and compressive strength that clearly affect the value of E_c, such as coarse aggregate content in concrete and properties of the aggregates. Myers and Carrasquillo (*6*) showed that elastic modulus appeared to be a function of the coarse aggregate content and type.

The prediction of the modulus of elasticity can be considerably improved if the influence of the modulus of elasticity of the particular type of aggregate used in the concrete is taken into account. This has been reflected in the Comité Euro-International du Beton-Fédération Internationale de la Précontrainte (CEB-FIP) Model Code (*7*), which introduced the empirical coefficient α_E to reflect the strength of the aggregate used:

$$E_c = 3100\alpha_E (f_{cm}/1.44)^{1/3} \qquad \text{(ksi)}$$
$$E_c = 21500\alpha_E (f_{cm}/10)^{1/3} \qquad \text{(MPa)} \tag{3}$$

where: E_c = tangent modulus of elasticity at zero stress and at a concrete age of 28 days and f_{cm} = mean compressive strength of concrete. The values of the empirical coefficient α_E are 1.2 for basalt and dense limestone, 1.0 for quartz aggregates, 0.9 for limestone, and 0.7 for sandstone.

Figure 5.3 of the ACI-363 Committee Report compares values for the modulus of elasticity of concrete experimentally determined from previous research with those predicted by the ACI-318 Building Code formula and based on a dry unit weight of 0.145 kip/ft^3. This chart was reproduced and is included in Figure 2, which also includes experimental data collected from the FHWA Showcase (*8*). Deviations from predicted values are highly dependent on the properties of the coarse aggregate.

The research work at the University of Minnesota indicated, based on the use of local materials, that the AASHTO-LRFD equation overestimated the modulus of elasticity of high-strength concrete (Ahlborn [*9*]). Researchers at the University of Texas (*6*) reported all high-strength concrete mixes tested in their research had moduli of elasticity larger than those predicted by ACI Committee 363 formula. Huo (*10*) and Huo et al. (*11*) indicated that both the AASHTO-LRFD and the

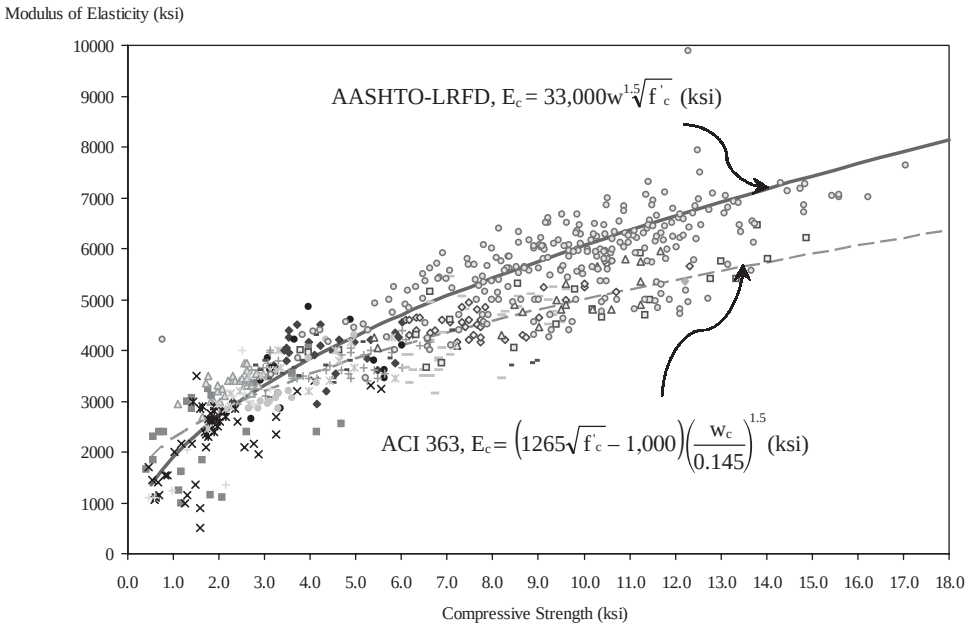

Figure 2. Modulus of elasticity versus compressive strength data obtained from ACI-363 Report (5) and FHWA Showcase (8).

ACI Committee 363 equations underestimated the modulus of elasticity of three high-strength concrete mixes studied in that research.

The differing opinions among researchers on the prediction equations for the modulus of elasticity have raised a question as to how to correctly predict the value of E_c for high-strength concrete. Although all the prediction equations for modulus of elasticity have compressive strength of concrete f'_c as a variable, other factors clearly affect the value of E_c, such as coarse aggregate content in the concrete and properties of the aggregates. These factors will be further explored in Chapter 3.

FACTORS INFLUENCING SHRINKAGE

Shrinkage depends on many variables, including water-to-binder ratio, moisture, relative humidity of the environment, ambient temperature, aggregate properties, and size and shape of the structural member. It is assumed to be independent of loading and results primarily from shrinkage of the cement paste. Because aggregates tend to restrain the shrinkage of the paste, the stiffness and proportion of aggregates influence shrinkage.

Shrinkage is conveniently expressed as a dimensionless strain under steady conditions of relative humidity and temperature. The AASHTO-LRFD formula for estimating shrinkage strain, ϵ_{sh}, as a function of a time-development factor, k_{td}, and the ultimate shrinkage (at time infinity), $\epsilon_{sh,\,u}$, is:

$$\epsilon_{sh} = k_{td}\epsilon_{sh,u} \tag{4}$$

$$\epsilon_{sh,u} = 560 \times 10^{-6}\gamma_{sh} \quad \text{for accelerated curing} \tag{5}$$

$$\epsilon_{sh,u} = 510 \times 10^{-6}\gamma_{sh} \quad \text{for moist curing} \tag{6}$$

$$k_{td} = \frac{t}{55 + t} \quad \text{after 1–3 days of accelerated curing} \tag{7}$$

$$k_{td} = \frac{t}{35 + t} \quad \text{after 7 days of moist curing} \tag{8}$$

$$\gamma_{sh} = k_s k_{hs} \tag{9}$$

k_s = V/S ratio (size) correction factor

$$= \left[\frac{\frac{t}{26e^{0.36V/S} + t}}{\frac{t}{45 + t}}\right]\left[\frac{1064 - 94V/S}{923}\right] \tag{10}$$

k_{hs} = humidity factor for shrinkage

$$= \frac{140 - H}{70} \quad \text{for } H < 80\%, \tag{11}$$

$$= \frac{3(100 - H)}{70} \quad \text{for } H \geq 80\% \tag{12}$$

In these equations, t is drying time after end of curing in days, H is relative humidity of ambient air, and V/S ratio is volume-to-surface ratio in inches. Other methods of predicting shrinkage strain such as the PCI-BDM, the ACI-209 (*12*), and the CEB-FIP are presented in Appendix A.

FACTORS INFLUENCING CREEP

The creep of concrete depends on many factors other than time, such as volume content of hydrated cement paste, relative humidity, the type and volume of the aggregate, the age of the concrete at the time of loading, the stress level, the duration the concrete is stressed, and the geometry of the member. The size and shape of a concrete member can significantly influence the rate and the magnitude of creep. Hansen (*13*) observed that the rate and magnitude of ultimate creep were substantially smaller for larger members.

Creep in high-strength concrete is generally smaller than in normal-strength concrete loaded to a similar stress level because of the lower water-to-binder ratio of high-strength concrete. At any time, the creep strain can be related to the initial elastic strain by a creep coefficient, $\psi\,(t, t_i)$, which is the ratio of creep strain to elastic strain. Creep strain will reach its ultimate value with an ultimate creep coefficient, ψ_u, at the end of the service life of the structure.

The AASHTO-LRFD creep prediction formulas are presented here. Other methods, for example, the PCI-BDM, the ACI-209, and the CEB-FIP are presented in Appendix B.

$$\psi(t, t_i) = k_{td}\psi_u \tag{13}$$

$$\psi_u = 3.5\gamma_{cr} \tag{14}$$

$$\gamma_{cr} = k_f k_c k_{hc} k_{la} \tag{15}$$

k_f = concrete strength factor

$$= \frac{1}{0.67 + \frac{f'_c}{9}} \quad \text{with } f'_c \text{ in ksi} \tag{16}$$

k_c = size factor

$$= \left[\frac{\frac{t}{26e^{0.36V/S} + t}}{\frac{t}{45 + t}}\right]\left[\frac{1.80 + 1.77e^{-0.54V/S}}{2.587}\right] \tag{17}$$

$$k_{hc} = \text{humidity factor for creep} = \frac{1.58 - H}{120} \tag{18}$$

$$k_{la} = \text{loading age factor} = t_1^{-0.118} \tag{19}$$

$$k_{td} = \text{time-development factor} = \frac{(t - t_i)^{0.6}}{10 + (t - t_i)^{0.6}} \qquad (20)$$

t_i = age of concrete, in days, when load is initially applied for accelerated curing or the age minus 6 days for moist curing.

FACTORS INFLUENCING RELAXATION OF STRANDS

If a strand is stressed and then held at constant strain, the stress decreases with time. The decrease in stress is called intrinsic relaxation loss. The intrinsic relaxation loss is larger with larger initial stress and higher temperature. Strands used in current practice are low-relaxation strands, which undergo considerably less relaxation than stress-relieved strands. As a result, the relaxation component of prestress loss has become a very small one.

The intrinsic relaxation loss for stress-relieved strand 1:

$$\Delta f_{pR1} = \frac{\log(24.0t)}{10.0}\left[\frac{f_{pi}}{f_{py}} - 0.55\right] f_{pj} \qquad (21)$$

The intrinsic relaxation loss for low-relaxation strand 1:

$$\Delta f_{pR1} = \frac{\log(24.0t)}{40.0}\left[\frac{f_{pi}}{f_{py}} - 0.55\right] f_{pj} \qquad (22)$$

where: t is time in days from time of initial stressing, f_{pj} (ksi), f_{py} (ksi) is yield strength of prestressing steel estimated at 85% of ultimate strength for stress relieved strands and 90% for low-relaxation strands. Relaxation loss in prestressing strands after transfer is given by the formulas:

For stress-relieved strand:

$$\Delta f_{pR2} = 20.0 - 0.4\Delta f_{pES} - 0.2\left(\Delta f_{pSR} + \Delta f_{pCR}\right) \qquad \text{(ksi)} \qquad (23)$$

For low-relaxation strand:

$$\Delta f_{pR2} = 6.0 - 0.12\Delta f_{pES} - 0.06\left(\Delta f_{pSR} + \Delta f_{pCR}\right) \qquad \text{(ksi)} \qquad (24)$$

where: Δf_{pES} is loss due to elastic shortening, Δf_{pSR} is loss due to shrinkage, and Δf_{pCR} is loss due to creep. Low-relaxation strands are the standard product for concrete girders. In most applications, the relaxation loss after transfer is in the 1.8 to 3.0 ksi range—a relatively small component of the total prestress loss.

TIME-DEPENDENT STRESS ANALYSIS

Stress-Strain Relationships

The strain that occurs upon initial loading in a concrete specimen subjected to a sustained axial load is the elastic strain. Additional strain then develops with time due to creep and shrinkage. Shrinkage strain is stress-independent. The ratio of creep strain at time t to elastic strain for a concrete specimen loaded at time t_i is creep coefficient, $\psi(t, t_i)$. Figure 3 shows

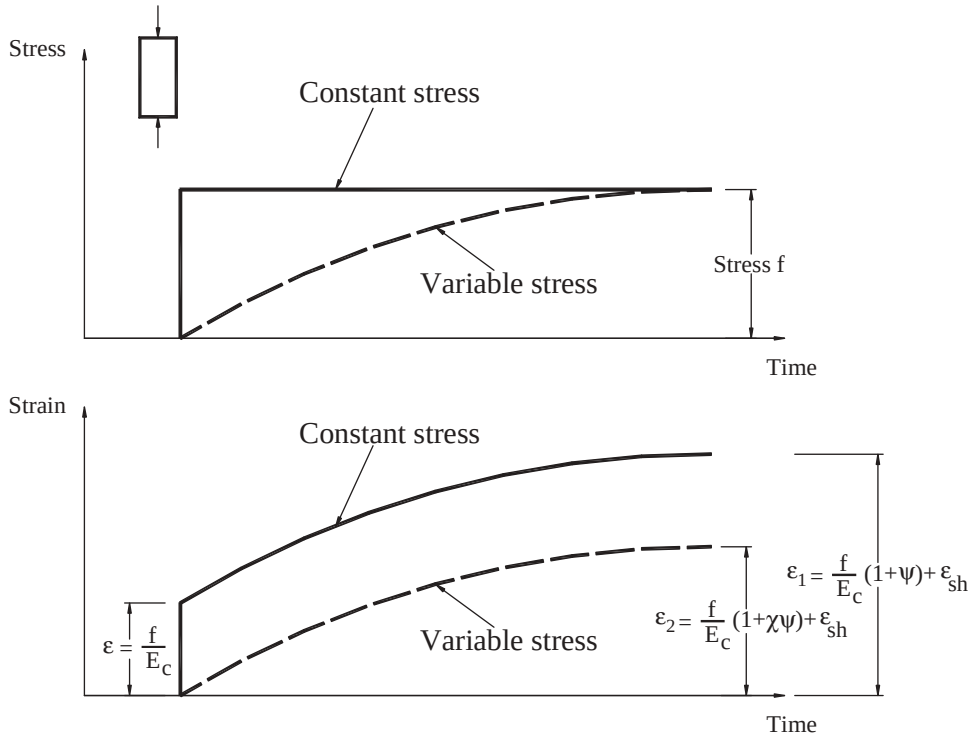

Figure 3. Creep strain for constant and variable stress conditions.

creep strain versus time for constant and variable concrete stress conditions.

Age-Adjusted Effective Modulus

Elastic and creep strains of concrete can be combined and treated as if they were elastic deformations through use of an "age-adjusted" effective modulus of elasticity. For constant sustained stress, the elastic-plus-creep strain is equal to $(1 + \psi)$ times the elastic strain. Thus, the elastic-plus-creep strain can be thought of as elastic-only strain if an effective modulus of elasticity is used to calculate that pseudo-elastic strain.

$$E_c' = \frac{E_c}{1 + \psi} \tag{25}$$

Therefore, the total concrete strain under long-term conditions is:

$$\epsilon_1 = \frac{f_c}{E_c'} + \epsilon_{sh} \tag{26}$$

If the concrete stress varies with time, the elastic-plus-creep strain becomes $(1 + \chi\psi)$ where the coefficient χ is the aging coefficient, initially proposed by Trost (*14*) and further developed by Bazant (*15*) and Dilger (*16*). It varies between 0 and 1 depending on concrete stress variability and the aging process of the member being considered. The age-adjusted effective modulus of elasticity of concrete is thus defined as:

$$E_c'' = \frac{E_c}{1 + \chi\psi} \tag{27}$$

The total concrete strain is:

$$\epsilon_2 = \frac{f_c}{E_c''} + \epsilon_{sh} \tag{28}$$

Thus, the time-dependent analysis for the effects of all constant sustained loads (initial prestress, self weight, deck weight, and SIDL) can be carried out using an effective elasticity modulus E_c' as defined by Equation 25, and for variable stress inducing effects (prestress loss and differential creep and shrinkage between the precast and cast-in-place components of section) using the age-adjusted effective modulus defined by Equation 27. Tadros et al. (*17*, *18*) demonstrated that, for precast prestressed concrete members, the aging coefficient ranges between 0.6 and 0.8.

Procedure for Time-Dependent Stress Analysis

The procedure presented by Dilger (*16*) may be used for computing time-dependent stresses in prestressed concrete members. The analysis is based on initial strain theory often employed in finite-element analysis of the effects of temperature change in structures.

The following three steps illustrate this analysis for simply supported precast concrete members.

Step 1: Immediately after transfer of prestress, separate the various components of the cross section into free-to-deform elements to allow deformation due to creep, shrinkage, and relaxation. Deformation of mild reinforcement is assumed to be zero. Concrete deformation will occur due to creep and shrinkage, and prestressing steel deformation will be related to its relaxation.

Step 2: The deformation of each of the components is brought to zero by applying axial force and bending moment to the concrete and axial force to the prestressing steel, using age-adjusted concrete modulus of elasticity.

Step 3: The various components are then reconnected assuming full bond between them to restore equilibrium. This is done by applying equal and opposite forces to the restraining forces calculated in Step 2. These new forces are combined into an axial force and a bending moment introduced to the age-adjusted equivalent transformed composite section. The deformation of the member due to this step is the total deformation. The stresses in the various components are the sum of the stresses obtained in Step 2 and Step 3.

PRESTRESS LOSS CALCULATION METHODS

Estimating prestress loss requires an accurate prediction of material properties and of the interaction between creep and shrinkage of concrete and the relaxation of steel. In addition, prestress losses are influenced by composite action between the cast-in-place concrete deck and the precast concrete girders. Use of high-strength concrete in precast prestressed concrete allows for high levels of prestress and long span capacities. However, experience in estimating prestress loss for high-strength concrete is limited. Approaches for estimating prestress losses can be divided into the following three major categories, listed in descending order of complexity and accuracy:

(a) Time-Step methods
(b) Refined methods
(c) Lump-Sum methods

TIME-STEP PRESTRESS LOSS METHODS

These methods are based on a step-by-step numerical procedure implemented in specialized computer programs for the accurate estimation of long-term prestress losses. This approach is especially useful in multi-stage bridge construction such as spliced girder and segmental box girder bridges. As concrete creeps and shrinks, the prestressing strands shorten and decrease in tension. This, in turn, causes the strands to relax less than if they were stretched between two fixed points. Hence, "reduced" rather than "intrinsic" relaxation loss takes

place. As the prestressing strand tension is decreased, concrete creeps less, resulting in some recovery.

To account for the continuous interactions between creep and shrinkage of concrete and the relaxation of strands with time, time will be divided into intervals; the duration of each time interval can be made progressively larger as the concrete age increases. The stress in the strands at the end of each interval equals the initial conditions at the beginning of that time interval minus the calculated prestress losses during the interval. The stresses and deformations at the beginning of an interval are the same as those at the end of the preceding interval. With this time-step method, the prestress level can be estimated at any critical time of the life of the structure. More information on these methods is given in Tadros et al. (*19*), Abdel-Karim (*20*) and the PCI-BDM (*4*).

REFINED PRESTRESS LOSS METHODS

In these methods, individual components of prestress loss are calculated separately and the total prestress losses are then calculated by summing up the separate components. However, none of these methods accounts for composite action between deck slabs and precast girders. Because the deck concrete shrinks more and creeps less than the precast girder concrete, prestress gain rather than prestress loss may occur.

Data representing the properties of materials, loading conditions, environmental conditions, and pertinent structural details have been incorporated in the prediction formulas used for computing the individual prestress loss components. Over the years, several methods have been developed. Among these methods, are the current AASHTO-LRFD Refined method (*1*), the AASHTO Standard Specifications method (*2*), and the PCI-BDM method (*4*).

In the eleventh edition of the AASHO (currently called AASHTO) Specifications, total losses were estimated as a sum of individual components. The provisions for prestress loss that appeared in the 1973 Specifications (*21*) were first introduced in the 1971 Interim Specifications. These provisions marked the first use of a rational method of estimating loss of prestress in the AASHO/AASHTO Specifications. The following equation was introduced in the 1971 Interim Specifications:

$$\Delta f_s = ES + SH + CR_C + CR_S \tag{29}$$

where: Δf_s = total loss of prestress, ES = loss due to elastic shortening, SH = loss due to concrete shrinkage, CR_C = loss due to creep of concrete, and CR_S = loss due to relaxation of prestressing steel.

Elastic Shortening Losses

Elastic shortening losses were estimated using the following equation:

$$ES = 7f_{cgp} \tag{30}$$

where: f_{cgp} = average concrete stress at the center of gravity of the prestressing steel at time of release. The coefficient 7 in this equation was apparently an estimate of the modular ratio of E_s to E_{ci}. Losses due to elastic shortening after release of prestressing force in the AASHTO 1977 Specifications (*22*) were given by:

$$ES = \frac{E_s}{E_{ci}} f_{cgp} \tag{31}$$

where: E_s = modulus of elasticity of prestressing steel and E_{ci} = modulus of elasticity of concrete at time of release.

Shrinkage Losses

Losses due to concrete shrinkage provided in the 1973 Specifications (*21*) are given in Table 1. These values correspond to a value for ultimate shrinkage strain of approximately 550×10^{-6} for concrete and a modulus of elasticity of approximately 28,000 ksi for prestressing tendons. A reduction factor, of 0.77 was used to adjust the ultimate shrinkage strain for a V/S ratio of approximately 4 in. Correction factors for average ambient relative humidity were applied by the PCI Committee on Prestress Losses (*23*); the final values appearing in the Standard Specifications are shown in Table 2.

Starting with the twelfth edition in 1977, the AASHTO Specifications (*22*) provisions for estimating loss of prestress have remained essentially unchanged. The prestress losses formula was repeated in its original form from the 1973 Specifications (*21*), but changes in equations for estimating the components were made. These changes were first introduced into the Specifications with the 1975 Interim AASHTO Specifications. Losses due to shrinkage of concrete were given by:

$$SH = 17,000 - 150H \tag{32}$$

where: H = mean annual ambient relative humidity, in percent. This equation was developed to yield similar results as those

TABLE 1 Shrinkage losses versus humidity in 1973 AASHO Specifications (*21*)

Average ambient relative humidity (percent)	SH losses (ksi)
100 - 75	5
75 - 25	10
25 - 0	15

TABLE 2 Shrinkage loss prediction using PCI Committee method (*23*)

Humidity (percent)	Shrinkage strain	Steel modulus of elasticity (ksi)	V/S ratio factor	Humidity factor	Shrinkage loss (ksi)
100 - 75	$550x10^{-6}$	28,000	0.77	0.3	3.56
75 - 25	$550x10^{-6}$	28,000	0.77	1.0	11.86
25 - 0	$550x10^{-6}$	28,000	0.77	1.3	15.42

in the table contained in the 1973 Specifications, but eliminated the abrupt change in shrinkage loss between the three humidity ranges given in the PCI Committee Report (*23*). Figure 4 depicts the shrinkage losses predicted by the AASHTO 1977 Specifications and provides a comparison with the 1973 Specifications.

Creep Losses

Losses due to creep of concrete in the 1973 AASHO Specifications were given by:

$$CR_C = 16f_{cd} \tag{33}$$

where: f_{cd} is the average concrete compressive stress at the center of gravity of the prestressing steel under full dead load. The factor 16 is approximately the product of a modular ratio of 7 and an ultimate creep coefficient of 2.3.

Losses due to creep of concrete in the 1975 AASHTO Interim Specifications were:

$$CR_C = 12f_{cgp} - 7f_{cds} \tag{34}$$

where: f_{cgp} is as defined for elastic shortening losses and f_{cds} = concrete tensile stress at the center of gravity of the prestressing steel due to all dead loads except the self weight of the beam.

Relaxation Losses

The 1973 AASHO Specifications did not provide an equation for estimation of relaxation losses for low-relaxation strands; it provided the following equation for stress-relieved strands.

$$CR_S = 20,000 - 0.125(SH + ES + CR_C) \tag{35}$$

The constants in the above equation can be derived if one assumes an intrinsic relaxation loss of approximately 10% of f_{pi}, and a relaxation reduction factor of one-eighth of the combined SH, ES, and CR_C values, to account for the effects of member shortening on the intrinsic relaxation loss. The 1975 AASHTO gave the following formulas for stress-relieved and low-relaxation strands.

(a) For stress-relieved strands, losses due to relaxation were given by:

$$CR_S = 20,000 - 0.4ES - 0.2(SH + CR_c) \tag{36}$$

(b) For low-relaxation strands, losses due to relaxation were given by:

$$CR_S = 5,000 - 0.1ES - 0.05(SH + CR_C) \tag{37}$$

The first edition of AASHTO-LRFD Bridge Design Specifications (*24*) was adopted and published in June 1994. In this edition, the refined method of estimating time-dependent losses was basically the same as the one used in the previously published AASHTO Standard Specifications. However, relaxation loss after transfer for low-relaxation strands was taken as 30% of the relaxation loss for stress-relieved strands.

The current AASHTO-LRFD Refined Estimates method computes the prestress losses in members constructed and prestressed in a single stage, relative to the stress immediately before transfer, as a sum of individual loss components:

$$\Delta f_{pT} = \Delta f_{pES} + \Delta f_{pSR} + \Delta f_{pCR} + \Delta f_{PR2} \tag{38}$$

where: Δf_{pT} is total loss of prestress, Δf_{pES} is loss due to elastic shortening, Δf_{pSR} is loss due to concrete shrinkage, Δf_{pCR} is loss due to creep of concrete, Δf_{PR2} is loss due to relaxation *n* of prestressing steel.

The elastic shortening loss in pretensioned members is given by:

$$\Delta f_{pES} = f_{cgp} E_p / E_{ci} \tag{39}$$

where: E_p is modulus of elasticity of prestressing strands and E_{ci} is modulus of elasticity of concrete at transfer.

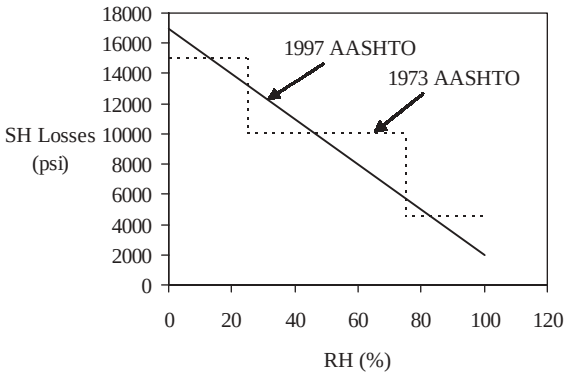

Figure 4. Losses due to concrete shrinkage.

Loss due to shrinkage of concrete is taken as a function of the relative humidity only, and does not take into account the variability of shrinkage with other parameters as indicated in Section 5.4.2.3.3 of the AASHTO-LRFD. Shrinkage loss is estimated by the following equation:

$$\Delta f_{pSR} = 17.0 - 0.15\,H \quad (40)$$

where: H = mean annual ambient relative humidity.

Loss due to creep may be taken as:

$$\Delta f_{pCR} = 12.0\,f_{cgp} - 7.0\,\Delta f_{cdp} \geq 0 \quad (41)$$

where: Δf_{cdp} = change in concrete stress at the center of gravity of the prestressing strands due to the permanent loads, with the exception of the load acting at the time the prestressing force is applied. Values of Δf_{cdp} should be calculated at the same section or at the sections for which f_{cgp} is calculated.

The relaxation after transfer is:

$$\Delta f_{pR2} = 6.0 - 0.12\,\Delta f_{pES} - 0.06\left(\Delta f_{pSR} + \Delta f_{pCR}\right) \quad (42)$$

Other methods of prestress losses prediction such as the PCI-BDM method (*4*), CEB-FIP Model Code method (*25*), Ontario Bridge Design Code method (*26*), ACI-ASCE Committee 423 method (*27*), Concrete Technology Associates (CTA) method (*28*), Modified Rate of Creep method (*29*), and Tadros et al. method (*19*) and are given in Appendix C.

LUMP-SUM METHODS

Lump-sum methods represent average conditions. They are useful in preliminary design, but the estimated loss should be recalculated in the final design. According to the current AASHTO-LRFD Approximate method, prestress loss for girders with 270 ksi low-relaxation strands is given by the following formulas:

$19 + 4\,PPR - 4(ksi)$ for Box Girders; (43)

$26 + 4\,PPR - 6(ksi)$ for Rectangular Beams and Solid Slabs; (44)

$33\left[1 - 0.15(f'_c - 6)/6\right] + 6\,PPR - 6(ksi)$ for I-Girders; (45)

$33\left[1 - 0.15(f'_c - 6)/6\right] + 6\,PPR - 8(ksi)$ for Double Tees and Voided Slabs; (46)

where: PPR is the partial prestress ration, which normally = 1 for precast pretensioned members. These formulas reflect trends obtained from a computerized time-step analysis of different beam sections for an ultimate concrete creep coefficient ranging from 1.6 to 2.4, ultimate concrete shrinkage strain ranging from 0.0004 to 0.0006, and relative humidity ranging from 40% to 100%.

This procedure recognizes reduction in prestress loss for concrete compressive strengths above 6.0 ksi. However, it does not recognize higher prestress levels for higher concrete strengths. It assumes, without justification, a large difference in prestress loss prediction for box girders and I-girders, and conversely no difference in loss values for vastly different product types: I-girders, double tee beams, and voided slabs.

Based on a review of available information, it was evident that additional research is required to establish realistic estimates of modulus of elasticity, creep, and shrinkage of high-strength concrete. The AASHTO-LRFD provisions need to be updated (1) to consider high-strength concrete in Sections 5.4.2.3 and 5.4.2.4, (2) to improve the prestress loss calculation methods of Section 5.9.5 for high-strength concrete, and (3) to link the material property formulas of Sections 5.4.2.3. and 5.4.2.4 with prestress loss prediction formulas of Section 5.9.5 into one integrated approach. Both detailed and approximate estimation of prestress losses are needed in design depending on the design stage and the type of member.

CHAPTER 3

RESEARCH RESULTS

INTRODUCTION

This chapter presents the prediction formulas of modulus of elasticity, creep, and shrinkage of high-strength concrete. The experimental basis for the proposed prediction formulas is given. Seven bridge girders in the states of Nebraska, New Hampshire, Texas, and Washington were instrumented for prestress loss measurement. Two methods are proposed for the estimation of prestress losses, a detailed method and an approximate method. The laboratory and field measurements were used to verify and calibrate the prediction methods.

In applying the proposed prediction methods, two alternatives for the input material properties were used. The first alternative was to use the measured material properties for the bridge girders that had been instrumented for prestress loss. The second alternative was to use specified and predicted material values that would normally be available to designers. In the latter alternative, specified concrete strength, assumed construction schedule, and the corresponding estimated modulus of elasticity, creep, and shrinkage were input into the loss prediction formulas. Comparisons were also given between measured loss values and those predicted by other methods in order to demonstrate the improvements offered by the proposed method.

Formulas presently used by various codes for computing concrete modulus of elasticity, shrinkage, and creep have been empirically established based primarily on data for normal-strength concrete with compressive strength up to 6.0 ksi (*30*). There has been recent interest in reevaluating these formulas and extending their applicability to concrete strengths between 8.0 and 12.0 ksi. Experimental work included both laboratory tests and field measurements.

This section covers the material testing program of concrete mixes used in Nebraska, New Hampshire, Texas, and Washington for pretensioned concrete girders and presents the results of previously reported research. For each material property, a summary of measured values is presented, followed by a proposed estimation method. A record of all data collected in this research is given in the appendixes (which are not published herein) for the various parameters evaluated.

EXPERIMENTAL PROGRAM

The materials testing program consisted of laboratory material tests conducted at the University of Nebraska (laboratory tests) and material tests conducted at girder production plants and at construction sites (on-site tests).

Laboratory Material Tests

The precast concrete producer in each of the four states provided three concrete mix designs and furnished raw materials for making and testing specimens at the University of Nebraska. One of the mixes represented the concrete intended to be used in the instrumented bridge girders. In addition, each participating state highway agency arranged for shipping raw materials and for producing this mix in laboratories that provided one mix design for the normal-strength concrete used in bridge deck construction. Proportions of state highway agency mixes are given in Tables 3 through 6. Additional details are given in Appendix D.

Twenty-seven 4 in. by 8 in. concrete cylinders were made for each of the three high-strength concrete mixes and for the normal-strength concrete deck mix. For each concrete mix, a set of three cylinders was tested for concrete compressive strength and modulus of elasticity at each of the following ages—1, 3, 7, 14, 28, 56, 90, 128, and 256 days. Shrinkage measurements were performed using three 4 in. by 4 in. by 24 in. specimens per concrete mix design. A total of 12 specimens were required for testing three high-strength mixes for the girder mix and one normal-strength mix for the deck. A total of 48 specimens were tested.

Four 4 in. by 4 in. by 24 in. specimens were used to obtain the creep measurements for each of the three girder mixes. Three specimens were loaded at the age of 1 day, and one specimen was loaded at 56 days. Twelve specimens were required for the three high-strength concrete mixes produced for each state. A total of 48 creep tests were performed.

On-Site Materials Testing

In addition to the laboratory specimens, similar specimens were made and monitored in the field. They were subjected to the same curing and environmental conditions as the bridge girders. The on-site testing program consisted of the following. Eighteen 4 in. by 8 in. cylinders were produced at each of the four plants. Sets of three cylinders were tested for concrete compressive strength and modulus of elasticity at the ages of 1, 3, 7, 14, 28, and 56 days. A set of three 4 in. by 4 in. by

24 in. shrinkage specimens were produced from the same mix design used for the pretensioned bridge girders; measurements were taken for 3 months. The results from the laboratory tests were compared with those obtained from various sites, to determine the effects of the various curing and environmental conditions.

Mixing and Sampling Procedures

Concrete mixing in the laboratory was done using 5.5-cf batches in a 9-cf capacity rotary drum. ASTM C192 (*31*), "Standard Practice for Making and Curing Concrete Test Specimens in the Laboratory" was followed for making the

TABLE 3 Mix properties for Nebraska girders and deck

Mix designation		NE09G	NE10G	NE12G	NE04D
Crushed limestone	Size (in.)/Type	0.75, ASTM Grade 5	0.5, ASTM Grade 5	0.375, ASTM Grade 5	1.5, ASTM Grade 5
	Quantity (pcy)	1530	1860	1913	883
Sand and gravel	Size/Type	Nebraska 47B	None	Nebraska 47B	Nebraska 47B
	Quantity (pcy)	765	None	933	2039
Sand	Size/Type	ASTM C33	ASTM C33	None	None
	Quantity (pcy)	765	990	None	None
Potable water	Quantity (pcy)	250	240	254	263
Cement type	Type	III	I	III	I
	Quantity (pcy)	705	750	680	658
Silica fume	Quantity (pcy)	None	50	None	None
Fly ash	Type	None	Class C	Class C	None
	Quantity (pcy)	None	200	320	None
High-range water reducer	Type	Prokrete N	Prokrete N	WRDA 19	Prokrete N
	Quantity (oz/100 lb of binder)	30	30	34.2	5-14
Water-reducer	Type	Conchem SP-L	Type A	None	Conchem SP-L
	Quantity (oz/100 lb of binder	10-20	4	None	3-5
Retarder	Type	None	None	Daratar 17	None
	Quantity (oz/100 lb of binder)	None	None	4	None
Air content	Amount (%)	5-7	5-7	5-7	6

TABLE 4 Mix properties for New Hampshire girders and deck

Mix designation		NH10G	NH11G	NH12G	NH04D
Crushed river gravel	Size (in.)/Type	0.75, ASTM Grade 5	0.75, ASTM Grade 5	0.75, ASTM Grade 5	1.0, ASTM Grade 5
	Quantity (pcy)	1850	1850	1850	1805
Sand	Quantity (pcy)	940	925	950	1205
Potable water	Quantity (pcy)	250	250	242	250
Cement	Type	II	II	II	II
	Quantity (pcy)	800	800	800	658
Silica fume	Quantity (pcy)	56	75	100	None
Fly ash	Type	None	None	None	Class F
	Quantity (pcy)	None	None	None	132
High-range water reducer	Type	Adva Flow	Adva Flow	Adva Flow	None
	Quantity (oz/cy)	51.4	53	63	None
Water-reducer	Type	Mira	Mira	Mira	Daracem 100
	Quantity (oz/cy)	51.4	53	63	118
Air entraining admixture	Type	Darex II	Darex II	Darex II	Darex II
	Quantity (oz/cy)	3	3	4	10
Corrosion inhibitor	Type	DCI-S	DCI-S	DCI-S	None
	Quantity (oz/cy)	33	33	33	None

test specimens. The concrete cylinders were made according to ASTM C192 and cured in the laboratory curing room at an ambient temperature of about 73°F for 24 hours. The cylinders were then de-molded and returned to the curing room until the test age. Creep and shrinkage specimens were cast for each of the three girder concrete mixes. After placement and consolidation, the surface was screeded and trowel finished and then covered with burlap. The forms were removed after 24 hours. The specimens were then left to cure at a room ambient temperature of 73°F.

TABLE 5 Mix properties for Texas girders and deck

Mix designation		TX08G	TX09G	TX10G	TX04D
Crushed limestone	Size (in.)/Type	0.75, ASTM Grade 5	0.75, ASTM Grade 5	0.75, ASTM Grade 5	None
	Quantity (pcy)	2029	2011	1975	None
Gravel	Size/Type	None	None	None	1.5, River gravel
	Quantity (pcy)	None	None	None	1811
Sand	Size/Type	Natural river sand	Natural river sand	Natural river sand	Natural river sand
	Quantity (pcy)	1237	1340	1237	1192
Potable water	Quantity (pcy)	206	192	197	244
Cement	Type	III	III	III	I
	Quantity (pcy)	611	564	705	611
Silica fume	Quantity (pcy)	None	None	None	None
Fly ash	Type	None	None	None	Class C
	Quantity (pcy)				152
High-range water reducer	Type	Rheobuild 1000	Rheobuild 1000	Rheobuild 1000	None
	Quantity (oz/100 lb of binder)	27	21	29	None
Water-reducer	Type	Pozzolith 300R	Pozzolith 300R	Pozzolith 300R	None
	Quantity (oz/100 lb of binder	3.5	3.0	3.5	None
Retarder	Quantity (oz/100 lb of binder)				6
Air content	Amount (%)	2	2	2	2

TABLE 6 Mix properties for Washington girders and deck

Mix designation		WA10G	WA11G	WA12G	WA04D
Gravel	Size/Type	0.75, ASTM Grade 5	0.75, ASTM Grade 5	0.75 ASTM Grade 5	1.0, ASTM Grade 5
	Quantity (pcy)	2010	1877	1959	1810
Sand	Size/Type	Natural river sand	Natural river sand	Natural river sand	Natural river sand
	Quantity (pcy)	1235	1383	1204	1046
Potable water	Quantity (pcy)	219	217	213	263
Cement	Type	III	III	III	I-II
	Quantity (pcy)	705	658	752	660
Silica fume	Quantity (pcy)	None	None	50	None
Fly ash	Type	None	None	None	Class F
	Quantity (pcy)	None	None	None	75
High-range water reducer	Type	Advacast	Advacast	Advacast	None
	Quantity (oz/100 lb of binder)	7	7	7	None
Water-reducer	Type	WRDA-64	WRDA-64	WRDA-64	Pozz-80
	Quantity (oz/100 lb of binder)	4	4	4	6
Air content	Amount (%)	1.5	1.5	1.5	2

MODULUS OF ELASTICITY

Experimental Results

The modulus of elasticity of concrete was determined in accordance with ASTM C469 (*32*). At any given concrete age, the reported modulus was the average of the results of two cylinders. The applied loads and the longitudinal strains were recorded until the applied load reached 40% of the concrete ultimate strength at the age of loading.

Appendix E shows the measured compressive strength and modulus of elasticity. Figure 5 shows modulus of elasticity versus compressive strength test results reported in the literature and those produced in this study. The figure shows the high variability in the experimental data. This variability may be attributed to a combination of factors including the degree of dryness of the specimens at the time they were tested, mixture proportions, properties of the concrete mix ingredients, method of testing, speed of load application, equipment accuracy, and operator experience.

Proposed Formula

The prediction formula given in both the ACI-318 and the AASHTO Specifications provided better correlation with the test results than those obtained from the ACI-363 formula. Neither prediction method accounted for the effects of aggregate type on modulus of elasticity and strength. Figure 6 shows the relationship between unit weight and compressive strength. These data indicate that nearly all the high-strength mixes included in this investigation had a unit weight less than 0.155 kcf. The relationship shown in the figure can be represented by the following formula, which accordingly has an upper limit of 0.155 kcf:

$$w_c \text{ in (kcf)} = 0.140 + \frac{f_c'}{1000}$$

$$\text{but not greater than } 0.155 \text{ kcf} \qquad (47)$$

The unit weight formula is proposed to be incorporated into modulus of elasticity calculation. Also, it is proposed that two factors be included: K_1 representing the difference between national average and local average (if tests results with local materials are available), and K_2 representing whether an upper-bound or a lower-bound value is desired in the calculations. An upper-bound value would be conservative to use for crack control analysis and a lower-bound value would be appropriate for prestress loss and deflection calculations. The proposed formula for modulus of elasticity is:

$$E_c = 33{,}000 K_1 K_2 \left(0.140 + \frac{f_c'}{1000}\right)^{1.5} \sqrt{f_c'} \qquad (48)$$

A correction factor $K_1 = 1.0$ corresponds to an equal average of all predicted values and all measured values of the modulus of elasticity. Individual averages of data groups from each of the participating states correspond to K_1 values other than unity, representing the effect of local material variability. The correction factor K_2 is based on the 90th percentile upper-bound and the 10th percentile lower-bound for each of the four states and for the entire data bank. The K_1 and K_2 values determined in this research are given in Table 7. The table also shows that the ratio of predicted to experimental values is closest to unity, when the proposed Equation 48 is used, in

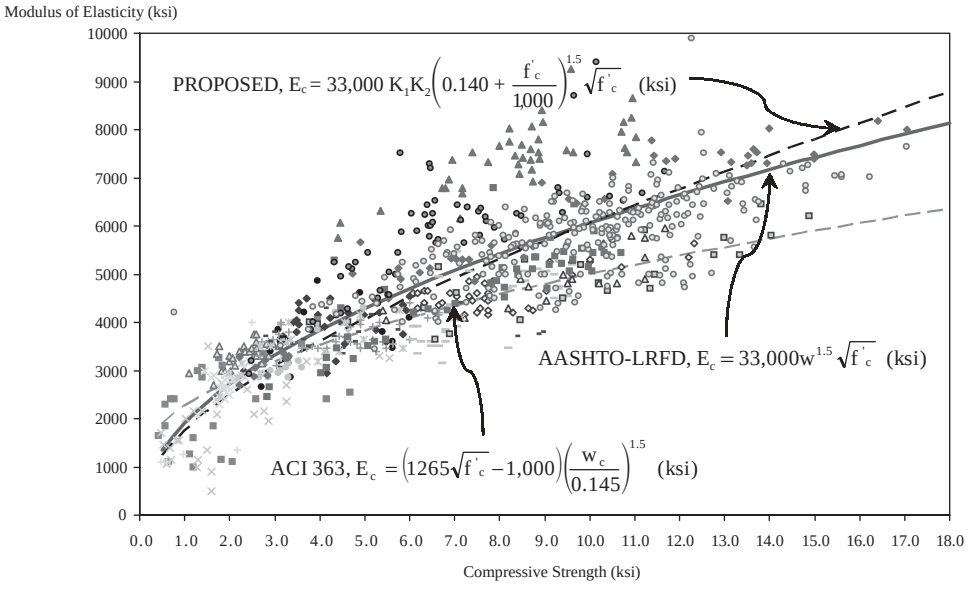

Figure 5. Modulus of elasticity versus compressive strength.

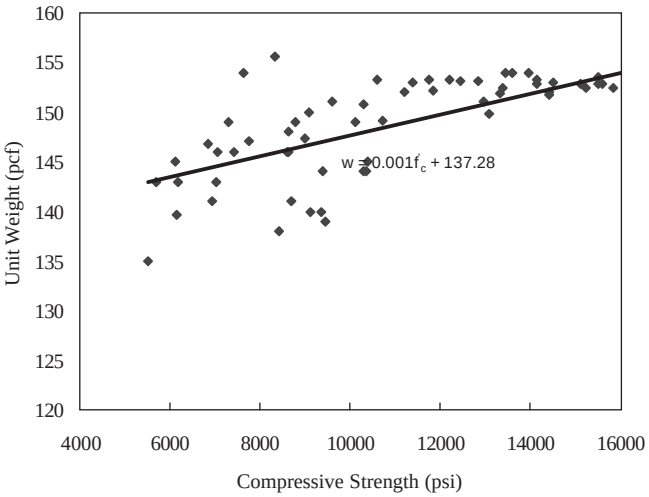

Figure 6. Relationship between unit weight and compressive strength of concrete.

comparison to the AASHTO-LRFD formula. Consider a Nebraska mix with a specified compressive strength of 8.0 ksi. According to Table 7, the value of $K_1 = 0.975$, the upper-bound $K_2 = 1.211$ and the lower-bound $K_2 = 0.788$. The predicted average, upper-bound, and lower-bound, values of the modulus of elasticity for this concrete strength may be estimated as follows:

$$\text{Average } E_c = 33{,}000(0.975)\left(0.140 + \frac{8}{1000}\right)^{1.5}\sqrt{8}$$

$$= 5{,}182 \text{ ksi}$$

$$\text{Upper-bound } E_c = 33{,}000(0.975)(1.211)\left(0.140 + \frac{8}{1000}\right)^{1.5}\sqrt{8} = 6{,}275 \text{ ksi}$$

$$\text{Lower-bound } E_c = 33{,}000(0.975)(0.788)\left(0.140 + \frac{8}{1000}\right)^{1.5}\sqrt{8} = 4{,}083 \text{ ksi}$$

Figure 7 shows the measured values versus those predicted using the proposed method. It demonstrates that the proposed method produces an accurate prediction of the average, lower-bound, and upper-bound, values of the modulus of elasticity of concrete. Appendix E contains additional comparisons between the proposed prediction method, the AASHTO-LRFD method, and other methods. Figure 8 illustrates a comparison between test results for a set of high-strength concrete mixes used in Washington State, with those predicted by the proposed formula and the AASHTO-LRFD formula. The significant difference between the two prediction methods illustrates the proposed formula's ability to more accurately account for local materials and for high-strength concrete.

EXPERIMENTAL SHRINKAGE RESULTS

Shrinkage specimens were cast at the same time and cured under the same conditions as the creep specimens. Readings were taken in parallel with the creep tests for each mix to compare the time-dependent strain of loaded and unloaded specimens. The creep and shrinkage specimens in this project had a V/S ratio of 1.0. The specimens were at an ambient relative humidity of 35% to 40%. Demountable mechanical (DEMEC) gages were used at a spacing of about 8 in. to measure the surface strains in the longitudinal direction. Five DEMEC points were used on each of two surfaces of each specimen. The DEMEC points were spaced at 4 in. This allowed for 3-to-8-in. gage lengths per surface, or 6 readings per specimen. Shrinkage readings were taken daily for the first week, weekly for the first month, and monthly for about 1 year. Figures 9 through 12 present the measured shrinkage strains of the

TABLE 7 K-values and predicted-to-measured ratios of modulus of elasticity of concrete

	Proposed K_1 and K_2			Ratio of Predicted to Measured	
	K_1	90th percentile K_2	10th percentile K_2	Proposed	AASHTO-LRFD
Nebraska NE09G, NE10G, NE12G	0.975	1.211	0.788	1.000	1.037
New Hampshire NH10G, NH11G, NH12G	0.911	1.123	0.878	1.000	1.122
Texas TX08G, TX09G, TX10G	1.321	1.115	0.886	1.000	0.768
Washington WA10G, WA11G, WA12G	1.154	1.182	0.817	1.000	0.889
All data	1.000	1.224	0.777	1.020	1.037

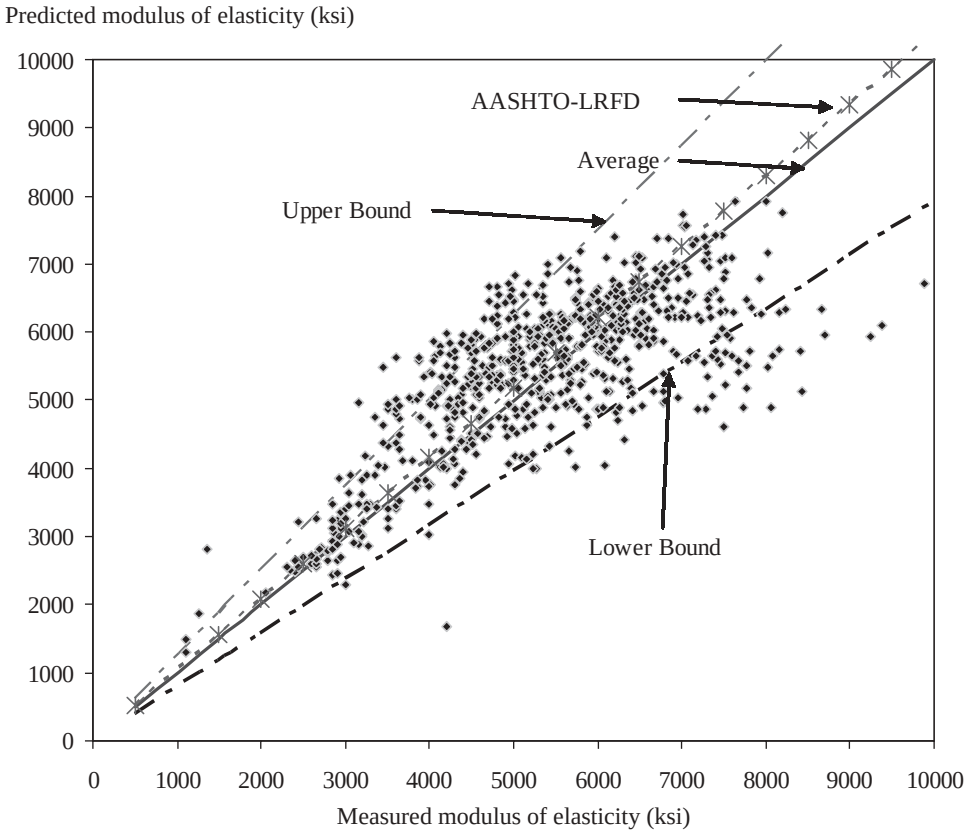

Figure 7. Predicted versus measured values of modulus of elasticity, nationwide experiments with wide strength range.

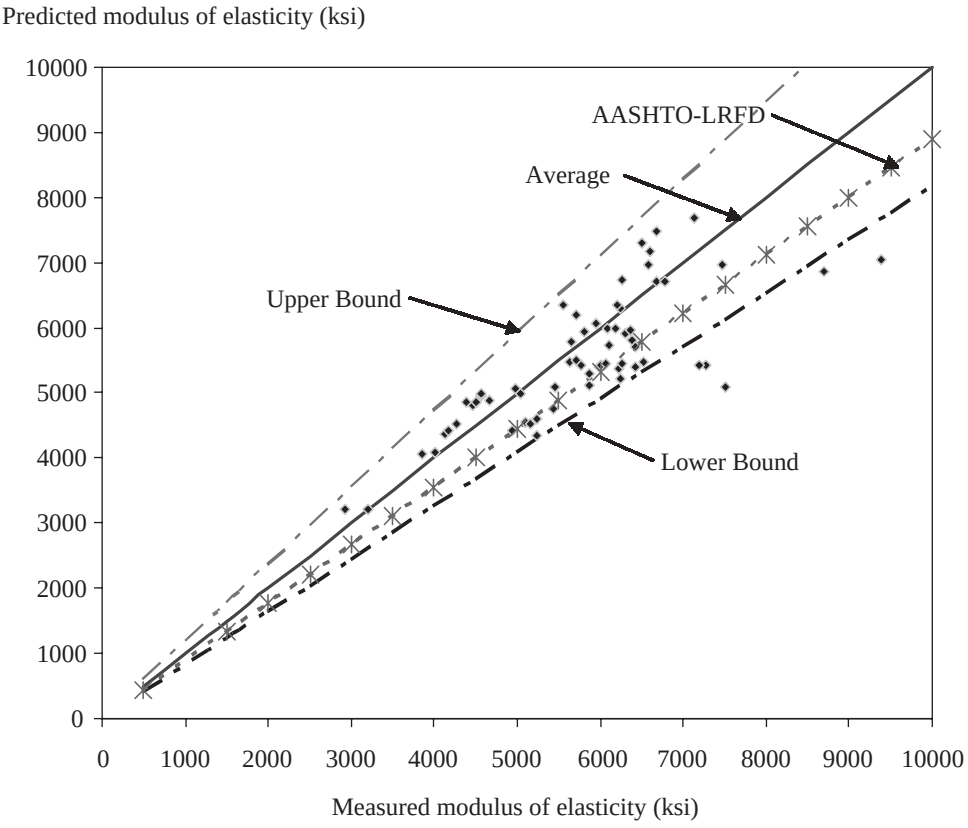

Figure 8. Predicted versus measured values of modulus of elasticity, Washington State high-strength concrete mixes.

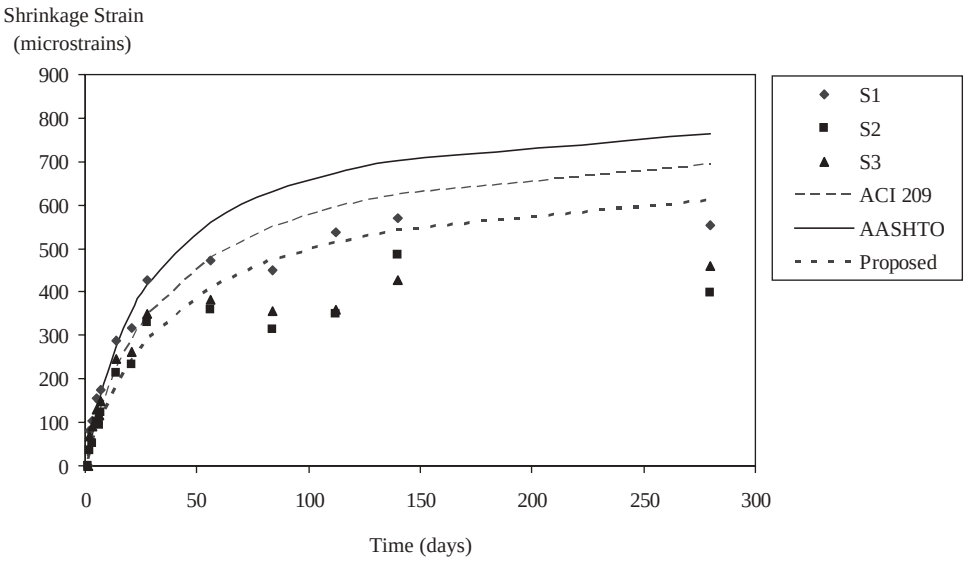

Figure 9. Shrinkage for Nebraska mix NE09G-S.

specimens produced in the laboratory. Appendix F contains data for all test specimens. The ratio of estimated shrinkage strains to measured values, with the AASHTO-LRFD and the ACI-209 formulas, are also shown in Table 8. It can be seen that the predicted shrinkage strains are generally much higher than the measured quantities confirming the need for improved shrinkage prediction formulas.

EXPERIMENTAL CREEP RESULTS

Creep tests were performed at the laboratory on the 12 high-strength concrete mixtures in accordance with the ASTM Standard C 512 (*33*). Similar to the shrinkage strain measurements, DEMEC mechanical strain gages were used. A total of four specimens were cast for each mix. Three of these specimens were loaded at the age of 1 day, and the fourth was loaded at the age of 56 days. The specimens were then loaded at an intensity of not more than 40% of the compressive strength at the age of loading.

The initial strain readings were taken immediately before and after loading. Creep measurements were then taken daily for the first week, weekly for the first month and monthly for about 1 year. The creep coefficients were calculated from the measured total strains, elastic strains, and shrinkage strains. Figures 13 through 16 show the test results for the four mixes

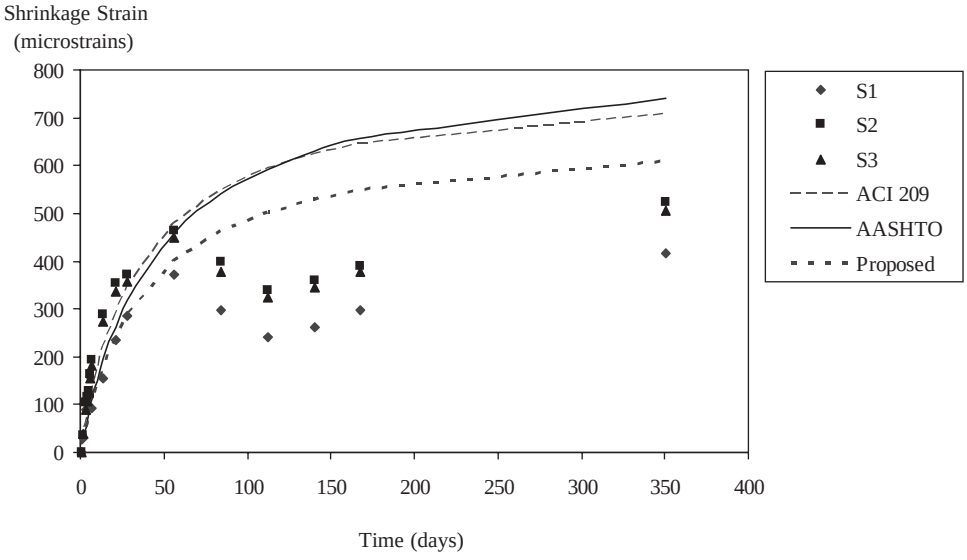

Figure 10. Shrinkage for New Hampshire mix NH10G-S.

of the instrumented girders. The calculated creep coefficients of the 12 high-strength concrete mixtures are given in Appendix G. Table 9 shows measured-to-estimated creep ratios using AASHTO-LRFD and ACI-209. It can be seen that the estimated creep coefficients are much higher than the measured quantities. The average of estimated to measured ratios, with the ACI-209 and the AASHTO-LRFD formulas, are 179% and 161%, respectively. It appears that the LRFD method, which includes a correction factor for concrete strength, is more accurate than the ACI-209 method; more comparisons are shown in the appendix.

These large differences in creep coefficients can have a substantial effect on the long-term prestress losses estimation. Similar observations were made in previous research (Huo et al. [*11*]), (Mokhtarzadeh [*34*]), (Gross [*35*]). It was noted that the creep strains developed rapidly during the early age then exhibited very little change after several months, see Figures 13 through 16.

PROPOSED CREEP AND SHRINKAGE CORRECTION FACTORS

Correction factors are used in various prediction methods to modify the ultimate values of creep coefficient, ψ (t, ti), and shrinkage strain, ϵ_{sh}, of concrete for any period of time

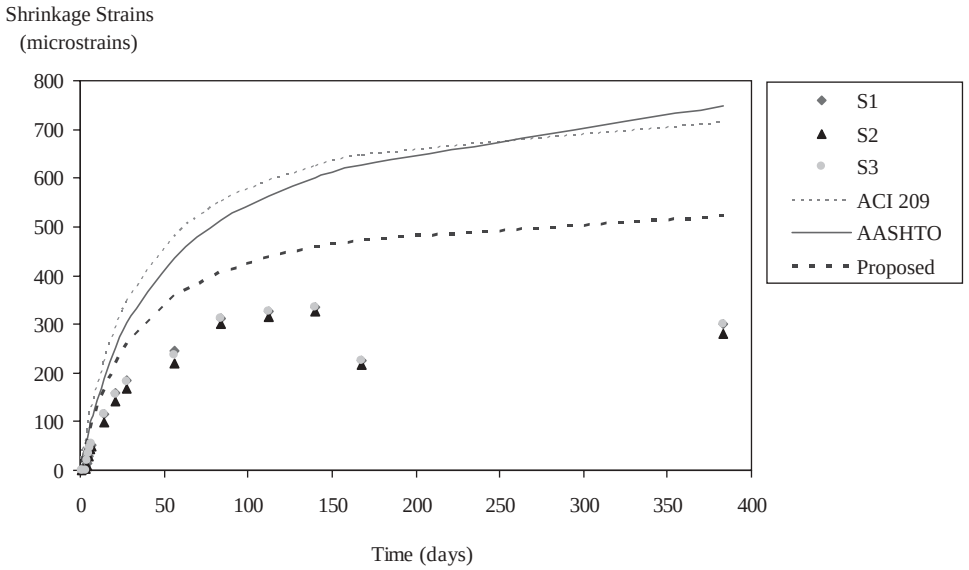

Figure 11. Shrinkage for Texas mix TX09G-S.

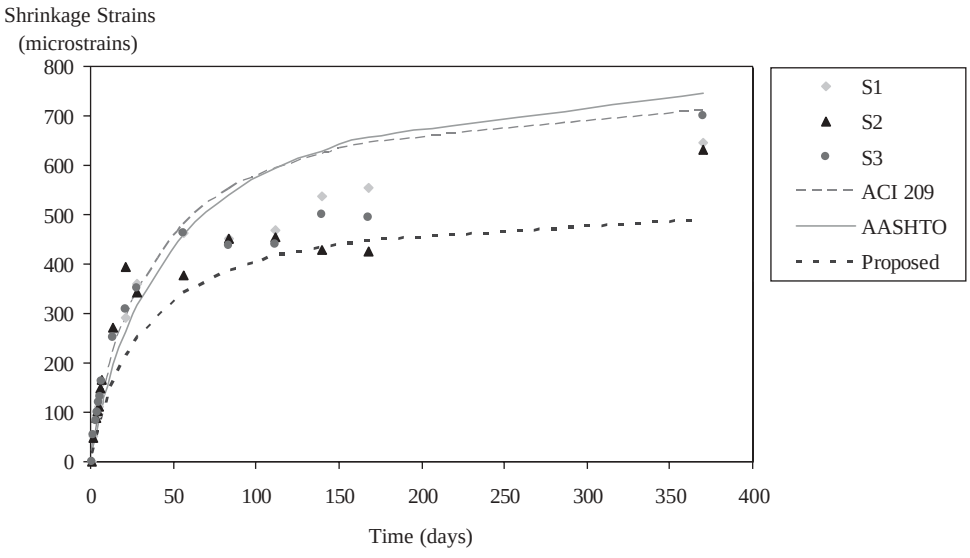

Figure 12. Shrinkage for Washington mix WA10G-S.

TABLE 8 Ratios of predicted-to-measured shrinkage strain for laboratory-stored specimens

Mix	Ratio of predicted-to-measured shrinkage strain	
	ACI-209	AASHTO-LRFD
Nebraska, NE09G, NE10G, NE12G	1.75	1.91
New Hampshire NH10G, NH11G, NH12G	1.13	1.27
Texas TX08G, TX09G, TX10G	2.26	2.60
Washington WA10G, WA11G, WA12G	1.05	1.18
Combined data	1.55	1.74

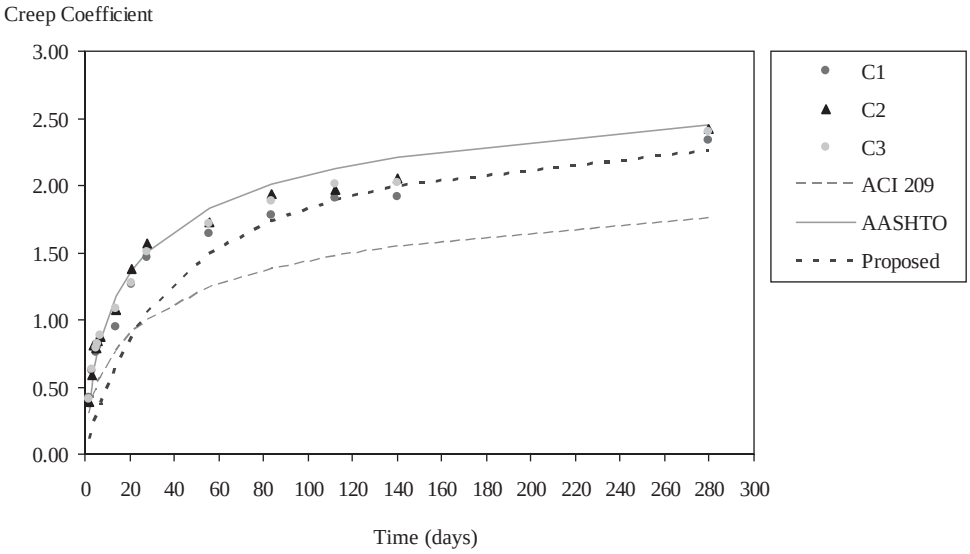

Figure 13. Creep for Nebraska mix NE09G-01 loaded at 1 day.

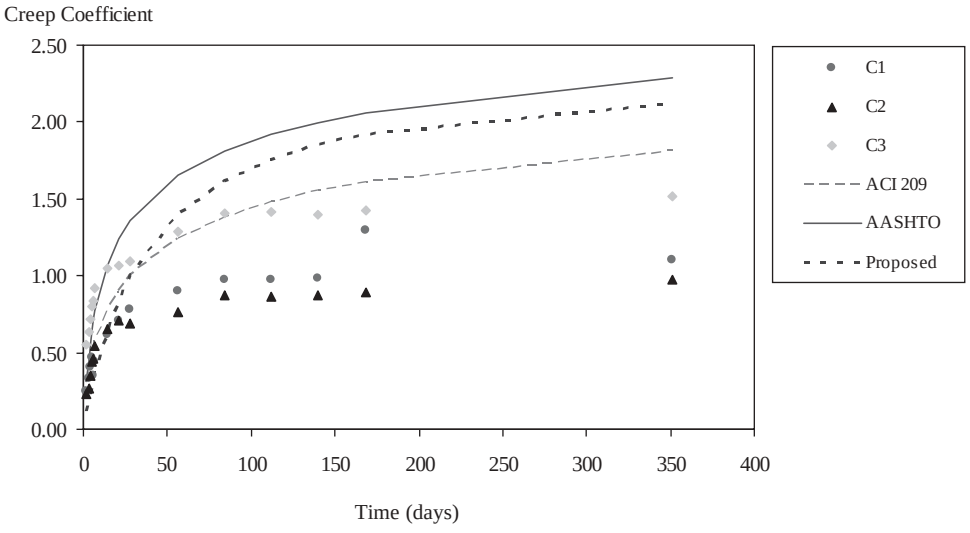

Figure 14. Creep for New Hampshire mix NH10G-01 loaded at 1 day.

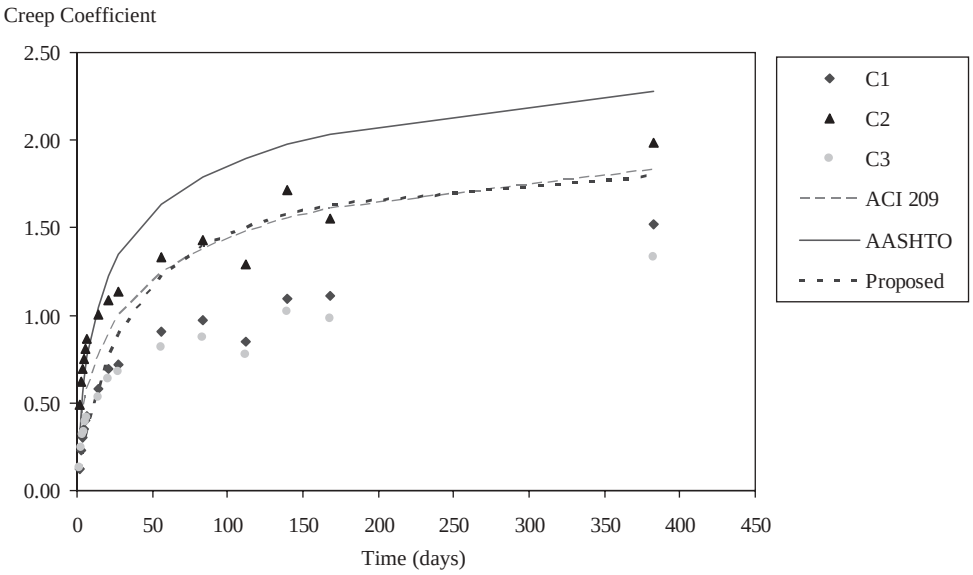

Figure 15. Creep for Texas mix TX09G-01 loaded at 1 day.

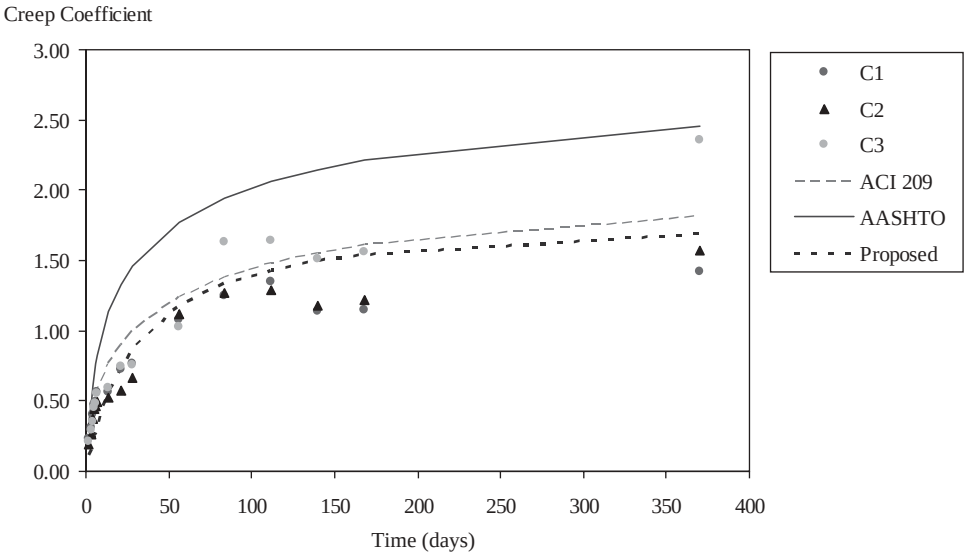

Figure 16. Creep for Washington mix WA10G-01 loaded at 1 day.

TABLE 9 Ratios of predicted-to-measured creep coefficients for laboratory-stored specimens

Mix	Ratio of predicted-to-measured creep coefficient	
	ACI-209	AASHTO-LRFD
Nebraska NE09G, NE10G, NE12G	1.69	1.31
New Hampshire NH10G, NH11G, NH12G	1.50	1.37
Texas TX08G, TX09G, TX10G	2.06	1.89
Washington WA10G, WA11G, WA12G	1.89	1.88
Average of all data	1.79	1.61

and for conditions other than the so-called "standard conditions." These standard conditions, in some methods, referred to laboratory specimen sizes and relative humidity conditions, which differed considerably from average bridge member sizes and environmental conditions. For example, for the ACI-209 method, a relative humidity of 40% is considered a standard condition, while most of the U.S. bridges are subject to an approximate average humidity of 70%. Another example is the V/S ratio of about 1.5 in. being considered representative of a standard member size in the LRFD creep and shrinkage prediction formulas, while most bridge members have an average V/S ratio of about 3.5 in. These uncommon conditions account for some of the apparently high creep coefficient and shrinkage strain given in the AASHTO-LRFD and ACI-209 formulas.

In the following presentation, factors are introduced to account as much as possible for the average conditions commonly encountered in practices (i.e., 70% annual average ambient relative humidity, V/S ratio of 3.5 in., loading age of 1 day for precast pretensioned members and 7 days for cast-in-place deck slabs, and accelerated curing for 1 day or moist curing for 7 days.)

Relative Humidity Correction Factor

Figure 17 shows the correction factor for a range of relative humidity when using the AASHTO-LRFD, the PCI-BDM, and the ACI-209 formulas to estimate creep coefficient and shrinkage strain. This figure shows essentially two trends when normalized to a default value of 1.0 at 70% relative humidity. Figure 18, adopted from AASHTO-LRFD (Figure 5.4.2.3.3-1), shows the range of the annual average ambient relative humidity for various parts of the United States and Canada. For the range of 30% to 80% ambient relative humidity encountered in the United States, one formula may be applied to shrinkage strain and another may be used for creep coefficient:

$$\text{Shrinkage: } k_{hs} = 2.00 - 0.0143H \quad (49)$$

$$\text{Creep: } k_{hc} = 1.56 - 0.008H \quad (50)$$

where: H = relative humidity, in percent.

Volume-to-Surface Ratio (Size) Correction Factor

Relatively thick members do not dry as easily as thin members when they are subjected to the ambient air. This effect is accounted for by using the V/S ratio factor. Member size affects short-term creep and shrinkage much more than it does ultimate value. Because the ultimate values are of primary importance for most bridges (except segmentally constructed box girder bridges), the V/S ratio factor formula can be greatly simplified when ultimate prestress loss and final concrete bottom fiber stress are the primary design values. The V/S ratio of the member may be computed as the ratio of cross-sectional area to the perimeter exposed to the environment.

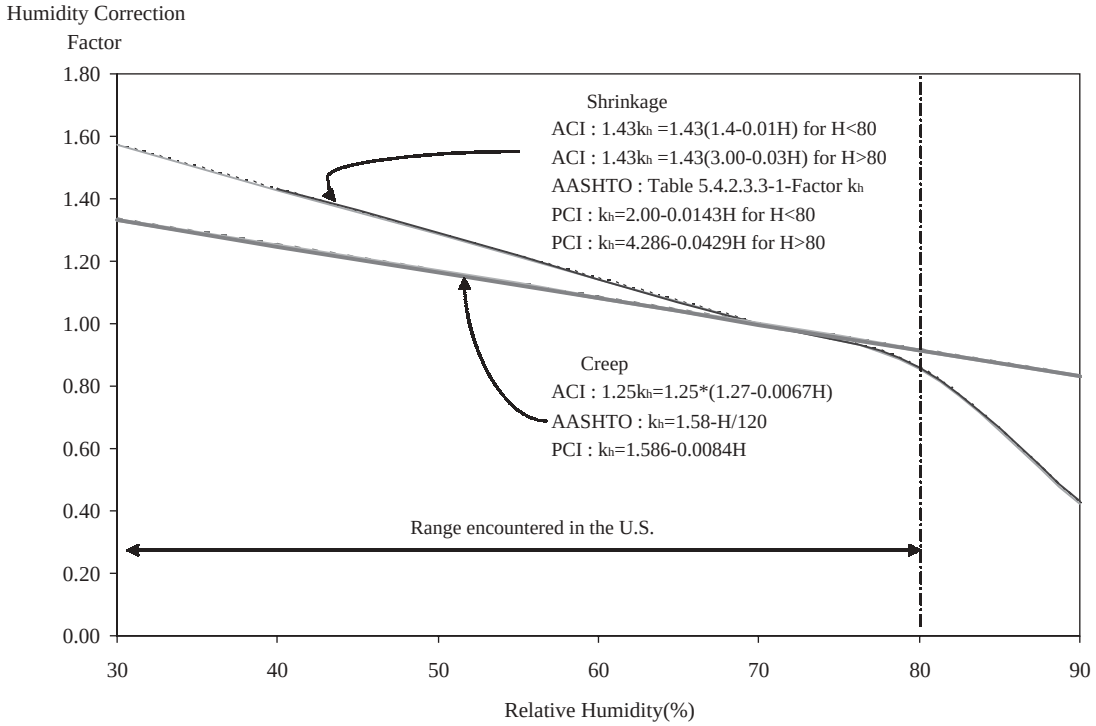

Figure 17. Humidity correction factor for the various prediction methods.

Figure 18. Average annual ambient relative humidity in percent, according to AASHTO-LRFD (1).

Figure 19 shows comparisons of the correction factor for a range of V/S obtained with the AASHTO-LRFD, the PCI-BDM, and the ACI-209 formulas. The AASHTO-LRFD formula produces negative values of correction factor for thick slabs and V/S ratios more than 11.32 in. All values shown in this figure were normalized to a default value of 1.0 for a V/S ratio of 3.5 in., which is equivalent to an I-girder web width of 7 in. The three formulas produce very close results when used for precast concrete stemmed members with a V/S ratio of 3 in. to 4 in. The simplest of these formulas, AASHTO-LRFD shrinkage factor, will be adopted here. Thus, the member size correction factor for both creep and shrinkage is as follows:

$$k_s = \frac{1064 - 94V/S}{735} \tag{51}$$

Loading Age Correction Factor

The AASHTO-LRFD and the ACI-209 prediction formulas were examined in computing the loading age correction factor, k_{la}, for both accelerated and moist curing. Figure 20 presents the correction factor for a range of loading ages normalized to a value of 1.0 for 1 day of accelerated curing or 7 days of moist curing. This figure indicates that the variation of the correction factor with loading age follows a similar trend for both types of curing. Thus, the AASHTO-LRFD formula should continue to be used for both types of curing, with a shift in datum used to represent the difference in curing type. Accordingly, the following equation may be used:

$$k_{la} = t_i^{-0.118} \tag{52}$$

where: t_i = age of concrete when load is initially applied for accelerated curing and age of concrete (in days) minus 6 days for moist curing.

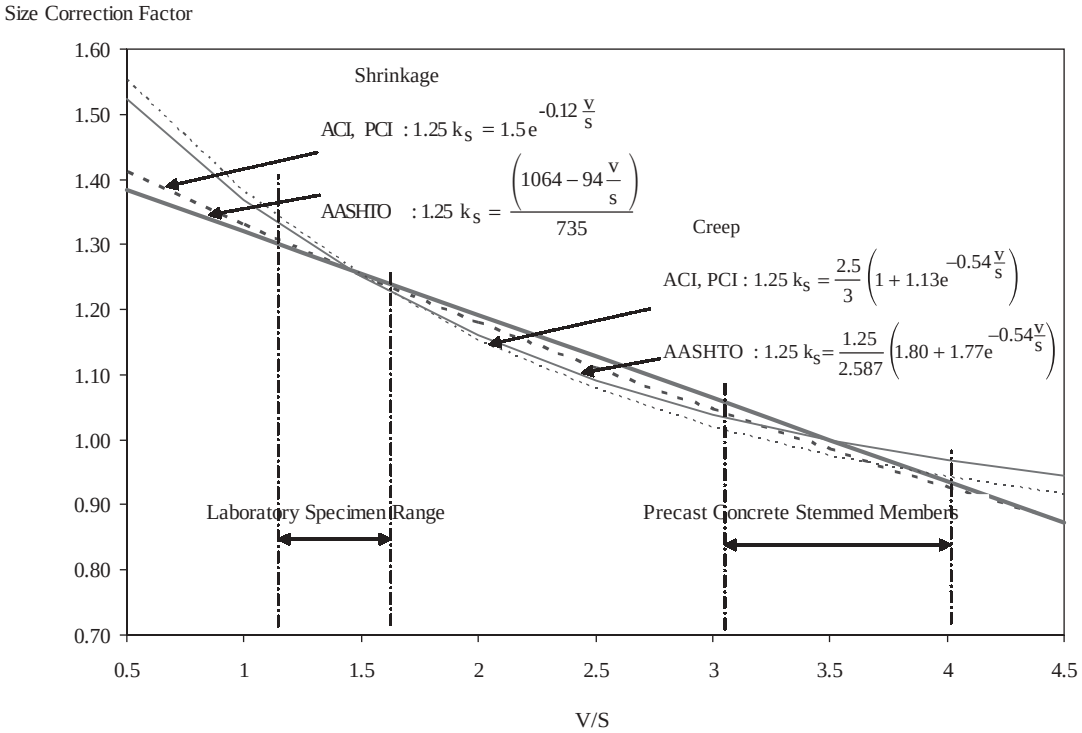

Figure 19. Size correction factor for the various methods.

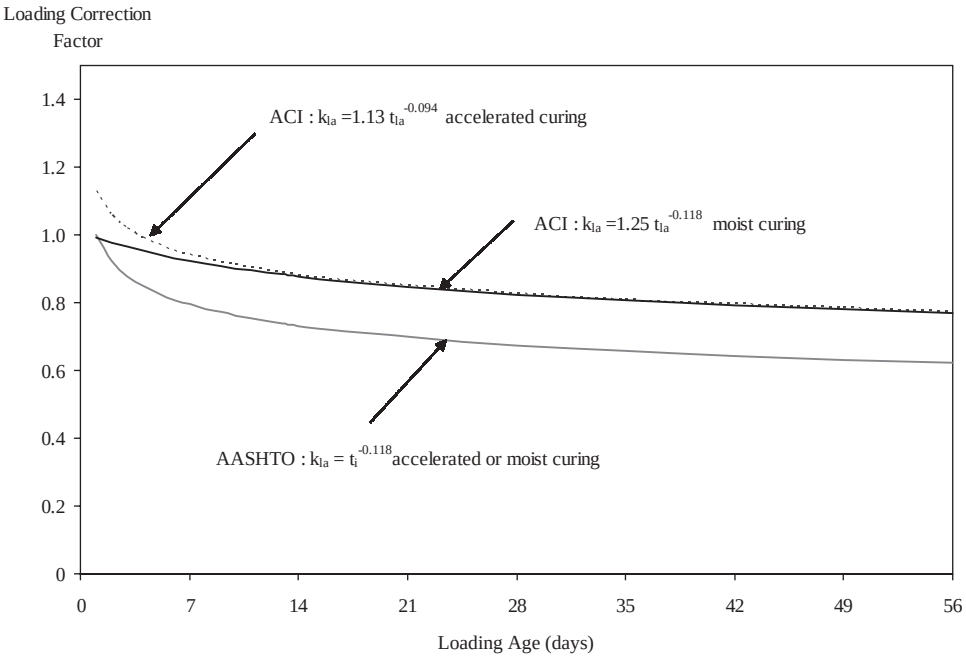

Figure 20. Loading age correction factor for the various methods.

Concrete Strength Correction Factor

Figure 21 shows a comparison of the correction factors for a range of compressive strength obtained with formulas used by the AASHTO-LRFD and Al-Omaishi (*30*). The strength correction used by Al-Omaishi was based on the concrete compressive strength at prestress transfer, which is more relevant than the compressive strength at 28 or 56 days. The concrete strength factor obtained with the AASHTO-LRFD formula was normalized to a value of 1.0 for final compressive strength at service of 5.0 ksi, which was assumed to be 1.25 of the initial compressive strength (at prestress transfer)

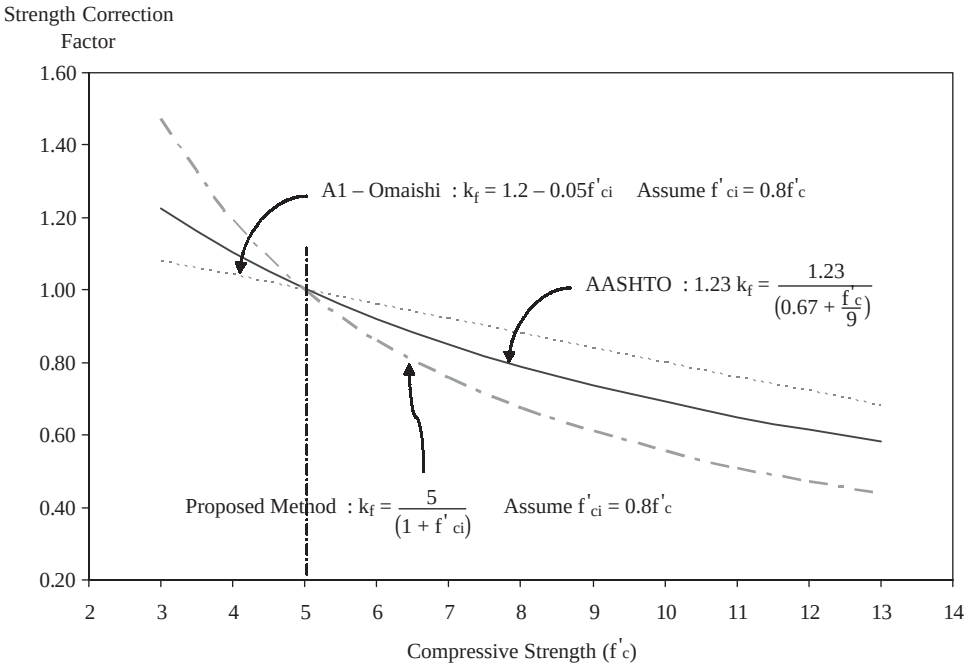

Figure 21. Comparison of strength correction factors.

of about 4.0 ksi. It is recommended that for non-prestressed members, such as the composite cast-in-place deck, an equivalent "initial" strength may be assumed to be 80% of the final strength at service. This assumption would validate usage of the same formulas for estimating creep and shrinkage of the deck slab. Therefore, the strength correction factor for both shrinkage and creep of concrete may be computed as follows:

$$k_f = \frac{5}{1 + f'_{ci}} \quad (53)$$

where: f'_{ci} is the specified compressive strength at prestress transfer for prestressed members or 80% of the strength at service for non-prestressed members.

Time-Development Correction Factor

The time-development correction factor is used to estimate creep and shrinkage effects at times other than time infinity. It can be used for calculating camber and prestress loss at the time of girder erection. The AASHTO-LRFD and the ACI-209 use the same time correction factor for predicting shrinkage of concrete. They also share another formula for predicting the time correction factor for creep. The following formula is proposed to be used for both shrinkage and creep for both conditions of curing:

$$k_{td} = \frac{t}{61 - 4f'_{ci} + t} \quad (54)$$

where: t = age of concrete after loading, in days (or at the end of curing for shrinkage applications).

Figure 22 shows a comparison of the time-development correction factors using the AASHTO-LRFD method, the modified ACI method (*11*), and the proposed method for compressive strength at service, $f'_c = 5$ ksi. The proposed time-development formula was developed to give reasonably close values to the other methods for this level of strength. Both the AASHTO-LRFD and the ACI-209 methods underestimate the reduction in ultimate creep and shrinkage with increasing concrete strength. Time-development of creep and shrinkage are impacted by concrete strength. Higher strength levels produce more accelerated creep and shrinkage at the early stages of a member's life. In all cases, the time-development correction factor approaches unity as time approaches infinity.

PROPOSED SHRINKAGE FORMULA

The extensive test data collected in this project were used to produce a reasonable estimate of ultimate shrinkage strain. In the absence of more accurate data, the ultimate shrinkage strain may be assumed to be 0.000480 in./in. The proposed formula is intended to represent the test data with a rectangular hyperbolic equation, similar to that in the ACI-209 Committee Report and AASHTO-LRFD, but with modifications to account for the effects of the high-strength concrete.

$$\epsilon_{sh} = 480 * 10^{-6} \gamma_{sh} \quad (55)$$

$$\gamma_{sh} = k_{td} k_s k_{hs} k_f \quad (56)$$

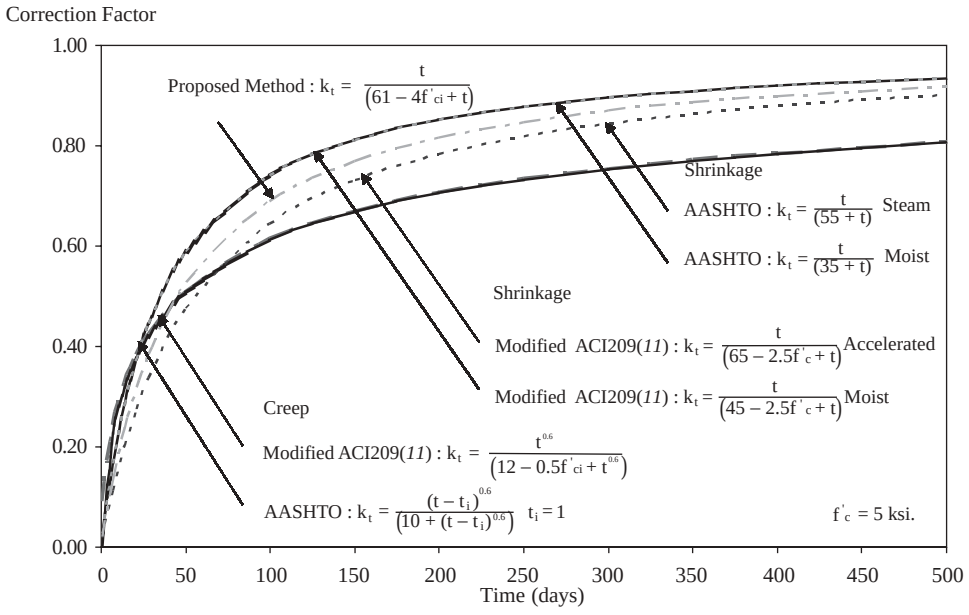

Figure 22. Time-development correction factor by various methods.

k_{td}, k_s, k_{hs}, and k_f were defined in Equations 54, 51, 49, and 53, respectively, as follows:

$$k_{td} = \text{time-development factor} = \frac{t}{61 - 4f'_{ci} + t}$$

k_{hs} = humidity factor for shrinkage = 2.00 – 0.0143H

$$k_s = \text{size factor} = \frac{1064 - 94V/S}{735}$$

$$k_f = \text{concrete strength factor} = \frac{5}{1 + f'_{ci}}$$

Other factors such as slump, cement content, percentage of fines, and air content that are included in the ACI-209 Committee Report have not been included here because of their minor effects. Similar to treatment of the modulus of elasticity, factors K_1 and K_2 may be used to represent average, and upper- and lower-bound values of shrinkage for local materials. Thus, the following equation results:

$$\epsilon_{sh} = 480 * 10^{-6} \gamma_{sh} K_1 K_2 \quad (57)$$

Values for K_1 and K_2 were not developed in this project. The data given in Appendix F may be used in future research as a basis for developing such values. Appendix F also includes a comparison of the experimental data with predictions of the ACI-209, the AASHTO-LRFD method, and the proposed method. A summary of this comparison is shown in Table 10. In general, the proposed method produced results in closer agreement with measured data than those obtained with the other methods.

PROPOSED CREEP FORMULA

The proposed formula for estimating the creep coefficient was developed in a similar manner to the shrinkage prediction formula. The standard conditions have been defined earlier as R.H. = 70%, V/S = 3.5 in., f'_{ci} = 4 ksi, loading age = 1 day for accelerated curing and 7 days for moist curing, and loading duration = infinity. The ultimate creep coefficient for these standard conditions equals 1.90, which is comparable to that predicted by the AASHTO-LRFD method.

$$\psi(t, t_i) = 1.90\gamma_{cr} \quad (58)$$

$$\gamma_{cr} = \text{product of the applicable correction factors} = k_{td} k_{la} k_s k_{hc} k_f \quad (59)$$

k_{td}, k_{la}, k_s, k_{hs}, and k_f were defined in Equations 54, 52, 50, and 53, respectively, as follows:

$$k_{td} = \text{time-development factor} = \frac{t}{61 - 4f'_{ci} + t}$$

$$k_{la} = \text{loading factor} = t_i^{-0.118} \quad (60)$$

$$k_{hc} = \text{humidity factor for creep} = 1.56 - 0.008H \quad (61)$$

$$k_s = \text{size factor} = \frac{1064 - 94V/S}{735}$$

$$k_f = \text{concrete strength factor} = \frac{5}{1 + f'_{ci}}$$

Similar to treatment of the modulus of elasticity and shrinkage, factors K_1 and K_2 may be used to represent average, upper- and lower-bound values of the creep coefficient for local materials. Thus, the following equation results:

$$\psi(t, t_i) = 1.90\gamma_{cr} K_1 K_2 \quad (62)$$

Appendix G contains a comparison of the experimental data with those predicted using the ACI-209, the AASHTO-LRFD, and the proposed creep prediction formulas; a summary of this comparison is shown in Table 11. The proposed formula produced results closer to the measured data than those obtained with the other methods.

RELAXATION OF PRESTRESSING STRANDS

The most commonly used type of prestressing steel is the low-relaxation strand. This type of strand undergoes an extra production step of controlled heating to about 660°F and then cooling while under tension, which reduces relaxation loss to about 25 percent of that for the stress-relieved strand. For low-

TABLE 10 Ratios of predicted-to-measured shrinkage strain specimens

Mix	Ratio of predicted-to-measured shrinkage strain		
	ACI-209	AASHTO-LRFD	Proposed
Nebraska NE09G, NE10G, NE12G	1.75	1.91	1.08
New Hampshire NH10G, NH11G, NH12G	1.13	1.27	0.80
Texas TX08G, TX09G, TX10G	2.26	2.60	1.57
Washington WA10G, WA11G, WA12G	1.05	1.18	0.74
Average of all data	1.55	1.74	1.05

TABLE 11 Ratios of predicted-to-measured creep coefficient specimens

Mix	Ratio of predicted-to-measured creep coefficient		
	ACI-209	AASHTO-LRFD	Proposed
Nebraska NE09G, NE10G, NE12G	1.69	1.31	1.00
New Hampshire NH10G, NH11G, NH12G	1.50	1.37	0.84
Texas TX08G, TX09G, TX10G	2.06	1.89	1.08
Washington WA10G, WA11G, WA12G	1.89	1.88	0.99
Average of all data	1.79	1.61	0.98

relaxation strands, the following formula, which is based on work of Magura et al. (*36*), has been the standard of practice in various references:

$$L_r = \frac{f_{pi}}{45}\left(\frac{f_{pi}}{f_{py}} - 0.55\right)\log\left(\frac{24t_2 + 1}{24t_1 + 1}\right) \quad (63)$$

where: L_r = intrinsic relaxation loss between t_1 and t_2 (days), f_{pi} = stress in prestressing strands at the beginning of the period considered; f_{py} = yield strength of strands, which is taken as 90% of the specified tensile strength of 270 ksi for Grade 270 steel; t_2 = age of concrete at the end of the period (days); t_1 = age of concrete at the beginning of the period (days). The relaxation loss is taken as zero if f_{pi}/f_{py} is less than 0.55. Due to the minimal amount of relaxation loss in low-relaxation strand, a total relaxation loss of 2.4 ksi is used for the detailed method and a more conservative 2.5 ksi is used for the approximate method.

PROPOSED AASHTO-LRFD REVISIONS

Proposed AASHTO-LRFD revisions are given in Appendix M. It is proposed that the modulus of elasticity, shrinkage, and creep prediction methods of Articles 5.4.2.3 and 5.4.2.4 be replaced with the methods described in the preceding sections.

NUMERICAL EXAMPLE OF MATERIAL PROPERTIES USING PROPOSED PREDICTION FORMULAS

The following example illustrates use of the proposed modulus of elasticity, creep, and shrinkage formulas to estimate these values for an interior girder of the New Hampshire bridge used in the experimental program. The beam data and the results obtained in this example will be used to illustrate the calculation of prestress losses at the end of this chapter.

Input Data

The girder type is New England NE1400BT, with an 8-in. thick cast-in-place composite deck slab. The effective slab width is 89 in. The ambient relative humidity is estimated to be 70% for that bridge site. Specified initial concrete compressive strength, f'_{ci}, is 5.7 ksi. The specified ultimate compressive strength, f'_c, for the girder concrete is 8 ksi and 5 ksi for the deck concrete. Precast girder V/S ratio is 3.34 in. Prestressing immediately before transfer f_{pi} is 200 ksi introduced with 40-0.6 in. diameter, low-relaxation strands. The concrete age at transfer is assumed to be 1 day. The concrete age at time of deck placement is assumed to be 56 days. The modulus of elasticity of concrete is calculated according to the formula developed in this research (Equation 48).

$$E_c = 33{,}000K_1\left(0.140 + \frac{f'_c}{1000}\right)^{1.5}\sqrt{f'_c} \qquad \text{(ksi)}$$

K_1 is a factor that accounts for the type of material used. It defaults to 1.0 if no test results are available. For a bridge built in New Hampshire, the information available shows a K_1 equal to 0.91. Thus, E_c at transfer = 33,000 (0.91) $(0.14 + 5.7/1000)^{1.5}\sqrt{5.7}$ = 3,978 ksi, and at service = 4,836 ksi; and the deck E_c = 3,707 ksi.

Shrinkage and Creep Between Transfer and Deck Placement

Girder shrinkage strain from transfer to deck placement, ϵ_{bid}, is calculated using Equation 55.

$$\epsilon_{bid} = 480 \times 10^{-6}\, k_{td}k_sk_{hs}k_f$$

$$k_{td} = \text{time-development factor} = \frac{t}{61 - 4.0f'_{ci} + t}$$

$$= \frac{56 - 1}{61 - 4(5.7) + (56 - 1)} = 0.59$$

$$k_s = \text{size factor} = \frac{1064 - 94V/S}{735} = \frac{1064 - 94(3.34)}{735} = 1.02$$

$$k_{hs} = \text{humidity factor} = 2.00 - 0.0143H$$
$$= 2.00 - 0.0143H(70) = 1.00$$

$$k_f = \text{concrete strength factor} = \frac{5}{1 + f'_{ci}} = \frac{5}{1 + 5.7} = 0.75$$

$$\epsilon_{bid} = 480 \times 10^{-6}\,(0.59)(1.00)(1.02)(1.00)(0.75) = 217 \times 10^{-6}$$

Girder creep coefficient from transfer to deck placement, ψ_{bid}, is calculated using Equation 58.

$\psi_{bid} = 1.90\ k_{td}k_{la}k_sk_{hc}k_f$

k_{la} = loading factor = $t_i^{-0.118}$ for accelerated curing, = 1.00 for loading age of 1 day

k_{hc} = humidity factor = 1.56 – 0.008(H) = 1.56 – 0.008(70) = 1.00

$\psi_{bid} = 1.90\ (0.59)(1.00)(1.02)(1.00)(0.75) = 0.86$

Girder creep coefficient from transfer to final time, ψ_{bif}

$\psi_{bif} = 1.90\ (1.00)(1.00)(1.02)(1.00)(0.75) = 1.45$

Shrinkage and Creep Between Deck Placement and Final Time

Shrinkage strain from deck placement to final, ϵ_{bdf}

$\epsilon_{bdf} = \epsilon_{bif} - \epsilon_{bid}$

$\epsilon_{bif} = 480 \times 10^{-6}\ k_{td}k_sk_{hs}k_f$

$\epsilon_{bif} = 480 \times 10^{-6}\ (1.00)(1.02)(1.00)(0.75) = 367 \times 10^{-6}$

$\epsilon_{bdf} = 367 \times 10^{-6} - 217 \times 10^{-6} = 150 \times 10^{-6}$

Deck shrinkage strain from deck placement to final, ϵ_{ddf}

$\epsilon_{ddf} = 480 \times 10^{-6}\, k_{td}k_sk_{hs}k_f$

$$k_s = \text{size factor} = \frac{1064 - 94V/S}{735} = \frac{1064 - 94(4)}{735} = 0.94$$

$$k_f = \frac{5}{1 + 0.8(5)} = 1.00$$

$$\epsilon_{ddf} = 480 \times 10^{-6}(1.00)(0.94)(1.00)(1.00) = 451 \times 10^{-6}$$

Girder creep coefficient from deck placement to final time, ψ_{bdf}

$\psi_{bdf} = 1.90\ k_{td}k_{la}k_sk_{hc}k_f$

k_{la} = for loading at deck placement = $t_i^{-0.118} = 56^{-0.118} = 0.62$

$\psi_{bdf} = (1.90)(1.00)(0.62)(1.02)(0.75) = 0.90$

Deck creep coefficient from deck placement to final time, ψ_{ddf}

$\psi_{ddf} = 1.90\ k_{td}k_{la}k_sk_{hc}k_f$

$\psi_{ddf} = (1.90)(1.00)(1.00)(0.94)(1.00)(1.00) = 1.79$

For comparison, the AASHTO-LRFD method was applied to the same example. The following values were obtained:

Modulus of elasticity of the girder concrete at transfer = 4350 ksi,
Modulus of elasticity of the girder concrete at service = 5153 ksi,
Modulus of elasticity of the deck concrete = 4074 ksi,
$\epsilon_{bid} = 163 \times 10^{-6}$,
$\psi_{bid} = 0.67$,
$\psi_{bif} = 1.76$,
$\epsilon_{bif} = 367 \times 10^{-6}$,
$\epsilon_{bdf} = 290 \times 10^{-6}$,
$\epsilon_{ddf} = 391 \times 10^{-6}$,
$\psi_{bdf} = 1.06$, and
$\psi_{ddf} = 2.39$.

PRESTRESS LOSS

This section covers measured prestress losses in seven instrumented girders at the four participating states. The proposed detailed method is verified by comparing its prediction results with the measured prestress losses. Measured material properties were used for this purpose. In addition, measured prestress losses will be compared with prestress losses estimates using various loss prediction methods for both measured and specified material properties. Material properties and other relevant information normally available to designers (e.g., concrete strength, modulus of elasticity, creep and shrinkage, relative humidity, and construction schedule) represent "estimated" properties.

EXPERIMENTAL PROGRAM

Concrete strains and temperatures, recorded at the level of the centroid of prestressing strands were used to measure the change of strain of the prestressing strands and calculate the loss in prestressing force. Measurements were taken at 15-min intervals during prestress transfer and deck placement and otherwise at 24-hour intervals. Vibrating wire strain gages for direct embedment in concrete were used for strain and temperature measurements of the four bridges. Readings were recorded by an automated data-acquisition system (ADAS) consisting of a multiplexer and a datalogger connected to a laptop computer.

Girders tested represented a range of the practices used in the United States:

(a) HWY91 East of Albion Bridge, Nebraska Department of Roads.
(b) Rollinsford 091/085 Bridge, New Hampshire Department of Transportation.
(c) Harris County FM-1960 Underpass, Texas Department of Transportation.
(d) La Center Bridge, Clark County, Washington.

Figures 23 through 26 show the plan and cross section of the each of the four bridges, and Table 12 provides geometric properties and loading data. Tables 13 and 14 show specified and measured concrete properties, respectively. Table 15 lists measured and predicted shrinkage and creep for the concrete mixes used. Appendix D provides details of the concrete mixes used in the bridge girders; designated NE09G, NH10G, TX09G, and WA10G for Nebraska, New Hampshire, Texas, and Washington, respectively.

Concrete Industries of Lincoln, Nebraska, produced the NU2000 girders on May 9 and 10, 2000. The girders were shipped to the site and the deck was placed April 10, 2001. Northeast Concrete Products of Plainville, Massachusetts, fabricated the NE 1400 BT girders June 8, 2000. The casting of the deck was completed October 18, 2000. Texas Concrete Company of Victoria, Texas, produced the Texas U54B girder June 15, 2000. The deck was placed January 9, 2001. Concrete Technology Corporation of Tacoma, Washington, produced the W74G girders for La Center Bridge. The girder concrete was placed September 13 and 14, and the deck was completed March 24, 2001.

Girder Instrumentation

The testing program included instrumentation of two girders per bridge, designated Girders 1 and 2, in Nebraska, New Hampshire, and Washington. Because U-beams were

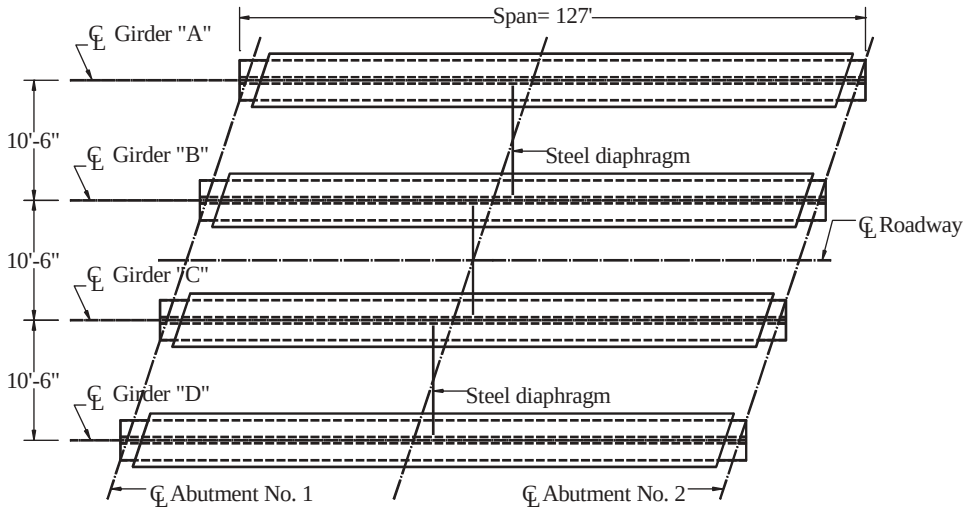

Girder Layout

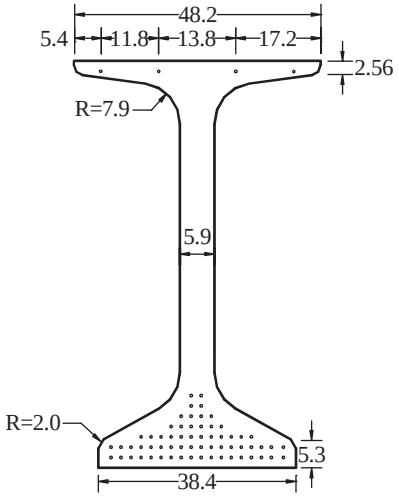

Girder Cross-section

Figure 23. Plan and cross section of HWY91 East of Albion Bridge, Nebraska.

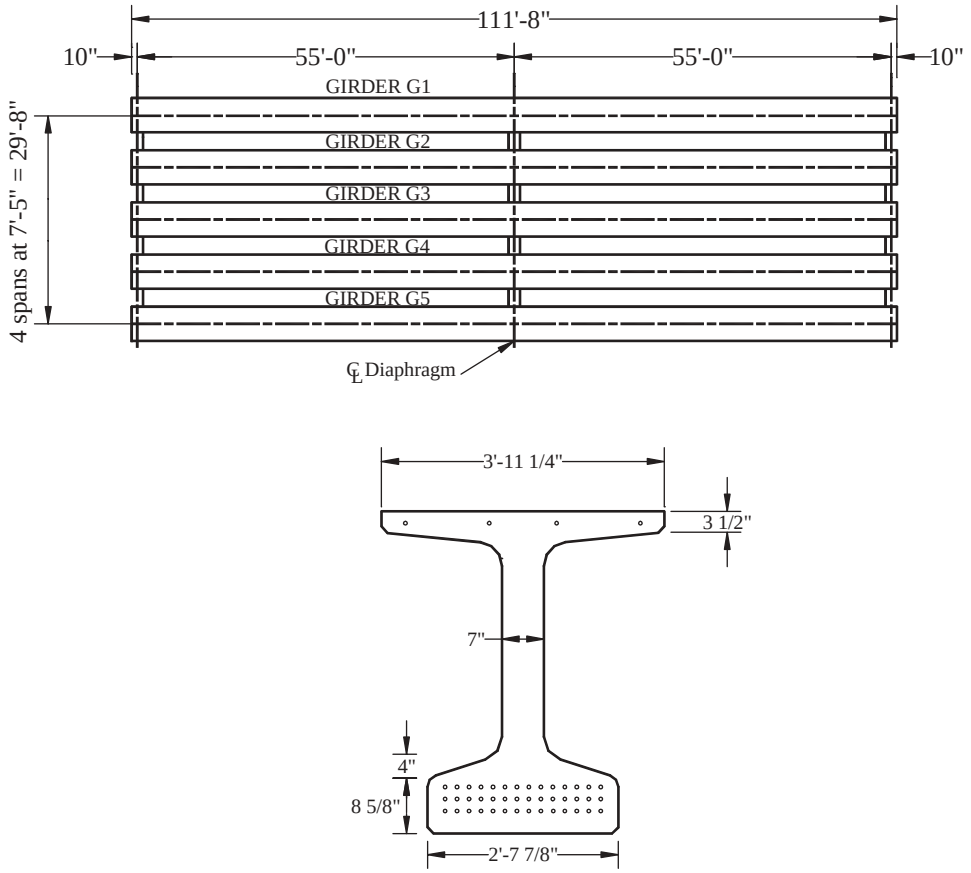

Figure 24. Plan and cross section of Rollinsford 091/085 Bridge, New Hampshire.

used in Texas, only one girder (Girder 1) was instrumented. Girder 1 was instrumented at two locations along the span length (mid-span and a location from the end of the girder equal to the greater of 6 ft or the girder height.) The second girder was instrumented at mid-span only.

Figure 27 shows the locations of the five vibrating strain gages used at each cross-section of the I-girders. Two gages were placed transversely at the same depth as the center of gravity of the prestressing force close to mid-span, one gage was positioned at web mid-depth, one gage was placed at the center of gravity of the top flange, and the fifth gage was placed within the cast-in-place deck. For the Texas U-beam, two gages were placed at the top flange and two gages were placed within the cast-in-place part of the deck. The vertical distribution of longitudinal strain can be used to identify the behavior of the complete cross-section through the linear strain gradient.

Table 16 lists the type of instrumentation used, the measured data, and their relevance to prestress losses. Figure 28 shows vibrating wire gages placed within girders prior to concrete casting. Once the girders were moved to the bridge site, one vibrating wire gage was installed in the deck at each of the instrumented deck sections with the exception of Texas where two gages were installed in the deck per section. The gage wires were run along the top of the deck's longitudinal reinforcement toward the location of the multiplexer near the end at the abutment or the pier. An ADAS was then attached to the bridge structure.

Readings were taken at 15-min intervals just before, during, and immediately after deck placement to capture the instantaneous deformation due to deck weight. Afterwards, the datalogger was reprogrammed for long-term measurements at the rate of once every 24 hours. A conventional telephone line was used as a communication means between the ADAS at the job site and the monitoring station at the University of Nebraska in Omaha. Accessing through a telephone module located within the ADAS system allowed a computer equipped with a modem to reprogram and collect data on a regular basis without the need to travel to the job site.

Concrete Temperature

High-strength concrete develops high heat of hydration that affects member performance especially in the first several days of member age. Therefore, data acquisition of member temperature began as soon as the concrete was placed and continued until the concrete temperatures fell to near ambient.

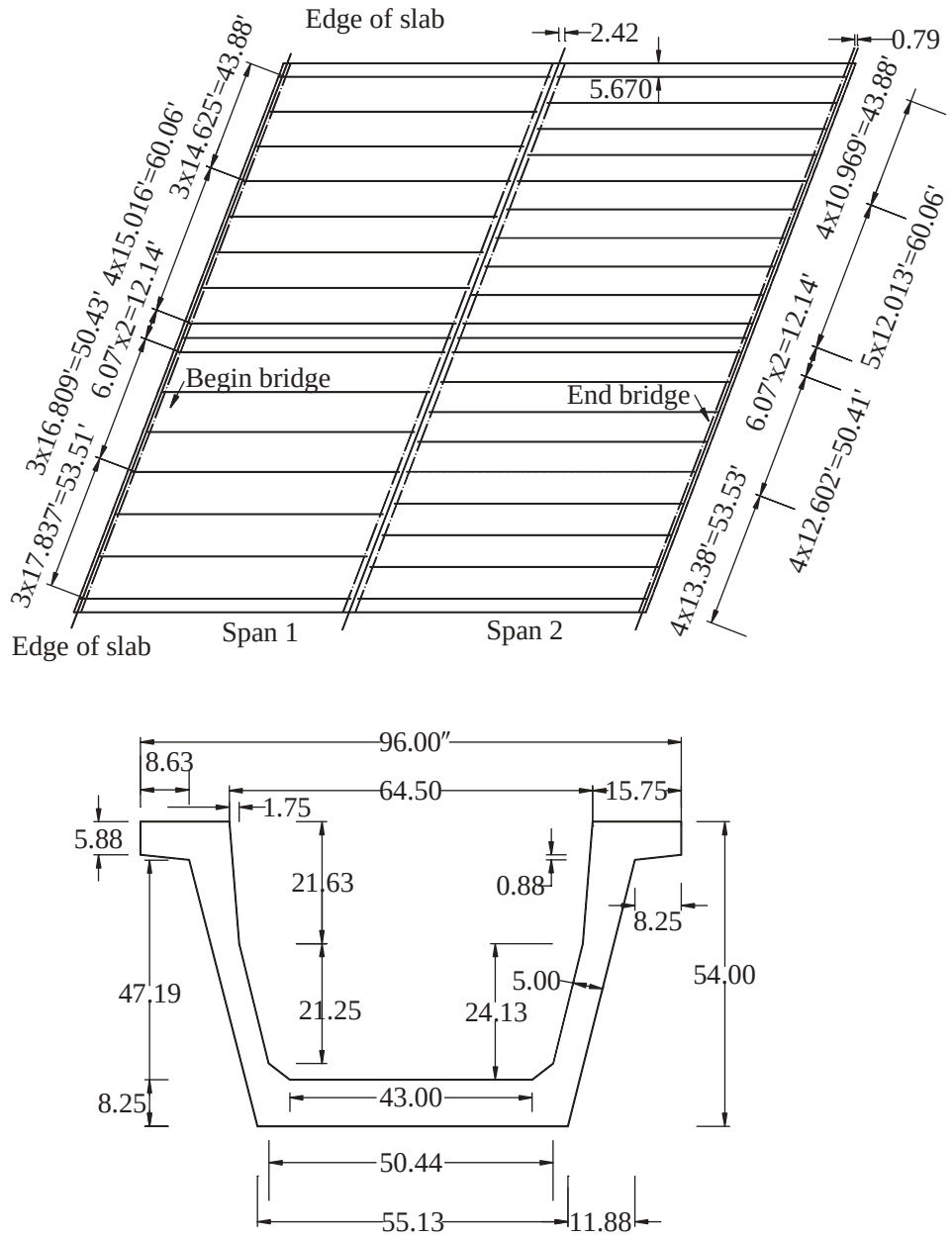

Figure 25. Plan and cross section of Harris County FM 1960 Underpass, Texas.

A typical time-temperature curve is shown in Figure 29. Temperature readings of the seven bridge girders were recorded in both the pretensioned girders and the cast-in-place decks, as shown in Table 17. Examples of temperature variations during girder casting are shown in Figure 30. A typical plot of temperature at mid-span of the composite section is presented in Figure 31. A more complete record of temperature readings at all significant construction events is given in Appendix H. The maximum temperature difference across the depth of the precast sections ranged from 35°F to 12°F, and occurred for most girders shortly after the removal of forms. A sharp drop in the girder temperature usually occurs immediately after removal of the forms at the end of the accelerated curing period.

Concrete Strains

Table 18 presents a summary of the strain measurements for the seven instrumented pretensioned bridge girders; all strain measurements are included in Appendix I. The measurement of concrete strain prior to transfer is very sensitive to the heat of hydration. The highest temperature recorded was 165°F during the casting of Washington girder W83G. Interpretation of concrete strain prior to transfer, especially in high-strength

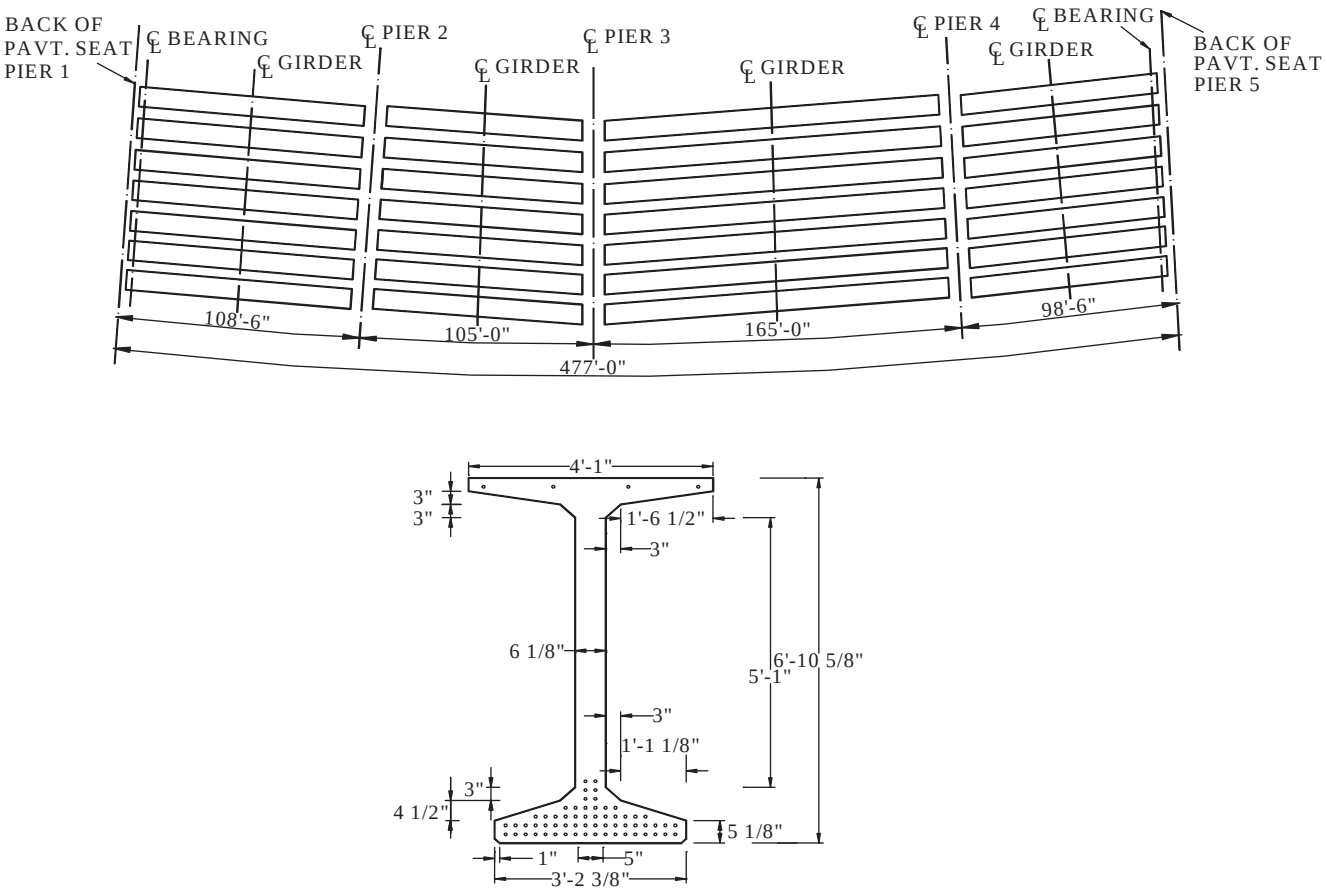

Figure 26. Plan and cross section of Clark County La Center Bridge, Washington.

concrete, is rather complicated. It temporarily impacts the level of tension in the embedded strands because they would have a similar temperature to that of the surrounding concrete. When prestress is released to the concrete and the temperature of the concrete is still elevated, the amount of prestressing applied to the girder is significantly impacted by the temporary high temperature. The following equation represents strand stress loss due to a temperature rise, ΔT:

$$\Delta f_{pt} = \alpha_s E_p \Delta T \quad (64)$$

where α_s is the coefficient of the thermal expansion of steel.

Thermal and relaxation loss prior to concrete hardening can be considered to be "locked in" as the bond forms. Relaxation loss after concrete set can be computed in the same manner as that prior to concrete set. Thermal effects after concrete bonding to prestressing strands tend to change the strains along the strands because of the difference in the axial stiffness between the girder section and the free strands. After the forms are removed, the girder cools and the concrete begins to contract. In addition, drying shrinkage causes extensive contraction prior to transfer. The magnitude of contraction is affected by the level of restraint provided by the formwork, the temperature increase due to heat of hydration, and other factors such as concrete mix proportions, curing, environmental conditions, and geometry of the section.

Generally the top of the beam experiences some expansion (tensile strains) due to the higher temperature on the freer top flange than that on the restraint bottom flange. The magnitude of the tensile strains was highly variable. The top flange subsequently went into compression because the temperature-related compressive strain exceeded the tensile strain. Because of the presence of compressive strain prior to transfer, the "baseline" reading for strain measurements for elastic shortening was not taken at the stress-free conditions. In addition, measurement of the prestress losses may have been affected by the concrete strain prior to transfer, depending on when the bond between the concrete and the strands developed.

The residual compressive strain, due to heat of hydration just prior to transfer, was taken as the baseline for measuring the elastic deformation of the section. Therefore, the elastic strain at transfer was taken as the difference between strain just before transfer and that immediately after transfer. Figure 32 for Nebraska girder G1 illustrates that the strain decreases noticeably at transfer (44 hours) when the concrete temperature is about 72°F (as shown in Figure 30). In contrast, the

TABLE 12 Properties and loading data

	Nebraska-East Albion HWY91		New Hampshire Rollinsford 091/085		Texas-Harris County FM 1960 Underpass	Washington-Clark County La Center Bridge	
Girder ID	1W2-1	1W2-2	G3	G4	G7	G18	G19
Girder type	NU2000		NE1400BT		U54B	W83G	
Span, ft	127		110		129.2	159.0	159.8
Spacing, ft	10.6		7.42		11.22	7.17	
Girder details							
h, in.	78.7		55.1		54	82.6	
A_g, in.^{2}	903.8		857.2		1121	972	
y_b, in.	35.7		26.27		22.48	39.66	
I_g, in.^{4}	790,592		351,968		404,230	956,329	
Girder unit weight, k/ft	0.967		0.893		1.222	1.073	
Prestressing strands							
Number of strands	56		40		64	60	
Diameter of strands, in.	0.5		0.6		0.6	0.6	
A_p, in.^{2}	8.568		8.680		13.888	13.02	
Eccentricity at mid-span e_p, in.	31.20		20.62		19.01	34.66	
Eccentricity at x[1] from end e_p, in.	At 7 ft 22.91		At 7 ft 17.17		At 7 ft 19.01	At 8 ft 23.09	
Strands initial stress, ksi	202.48		202.76		202.30	202.49	
Strands modulus of elasticity, ksi	28,800		28,800		28,000	28,800	
Deck details							
t, in	7.5		8.0		8.0	7.5	
A_d, in.^{2}	945		623		1076.8	645	
Deck unit weight, k/ft	1.019		0.767		1.160	0.696	
e_d, in.	46.75		32.83		35.52	46.69	
Assumed superimposed dead loads							
SIDL unit weight, k/ft	0.473		0.334		0.505	0.323	

[1] x = 7 ft from the girder end or the girder depth, whichever is larger.

recorded residual strain just before transfer at 20 hours for a similar girder G2 was about 191 microstrains. When the girder temperature was about 100°F, the temperature correction would equal $\alpha_s (T_t - T_o) = 6.78 (100 - 72) = 190$ microstrains.

However, as the concrete cooled, similar readings were recorded for the two girders, which indicate that strain readings were affected by the high temperature. The only forces acting on the girder between the times of transfer and deck placement are the initial prestressing force and the self weight of the girder. During this period, the prestress losses are based on these two effects and on the long-term material properties of the concrete and prestressing strands. A typical graph of the variation of concrete strain with time is shown in Figure 33.

OTHER EXPERIMENTAL DATA

Prestress loss data obtained from other tests were compared to those estimated by the proposed methods to assess the methods' reliability to accurately estimate prestress losses.

TABLE 13 Specified concrete strength

	Nebraska East Albion HWY91	New Hampshire Rollinsford Bridge 091/085	Texas Harris County FM 1960 Underpass	Washington Clark County La Center Bridge
Girder concrete mix ID	NE09G	NH10G	TX09G	WA10G
Specified strength at transfer, ksi	5.500	5.700	6.960	7.500
Specified strength at service, ksi	8.000	8.000	9.410	10.000
Deck concrete mix ID	NE04D	NH04D	TX04D	WA04D
Specified strength at service, ksi	4.000	5.000	5.000	4.000

TABLE 14 Measured concrete strength and modulus of elasticity

	Nebraska East Albion HWY91	New Hampshire Rollinsford Bridge 091/085	Texas Harris County FM 1960 Underpass	Washington Clark County La Center Bridge
Girder concrete mix ID	NE09G	NH10G	TX09G	WA10G
Concrete unit weight, kcf	0.149	0.145	0.152	0.154
Age at transfer, days	44/24 = 1.8	20/24 = 0.8	24/24 = 1.0	20/24 = 0.8
Strength at transfer, ksi	6.250	5.790	7.230	7.530
Modulus of elasticity at transfer, ksi	4,091	4,688	6,280	5,586
Age of girder at deck placement, days	340	130	200	190
Strength of girder at deck placement, ksi	9.025	10.050	10.670	10.280
Modulus of elasticity at deck placement, ksi	5,088	5,396	7,395	6,114
Deck concrete mix ID	NE04D	NH04D	TX04D	WA04D
Strength at service, ksi	4.200	5.150	5.200	5.150
Modulus of elasticity at service, ksi	3,898	4,357	4,380	4,357

TABLE 15 Measured and predicted shrinkage and creep

	Nebraska East Albion HWY91		New Hampshire Rollinsford 091/085		Texas-Harris County FM 1960 Underpass		Washington-Clark County La Center Bridge	
Girder mix designation	NE09G		NH10G		TX09G		WA10G	
Volume-to-surface ratio, V/S, in.	2.95		3.34		2.88		2.95	
Ambient relative humidity, %	65		70		70		80	
	Planned	Actual	Planned	Actual	Planned	Actual	Planned	Actual
Age of girder at deck placement, days	56	340	56	130	56	200	56	190
Deck mix designation	NE04D		NH04D		TX04D		WA04D	
Volume-to-surface ratio, V/S, in.	3.75		4.00		4.00		3.75	
Ambient relative humidity, %	65		70		70		80	
Material properties	Predicted	Modified Measured	Predicted	Modified Measured	Predicted	Modified Measured	Predicted	Modified Measured
1. Shrinkage								
a) Girder								
Initial to final, ε_{bif}	422	334	364	388	325	248	258	328
Initial to deck placement, ε_{bid}	248	302	215	301	203	213	165	282
Deck placement to final, ε_{bdf}	175	32	149	88	122	34	93	46
b) Deck								
Deck placement to final, ε_{ddf}	496	392	373	425	373	296	397	377
2. Creep								
a) Girder								
Initial to final, ψ_{bif}	1.624	1.767	1.444	1.256	1.286	1.182	1.099	1.144
Initial to deck placement, ψ_{bid}	0.952	1.598	0.854	0.973	0.804	1.018	0.704	0.984
Deck placement to final (initial loadings) ($\psi_{bif} - \psi_{bid}$)	0.672	0.169	0.590	0.283	0.482	0.172	0.395	0.160
Deck placement to final (deck loads), ψ_{bdf}	1.010	0.924	0.898	0.707	0.800	0.632	0.683	0.616
b) Deck								
Deck placement to final, ψ_{ddf}	1.517	--	1.176	--	1.176	--	1.342	--

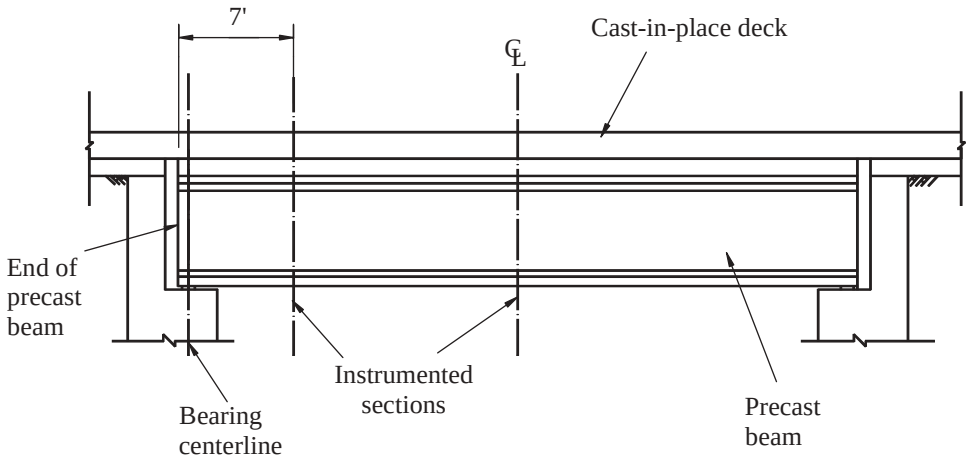

(a) Instrumented Locations along the Girder

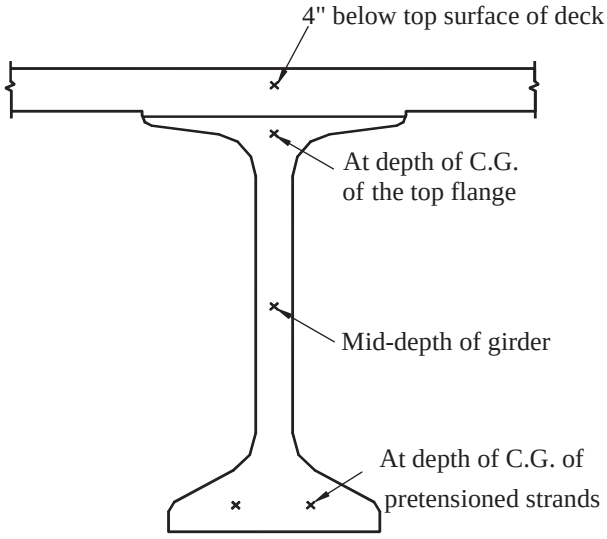

(b) Vibrating Wire Strain Gauge Locations

Figure 27. Instrumentation locations.

TABLE 16 Instrumentation and measured parameters

Instrumentation type	Measured data	Relevance of data
Vibrating wire gages	Concrete strains	Elastic shortening Long-term prestress losses
Thermistors	Concrete temperatures	Hydration temperature Thermal gradient Corrections for strain
Tension-wire system or Precise surveying	Beam camber/deflection	Elastic response to transfer of prestress force

Temperature readings were recorded during the first 24 hours of accelerated curing at 15-minute intervals to ensure measurement of the maximum temperature. Strain readings were taken at 15-minute intervals during transfer and deck casting. After the placement of the deck, the strain and temperature readings were taken once a day.

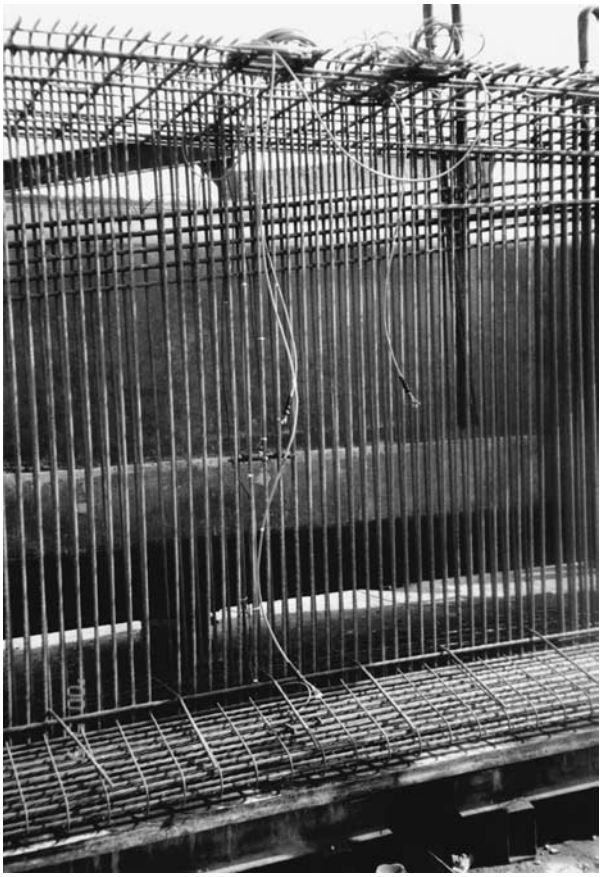

Figure 28. Attachment of vibrating wire gages at the end section of Nebraska NU2000 girder.

Prestress loss measurements were reported for tests on 31 pretensioned concrete girders in Connecticut, Illinois, Nebraska, Ohio, Pennsylvania, Texas, and Washington ranging in age from 200 days to 28 years. They represented a wide range of environmental conditions, material properties, and constructions practices. The girders had I and box sections. The spans ranged from 45 ft to 152 ft.

Specified compressive concrete strength ranged from 3.38 ksi to 7.86 ksi. The specified concrete compressive strengths ranged from 5.30 ksi to 14.00 ksi. When unavailable, data related to material properties such as shrinkage strain and creep coefficients were estimated using the proposed shrinkage and creep formulas. The measured prestress loss data were obtained from published reports and papers (Greuel et al. [*37*], Pessiki et al. [*38*], Mossiossian et al. [*39*] Kebraei et al. [*40*] Shenoy et al. [*41*], Stanton et al. [*42*], Seguirant et al. [*43*], and Gross et al. [*35*]). Details related to girder type and section properties, deck geometry, prestressing strands, loads and moments, and concrete material properties are included in Appendix J.

Reported prestress losses data were compared with the estimated prestress losses using the AASHTO-LRFD Refined, the AASHTO-LRFD Lump-Sum, the PCI-BDM, and the proposed detailed and approximate methods.

PROPOSED DETAILED PRESTRESS LOSS METHOD

The proposed detailed method uses the aging coefficient approach for computing prestress losses between transfer

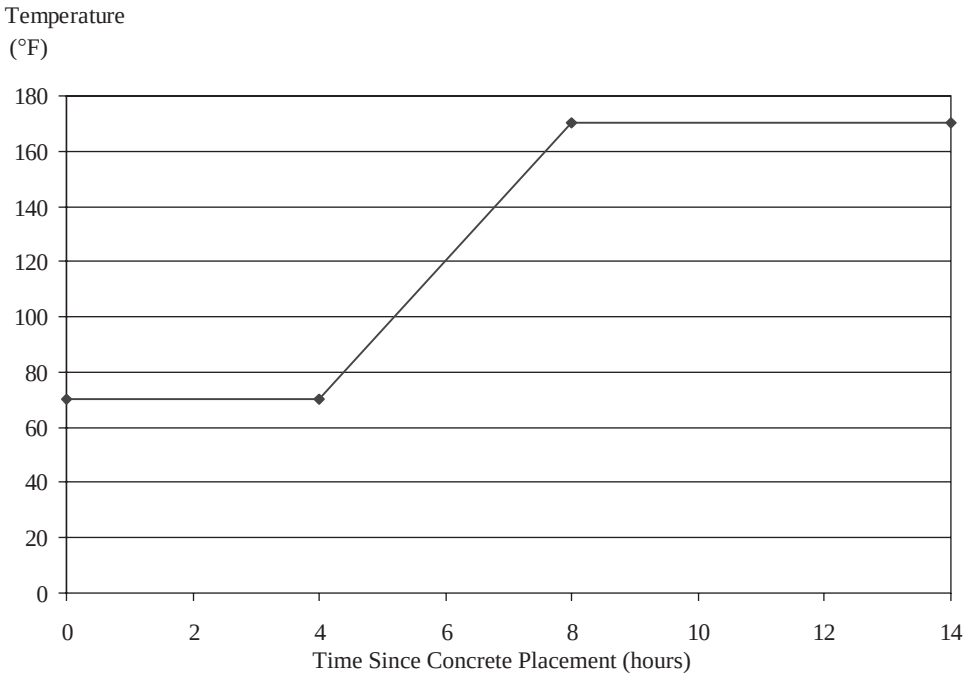

Figure 29. Typical time-temperature curing cycle (4).

TABLE 17 Measured concrete temperature

State	Nebraska		New Hampshire		Texas	Washington	
Bridge name	East Albion HWY91		Rollinsford Bridge 091/085		Harris County FM 1960 Underpass	Clark County La Center Bridge	
Girder ID	1W2-1	1W2-2	G3	G4	G7	G18	G19
Girder type	NU2000	NU2000	NE1400BT	NE1400BT	U54B	W83G	W83G
Girder temperature							
Casting date	May 9, 2000	May 10, 2000	June 8, 2000	June 8, 2000	June 15, 2000	September 13, 2000	September 14, 2000
Casting time	10:12 AM	11:05 AM	11:30 AM	11:00 AM	1:00 PM	12:30 PM	4:25 PM
Maximum concrete temperature, °F	161	128	138	135	141	165	163
Location of maximum temperature	Bottom Flange	Top Flange	Top Flange	Mid-Height Web	Bottom Flange	Bottom Flange	Top Flange
Maximum temperature difference, °F	20	19	20	12	35	15	20
Deck temperature							
Casting date	April 10, 2001		October 18, 2000		January 9, 2001	March 24, 2001	
Casting time	8:00 AM		9:00 AM		8:00 AM	8:00 AM	
Peak concrete temperature, °F	57		69		61	107	

and casting of decks described by Tadros et al. (*18*) and Gallt in the PCI-BDM (*4*) for precast noncomposite members. The approach was also adopted by the European CEB-FIP Recommendations (*25*). The theory is expanded here to cover composite action between precast concrete girders and cast-in-place deck slabs. The prestress losses of pretensioned members, Δf_{pT}, consist of the following four components, each of which relates to a significant construction stage:

(a) Instantaneous prestress loss due to elastic shortening at transfer, Δf_{pES}.
(b) Long-term prestress losses due to shrinkage of concrete, $(\Delta_{pSR})_{id}$, and creep of concrete, $(\Delta f_{pCR})_{id}$, and relax-

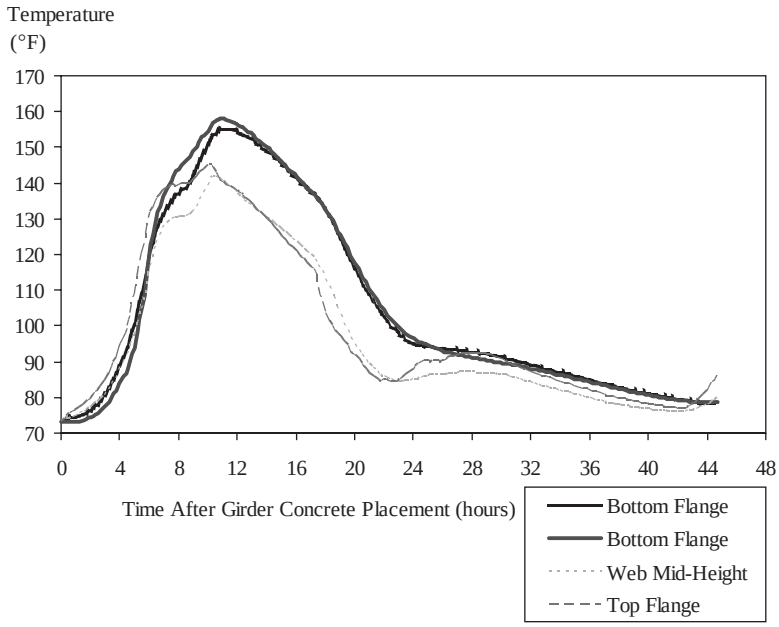

Figure 30. Temperature for girder G1 at mid-span during Nebraska girder casting.

ation of prestressing strands, $(\Delta f_{pR2})_{id}$, between the time of transfer and just before deck placement.

(c) Instantaneous prestress gain due to the placement of deck weight and SIDL, Δf_{pED}.

(d) Long-term prestress losses, between the time of deck placement and the final service life of the structure, due to shrinkage of the girder, $(\Delta f_{pSD})_{df}$, creep of the girder, $(\Delta f_{pCD1} + \Delta f_{pCD2})_{df}$, relaxation of prestressing strands, $(\Delta f_{pR3})_{df}$, and shrinkage of the deck concrete, $(\Delta f_{pSS})_{df}$.

Total prestress losses in pretensioned bridge girders, Δf_{pT}, relative to the stress immediately before transfer is thus given by the equation:

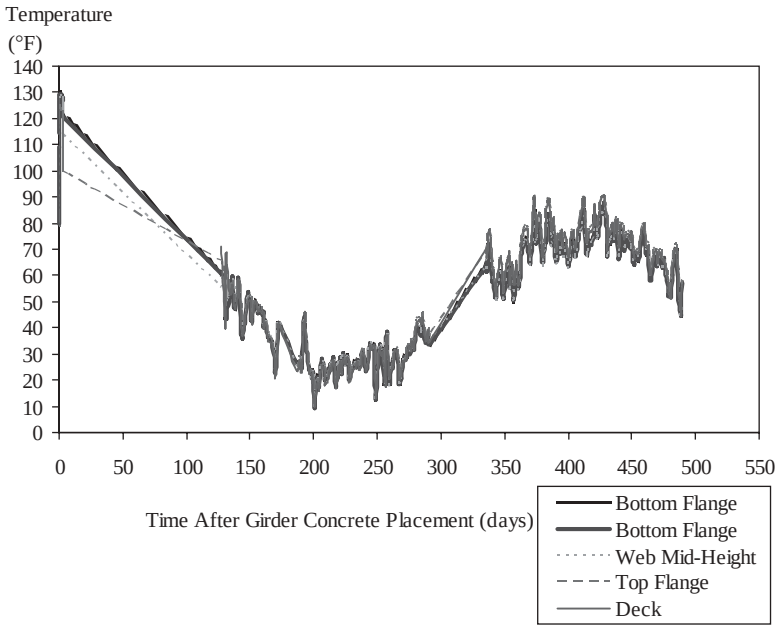

Figure 31. Temperature for New Hampshire girder G3 at mid-span from girder casting to final time.

TABLE 18 Summary of measured strains

Girder	Measured elastic strain at transfer	Measured long-term strain transfer to deck placement	Measured elastic strain at deck and superimposed dead loads	Measured long-term strain deck placement to final	Total measured strain	Age of girder at final, (days)
Nebraska G1 NU2000	591	543	-221	144	1057	470
Nebraska G2 NU2000	573	672	-218	148	1175	469
New Hampshire G3 NE1400BT	874	745	-234	64	1449	490
New Hampshire G4 NE1400BT	848	723	-228	66	1409	490
Texas G7 U54B	460	613	-267	46	852	400
Washington G18 W83G	959	457	-241	229	1404	380
Washington G19 W83G	885	463	-240	224	1332	380

All strains are in in. per in. x 10^{-6}.

$$\Delta f_{pT} = \Delta f_{pES} + \left(\Delta f_{pSR} + \Delta f_{pCR} + \Delta f_{pR2}\right)_{id} - \Delta f_{pED} + \left(\Delta f_{pSD} + \Delta f_{pCD1} + \Delta f_{pCD2} + \Delta f_{pR3} - \Delta f_{pSS}\right)_{df}$$

Instantaneous Prestress Loss Due to Elastic Shortening at Transfer

Elastic shortening loss is caused by instantaneous deformation of the concrete at the time prestress is transferred to the member. It does not need to be calculated if the transformed section analysis is used to calculate concrete stresses at transfer. Its calculation is given here only to show that it can be calculated using transformed section properties and to allow for a complete comparison with current prestress loss prediction methods. The concrete stress at steel centroid, f_{cgp}, is obtained by applying the initial prestressing force just prior to transfer, P_i, and the self weight moment, M_g, to a section transformed to precast concrete using a modular ratio at transfer n_i.

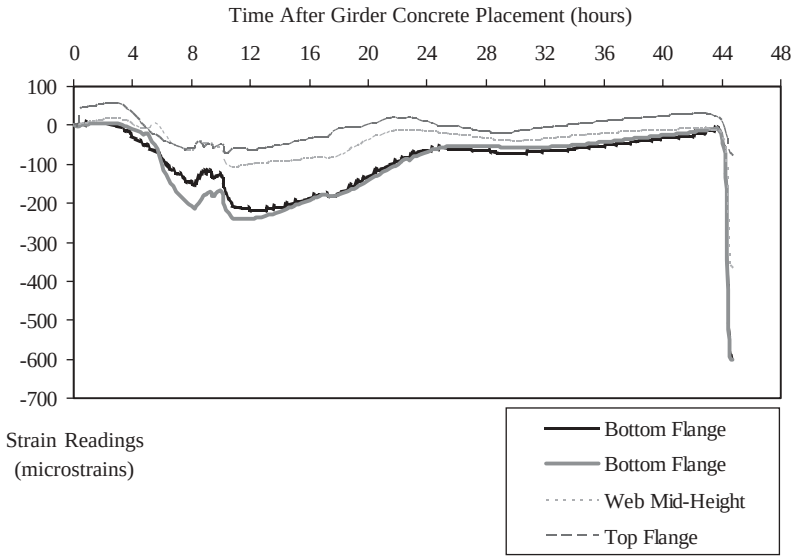

Figure 32. Strain readings at transfer for Nebraska girder G1 mid-span.

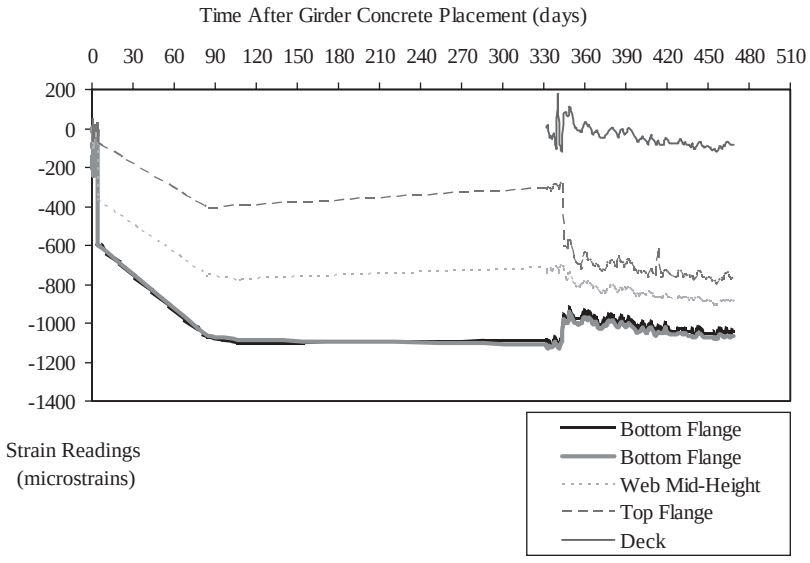

Figure 33. Long-term strain reading at mid-span of Nebraska girder G1.

$$f_{cgp=} = P_i\left(\frac{1}{A_{ti}} + \frac{e_{pti}^2}{I_{ti}}\right) - \frac{M_g e_{pti}}{I_{ti}}$$

where: A_{ti} = transformed area; I_{ti} = transformed moment of inertia; and e_{pti} = eccentricity of strands with respect to the transformed section centroid. The value of concrete stress at steel centroid is multiplied by the modular ratio to determine the change in steel stress:

$$\Delta f_{pES} = n_i f_{cgp} = \frac{E_p}{E_{ci}} f_{cgp}$$

Long-Term Prestress Losses Between the Times of Transfer and Deck Placement

Long-term prestress losses due to shrinkage and creep of concrete and relaxation of prestressing strands are estimated based on the net section properties of the noncomposite section.

Prestress Loss Due to Shrinkage

$$\Delta\epsilon_p = \Delta\epsilon_c$$

$$\frac{\Delta P_p}{A_{ps}E_p} = \epsilon_{bid} - \left(\frac{\Delta P_p}{E''_{c1}A_n} + \frac{\Delta P_p}{E''_{c1}}\frac{e_{pn}^2}{I_n}\right)$$

$$\frac{\Delta P_p}{A_{ps}}\left[1 + \frac{E_p}{E''_{c1}}\frac{A_{ps}}{A_n}\left(1 + \frac{A_n e_{pn}^2}{I_n}\right)\right] = \epsilon_{bid}E_p$$

$$E''_{c1} = \frac{E_{ci}}{1 + \chi\psi_{bif}}$$

$$\alpha_n = \left(1 + \frac{A_n e_{pn}^2}{I_n}\right)$$

$$\rho_n = \frac{A_{ps}}{A_n}$$

$$K_{id} = \frac{1}{1 + n_i\rho_n\alpha_n(1 + \chi\psi_{bif})}$$

$$\Delta f_{pSR} = \frac{\Delta P_p}{A_{ps}}$$

$$\Delta f_{pSR} = \epsilon_{bid}E_p K_{id}$$

where:

ϵ_{bid} = concrete shrinkage strain of the girder between transfer and deck placement,

ψ_{bif} = girder creep coefficient minus the ratio of the strain that exists at the final time to the elastic strain caused when the load is applied at the time of transfer,

α_n = factor for initial net (or approximately gross) section properties,

ρ_n = tensile reinforcement ratio for initial net section,

E''_{cl} = age-adjusted effective modulus of elasticity of concrete,

χ = aging coefficient that accounts for concrete stress variability with time and may be considered constant for all concrete members at age 1 to 3 days (Dilger [*16*] = 0.7, and

K_{id} = transformed section age-adjusted effective modulus of elasticity factor, for adjustment between time of transfer and deck placement.

Prestress Loss Due to Creep

$$\Delta\epsilon_p = \Delta\epsilon_{pc}$$

$$\frac{\Delta P_p}{A_{ps}E_p} = \frac{f_{cgp}}{E'_{c1}} - \left(\frac{\Delta P_p}{E''_{c1}A_n} + \frac{\Delta P_p}{E''_{c1}}\frac{e_{pn}^2}{I_n}\right)$$

$$\frac{\Delta P_p}{A_{ps}E_p} = \frac{f_{cgp}}{E_{ci}}\psi_{bid} - \left(\frac{\Delta P_p}{E_{ci}A_n} + \frac{\Delta P_p}{E_{ci}}\frac{e_{pn}^2}{I_n}\right)(1 + \chi\psi_{bif})$$

$$E'_{c1} = \frac{E_{ci}}{\psi_{bid}}$$

$$E''_{c1} = \frac{E_{ci}}{1 + \chi\psi_{bif}}$$

$$\frac{\Delta P_p}{A_{ps}}\left[1 + \frac{E_p}{E_{ci}}\frac{A_{ps}}{A_n}\left(1 + \frac{A_n e_{pn}^2}{I_n}\right)(1 + \chi\psi_{bif})\right] = \frac{E_p}{E_{ci}} f_{cgp}\psi_{bid}$$

$$K_{id} = \frac{1}{1 + n_i\rho_n\alpha_n(1 + \chi\psi_{bif})}$$

$$\Delta f_{pCR} = \frac{\Delta P_p}{A_{ps}}$$

$$\Delta f_{pCR} = n_i f_{cgp}\psi_{bid}K_{id}$$

where:

E'_{cl} = age-adjusted effective modulus of elasticity of concrete and

ψ_{bid} = girder creep coefficient minus the ratio of the strain that exists at the time of deck placement to the elastic strain caused when the load is applied at the time of transfer.

Prestress Loss Due to Relaxation

Relaxation loss from the time of transfer to deck placement, $\phi_i L_i$, can be estimated using the intrinsic relaxation loss, L_i, (Magura et al. [*36*]) and the reduction factor, ϕ_i, (Tadros et al. [*19*]) as follows:

$$\Delta f_{pR2} = \phi_i L_i K_{id}$$

$$\text{for } \frac{f_{po}}{f_{py}} \geq 0.50,\ L_i = \frac{f_{po}}{45}\left(\frac{f_{po}}{f_{py}} - 0.55\right)\log\left(\frac{24t_d + 1}{24t_i + 1}\right)$$

$$\text{for } \frac{f_{po}}{f_{py}} \leq 0.50,\ \text{no relaxation loss is assumed to take place}$$

where:

f_{po} = stress in prestressing strands just after transfer;
f_{py} = specified yield strength of strands;
t_d = age of the concrete at deck placement, days;
t_i = age of the concrete at transfer, days;
ϕ_i = reduction factor that reflects the steady decrease in strand prestressing due to creep and shrinkage of the concrete.

$$\phi_i = 1 - \frac{3(\Delta f_{pSR} + \Delta f_{pCR})}{f_{po}}$$

In general, the relaxation loss of low-relaxation strand is very small, ranging from 1.5 ksi to 4.0 ksi, it may be convenient to assume a constant value of 2.4 ksi, equally split between the two time periods: initial to deck placement and deck placement to time infinity.

Instantaneous Elastic Prestress Gain at the Time of Deck Placement and Superimposed Dead Loads

As indicated earlier, there is no need for the explicit calculation of elastic loss and gain because stress analysis using the transformed section automatically accounts for this component of steel stress change.

Long-Term Prestress Losses Between the Time of Deck Placement and the Final Time

Long-term prestress losses due to the shrinkage and creep of girder concrete, relaxation of prestressing strands, and shrinkage of deck concrete between the time of deck placement and the final service life of the structure are computed assuming a composite section to be in action shortly after deck placement.

Prestress Loss Due to Shrinkage of Girder Concrete in the Composite Section

$$\Delta\epsilon_p = \Delta\epsilon_c$$

$$\frac{\Delta P_p}{A_{ps}E_p} = \epsilon_{bdf} - \left(\frac{\Delta P_p}{E''_{c1}A_{nc}} + \frac{\Delta P_p}{E''_{c1}}\frac{e^2_{pnc}}{I_{nc}}\right)$$

$$\frac{\Delta P_p}{A_{ps}}\left[1 + \frac{E_p}{E''_{ci}}\frac{A_{ps}}{A_{nc}}\left(1 + \frac{A_{nc}e^2_{pnc}}{I_{nc}}\right)\right] = \epsilon_{bdf}E_p$$

$$E''_{c1} = \frac{E_{ci}}{1 + \chi\psi_{bif}}$$

$$\alpha_{nc} = 1 + \frac{A_{nc}e^2_{pnc}}{I_{nc}}$$

$$\rho_{nc} = \frac{A_{ps}}{A_{nc}}$$

$$K_{df} = \frac{1}{1 + n_i\rho_{nc}\alpha_{nc}(1 + \chi\psi_{bif})}$$

$$\Delta f_{pSD} = \frac{\Delta P_p}{A_{ps}}$$

$$\Delta f_{pSD} = \epsilon_{bdf}E_pK_{df}$$

where:

ϵ_{bdf} = shrinkage strain of the girder between the time of deck placement and the final time;
e_{pnc} = eccentricity of strands with respect to centroid of the net composite section at service, always taken as positive;
α_{nc} = factor for net composite section properties;
ρ_{nc} = tensile reinforcement ratio for net composite section
χ = aging coefficient = 0.7; and
K_{df} = transformed section factor based on age-adjusted effective modulus of elasticity of concrete, used to adjust the small gain in steel stress resulting from the continuous interaction between concrete and steel components of the member, between the time of deck placement and the final time.

Prestress Loss Due to the Creep of Girder Concrete in the Composite Section Caused by the Initial Prestressing Force and Self Weight

$$\Delta\epsilon_p = \Delta\epsilon_c$$

$$\frac{\Delta P_p}{A_{ps}E_p} = \frac{f_{cgp}}{E'_{c2}} - \left(\frac{\Delta P_p}{E''_{c1}A_{nc}} + \frac{\Delta P_p}{E''_{c1}}\frac{e^2_{pnc}}{I_{nc}}\right)$$

$$\frac{\Delta P_p}{A_{ps}E_p} = \frac{f_{cgp}}{E_{ci}}(\psi_{bif} - \psi_{bid}) - \left(\frac{\Delta P_p}{E_{ci}A_{nc}} + \frac{\Delta P_p}{E_{ci}}\frac{e^2_{pnc}}{I_{nc}}\right)(1 + \chi\psi_{bif})$$

$$E'_{c2} = \frac{E_{ci}}{\psi_{bif} - \psi_{bid}}$$

$$E''_{c1} = \frac{E_{ci}}{1 + \psi_{bif}}$$

$$\frac{\Delta P_p}{A_{ps}}\left[1+\frac{E_p}{E_{ci}}\frac{A_{ps}}{A_{nc}}\left(1+\frac{A_{nc}e_{pnc}^2}{I_{nc}}\right)(1+\chi\psi_{bif})\right] = \frac{E_p}{E_{ci}}f_{cgp}(\psi_{bif}-\psi_{bid})$$

$$K_{df} = \frac{1}{1+n_i\rho_{nc}\alpha_{nc}(1+\chi\psi_{bif})}$$

$$\Delta f_{pCD1} = \frac{\Delta P_p}{A_{ps}}$$

$$\Delta f_{pCD1} = n_i f_{cgp}(\psi_{bif}-\psi_{bid})K_{df}$$

where:

f_{cgp} = concrete stress at centroid of prestressing strands due to the initial prestressing force and self weight and

E'_{c2} = age-adjusted effective modulus of elasticity of concrete.

Prestress Loss Due to the Creep of Girder Concrete in the Composite Section Caused by Deck Weight and Superimposed Dead Loads

$$\Delta\epsilon_p = \Delta\epsilon_c$$

$$\frac{\Delta P_p}{A_{ps}E_p} = \frac{\Delta f_{cdp}}{E'_{c3}} - \left(\frac{\Delta P_p}{E''_{c1}A_{nc}} + \frac{\Delta P_p}{E''_{c1}}\frac{e_{pnc}^2}{I_{nc}}\right)$$

$$\frac{\Delta P_p}{A_{ps}E_p} = \frac{\Delta f_{cdp}}{E_c}\psi_{bdf} - \left(\frac{\Delta P_p}{E_{ci}A_{nc}} + \frac{\Delta P_p}{E_{ci}}\frac{e_{pnc}^2}{I_{nc}}\right)(1+\chi\psi_{bif})$$

$$E'_{c3} = \frac{E_c}{\psi_{bdf}}$$

$$E''_{c1} = \frac{E_{ci}}{1+\psi_{bif}}$$

$$\frac{\Delta P_p}{A_{ps}}\left[1+\frac{E_p}{E_{ci}}\frac{A_{ps}}{A_{nc}}\left(1+\frac{A_{nc}e_{pnc}^2}{I_{nc}}\right)(1+\chi\psi_{bif})\right] = \frac{E_p}{E_c}f_{cdp}\psi_{bdf}$$

$$K_{df} = \frac{1}{1+n_i\rho_{nc}\alpha_{nc}(1+\chi\psi_{bif})}$$

$$\Delta f_{pCD2} = \frac{\Delta P_p}{A_{ps}}$$

$$\Delta f_{pCD2} = n\Delta f_{cdp}\psi_{bdf}K_{df}$$

where:

Δf_{cdp} = change in concrete stress at centroid of prestressing strands due to long-term losses between transfer and deck placement, deck weight on noncomposite section, and superimposed weight on composite section;

ψ_{bdf} = girder creep coefficient minus the ratio of the strain that exists at the final time to the elastic strain caused when the load is applied at the time of deck placement; and

E'_{c3} = age-adjusted effective modulus of elasticity of the concrete.

Prestress Loss Due to the Relaxation of Strands in the Composite Section

Relaxation loss can be computed for the composite section, between the time of deck placement and the final time of the structure. However a constant value of total loss due to steel relaxation of low-relaxation prestressing strand of 2.4 ksi may be assumed.

Prestress Gain Due to Shrinkage of the Deck in the Composite Section

Prestress loss due to shrinkage of the deck in the composite section could be given by:

$$P_{sd} = \frac{\epsilon_{ddf}A_dE_{cd}}{(1+\chi\psi_{ddf})}$$

$$\Delta\epsilon_p = \Delta\epsilon_c$$

$$\frac{\Delta P_p}{A_{ps}E_p} = \frac{\Delta f_{cdf}}{E''_{c2}} - \left(\frac{\Delta P_p}{E''_{c1}A_{nc}} + \frac{\Delta P_p}{E''_{c1}}\frac{e_{pnc}^2}{I_{nc}}\right)$$

$$E''_{c2} = \frac{E_c}{1+\chi\psi_{bdf}}$$

$$\Delta f_{cdf} = \frac{P_{sd}}{A_{nc}} - \frac{P_{sd}e_{dc}e_{pnc}}{I_{nc}}$$

$$\frac{\Delta P_p}{A_{ps}}\left[1+\frac{E_p}{E_{ci}}\frac{A_{ps}}{A_{nc}}\left(1+\frac{A_{nc}e_{pc}^2}{I_{nc}}\right)(1+\chi\psi_{bif})\right] = \frac{E_p}{E_c}\Delta f_{cdf}(1+\chi\psi_{cdf})$$

$$\Delta f_{pSS} = \frac{\Delta P_p}{A_{ps}}$$

$$\Delta f_{pSS} = n\Delta f_{cdf}K_{df}(1+\chi\psi_{bdf})$$

where:

P_{sd} = horizontal force in the deck due to the shrinkage of the deck concrete;

Δf_{cdf} = change in the concrete stress at centroid of prestressing strands due to shrinkage of the deck concrete;

ϵ_{ddf} = shrinkage strain of the deck concrete between placement and the final time;

e_{dc} = eccentricity of the deck with respect to the transformed composite section at the time of application of SIDL, always taken as negative;
E''_{c2} = age-adjusted effective modulus of elasticity of concrete; and
ψ_{ddf} = deck creep coefficient minus the ratio of the strain that exists at the final time to the elastic strain caused when the load is applied at the time of deck loading.

Summary of Prestress Losses Formulas

The following is a summary of formulas used to estimate prestress losses:

(a) Instantaneous prestress loss due to elastic shortening at transfer (not needed in the calculation of concrete stresses when transformed section properties are used).
(b) Long-term prestress losses between transfer and deck placement due to shrinkage and creep of the girder concrete and relaxation of the prestressing strands.
- Prestress loss due to shrinkage of girder concrete:

$$\Delta f_{pSR} = \epsilon_{bid} E_p K_{id} \quad (66)$$

- Prestress loss due to creep of girder concrete:

$$\Delta f_{pCR} = n_i f_{cgp} \psi_{bid} K_{id} \quad (67)$$

- Prestress loss due to relaxation of strands:

$$\Delta f_{pR2} = \phi_i L_i K_{id} \quad \text{(approximately 1.2 ksi)} \quad (68)$$

(c) Instantaneous elastic gain at the deck (precast transformed section) and SIDL placement (composite transformed section) are accounted for in concrete stress analysis and need not be calculated separately.
(d) Long-term prestress losses between the deck placement and the final time (composite section) due to shrinkage and creep of concrete and relaxation of prestressing strands in the composite section between the deck placement and the final time:
- Prestress loss due to shrinkage of the girder concrete in the composite section:

$$\Delta f_{pSD} = \epsilon_{bdf} E_p K_{df} \quad (69)$$

- Prestress loss due to the creep of the girder under initial loads in the composite section:

$$\Delta f_{pCD1} = n_i f_{cgp} (\psi_{bif} - \psi_{bid}) K_{df} \quad (70)$$

- Prestress gain due to the creep of the girder under the deck and SIDL in the composite section:

$$\Delta f_{pCD2} = n \Delta f_{cdp} \psi_{bdf} K_{df} \quad (71)$$

- Prestress loss due to relaxation of strands in the composite section:

$$\Delta f_{pR3} = \phi_d L_d K_{df} \quad (72)$$

- Prestress gain due to shrinkage of the deck in the composite section:

$$\Delta f_{pSS} = n \Delta f_{cdf} K_{df} (1 + \chi \psi_{bdf}) \quad (73)$$

Spreadsheet Implementation

The spreadsheet given in Appendix L can be used as a design aid in place of manual calculations with a hand-held calculator. A sample output of the spreadsheet is shown in Table 19. It is given for the New Hampshire girder in the manual calculation examples at the end of this chapter.

Proposed AASHTO-LRFD Revisions

Proposed AASHTO-LRFD revisions are given in Appendix M. It is proposed that the detailed method described herein replace the current "REFINED ESTIMATES OF TIME-DEPENDENT LOSSES" in Article 5.9.5.4 of the Specifications.

PROPOSED APPROXIMATE PRESTRESS LOSS METHOD

A simplified derivation and a parametric study of prestress losses in pretensioned high-strength bridge girder were conducted. Factors considered included the level of prestressing, girder cross-section shape, and compressive strength of the concrete. The total long-term loss according to the proposed detailed method is given by the following formula:

$$\begin{aligned}\Delta f_{pLT} = {} & \epsilon_{bid} E_p K_{id} + \epsilon_{bdf} E_p K_{df} + n_i f_{cgp} \psi_{bid} K_{id} \\ & + n_i f_{cgp} (\psi_{bif} - \psi_{bid}) K_{df} + n \Delta f_{cdp} \psi_{bdf} K_{df} \\ & + n \Delta f_{cdf} K_{df} (1 + \chi \psi_{bdf}) + \phi_i L_i K_{id} + \phi_d L_d K_{df}\end{aligned}$$

The first two terms relate to the effects of shrinkage of the girder; the last two terms relate to the relaxation of the prestressing strands. The remainder of the terms relates to creep of the girder due to prestress, girder weight, deck weight, SIDL, and deck shrinkage. The relaxation loss for low-relaxation strands is a very small quantity and may be assumed to be 1.2 ksi between transfer and deck placement and 1.2 ksi for the remaining life. In this method, a total relaxation loss of 2.40 ksi will be assumed. Loss due to shrinkage of the girder, $\epsilon_{bid} E_p K_{id} + \epsilon_{bdf} E_p K_{df}$, is a function of E_p (which may be assumed a constant 28,500 ksi). The

TABLE 19 Spreadsheet sample output
Detailed method using specified/estimated material properties
Precast NE1400BT

Section Properties				Precast Net	Precast Transf. Release	Precast Transf. Final	Deck	Composite Net	Composite Transf.
Steel modular ratio, n_i	E_s/E_{ci}	7.14	A	848.32	910.29	899.42	545.86	1394.18	1445.27
Steel modular ratio, n	E_s/E_c	5.89	y_b	26.47	25.05	25.29	59.12	39.25	38.07
Deck modular ratio	E_d/E_c	0.77	I	349471	374508	370364	2911	706432	762092
			e_p	20.82	19.40	19.64		33.60	32.42
			e_d					-19.87	
			$\alpha = 1+A*e^2/I$	2.05				3.23	
Transfromed section factors, K			K_r Elastic	0.87	K_{dc} Elastic(at SIDL)				0.89
$K=1/(1+n*\alpha*A_s/A_c*(1+0.7*C))$			K_d Elastic	0.89					
			K_{rd} Long-term	0.77	K_{df} Long-term				0.77

Stress Calculation	Steel Stress Change	Steel Stress Net	Net Section Concrete Stress Change	Net Section Concrete Stress Net	Transformed Section Concrete Stress Change	Transformed Section Concrete Stress Net
		200.00				
(1) Elastic due to P_i; $P_i*\alpha*K_r*n_i/A$	26.08	173.92	3.65	3.65	3.65	3.65
(2) Elastic due to self weight; $M*e/I*K_r*n_i$	-5.99	179.92	-0.84	2.81	-0.84	2.81
(3) Shrinkage between release and deck placement; $\varepsilon_{bid}*E_p*K_{rd}$	4.71	175.21				
(4) Creep between release and deck placement; $n_i*f_{cir}*K_r*\psi_{bid}*K_{rd}$	13.41	161.80				
(5) Relaxation between release and deck placement	1.20	160.60	-0.41	2.41	-0.35	2.46
(6) Elastic due to deck weight; $n*\delta f_{cdp}*K_d$	-4.34	164.95	-0.74	1.67	-0.74	1.72
(7) Elastic due to SIDL; $n*\delta f_{csp}*K_{dc}$	-1.52	166.46	-0.26	1.41	-0.26	1.46
(8) Shrinkage of beam, deck placement to final; $\varepsilon_{bdf}*E_p*K_{df}$	3.29	163.18				
(9) Creep of beam due to initial loads, deck to final; $n_i*f_{pc}*(\psi_{bif}-\psi_{bid})*K_{df}$	9.36	153.81				
(10) Creep of beam due to deck and SIDL; $n*df_{pc}*\psi_{bdf}*K_{df}$	-5.85	159.66				
(11) Relaxation between deck placement and final time; $\phi_d*L_d*K_{df}$	1.20	158.46				
(12) Shrinkage of deck; $\varepsilon_{bdf}*E_{cd}/(1+0.7*\psi_{ddf})*A_d*\alpha/A*K_{df}*n*(1+0.7*\psi_{bdf})$	-0.84	159.30	-0.14	1.27	-0.13	1.34
Total Prestress Loss prior to Live Load Application	**40.70**					

shrinkage strain values of $\epsilon_{bid} + \epsilon_{bdf}$ = total shrinkage strain of the girder concrete. Most girders have V/S ratios such that the factor k_s is about 1.0. Most prestressing is transferred within the first day of concrete placement and the corresponding loading age factor is also about 1.0. The total shrinkage thus equals $480 \times 10^{-6}\ k_h\ k_f$. Although the transformed section factors K_{id} and K_{df} are different and vary with the section shape, the parametric study showed that their range of variability is relatively small for standard precast girder sections.

It is conservative for this approximate method to assume a value of $K_{id} = K_{df} = 0.8$, based on analysis of various section shapes. Thus, the shrinkage term may be approximated as $480(10^{-6})28{,}500(0.8)\ k_h k_f = 10.94\ k_h k_f$ ksi, where the factors k_h and k_f account for relative humidity and concrete strength factors, respectively. In the final form, the coefficient 10.94 was modified to 12 to produce a good upper-bound correlation with the test results. Long-term prestress loss due to girder creep takes the following form:

$$n_i f_{cgp} \psi_{bid} K_{id} + n_i f_{cgp} (\psi_{bif} - \psi_{bid}) K_{df} + n \Delta f_{cdp} \psi_{bdf} K_{df} + n \Delta f_{cdf} K_{df} (1 + \chi \psi_{bdf})$$

The first two terms account for the effects of concrete creep due to initial prestress and girder weight; the third term estimates loss due to additional superimposed loads, and the last term is loss due to the interaction between deck shrinkage and girder creep. Because a composite member (e.g., a precast I girder and a cast-in-place deck) becomes stiffer after the deck concrete has hardened, and deck shrinkage commonly creates prestress gain (rather than loss), ignoring the contribution of the increased stiffness due to composite action and the small prestress gain due to deck shrinkage will result in a conservative estimate of prestress loss. Assuming $K_{id} = K_{df} = 0.8$, the long-term creep is $n_i f_{cgp}\ (\psi_{bif})(0.80) + n\Delta f_{cdp}\ \psi_{bdf}\ (0.80)$.

Also, assuming average values for modular ratios of $n_i = 7$ and $n = 6$, the creep coefficient will be reduced to the following formula for loading age of 1 day, loading duration of infinity, and V/S ratio of 3 in. to 4 in. (corresponding to a web width of 6 in. to 8 in.).

$$\psi_{bif} = 1.90\, k_{td} k_{la} k_s k_h k_f = 1.90(1.00)(1.00)(1.00) k_h k_f = 1.9\, k_h k_f$$

It is further assumed that the creep coefficient for the deck and superimposed loads is 0.4 of that for the initial loads. Thus, the creep loss component reduces to $1.90(0.8)k_h k_f\ [7f_{cgp} - 0.4(6)\Delta f_{cdp}]$. It is possible to relate the concrete stresses f_{cgp} and Δf_{cdp}, due to initial loading and additional dead loads, respectively, to the amount of prestressing introduced. Generally, the concrete stress at the bottom fibers at service is kept close to zero. Thus, the individual stresses due to effective prestress, girder weight, deck weight, SIDL and live load add up to zero at time infinity. In beams of common spans, the stress due to external loads is about equally divided between girder weight, deck weight, and live load. Also, the total stress due to external load is equal and opposite to the stress due to effective prestress. Therefore, if the effective prestress is assumed to be 80% of the initial prestress, the relationship between f_{cgp}, Δf_{cdp}, and initial prestress P_i become: $\dfrac{0.8\ P_i \alpha}{A_g} = \dfrac{3 M_g e_p}{I_g}$

$$\text{Creep loss} = 1.90(0.8) k_h k_f \left(\frac{\alpha P_i}{A_g}\right)\left[7\left(0.8 - \frac{0.8}{3}\right) - (0.4)(6)\left(\frac{0.08}{3}\right)\right] = 4.70 k_h k_f \frac{\alpha P_i}{A_g}$$

Based on parametric analysis of standard cross section geometries, α of about 2.0 is reasonable. Thus, the creep loss can be approximated as $10.0 k_h k_f \dfrac{P_i}{A_g}$. In the detailed method, the relative humidity correction factor for shrinkage is different from that for creep. An average coefficient is used and the correction factor symbol is changed to avoid mix-up with the factors for the detailed method.

The final form of the approximate method loss formula is shown below:

$$\Delta f_{pLT} = 10.0 \frac{f_{pi} A_{ps}}{A_g} \gamma_h \gamma_{st} + 12.0 \gamma_h \gamma_{st} + 2.5 \tag{74}$$

$$\gamma_h = 1.7 - 0.01H \tag{75}$$

$$\gamma_{st} = \frac{5}{1 + f'_{ci}} \tag{76}$$

where: γ_h = correction factor for humidity; and γ_{st} = correction factor for concrete strength.

The following assumptions were made to arrive at the approximate method coefficients.

(a) Prestress losses are calculated for conditions at the maximum positive moment section.
(b) No mild steel reinforcement exists at that section.
(c) Elastic losses at transfer or elastic gains due to the application of external loads are not considered.
(d) Prestress is transferred to the concrete at 1 day in accelerated plant curing conditions.
(e) The cast-in-place deck weight (for composite construction) is applied to the precast concrete section without any shoring after at least 28 days from the time of prestress transfer.
(f) V/S ratio for the girder cross section is 3 in. to 4 in.

Proposed AASHTO-LRFD Revisions

Proposed AASHTO-LRFD revisions are given in Appendix M. It is proposed that the approximate method described herein replace the current "APPROXIMATE LUMP SUM ESTIMATE OF TIME-DEPENDENT LOSSES" in Article 5.9.5.3 of the Specifications.

COMPARISON OF MEASURED AND PREDICTED LOSSES

The purpose of estimating prestress losses is to determine the level of prestressing at service. While prestress losses do not affect the ultimate strength of pretensioned girders, they do have a significant impact on the serviceability conditions of the member. Table 20 presents a summary of measured prestress losses for mid-span sections of the seven instrumented bridge girders. It also lists prestress losses estimated with the use of the proposed detailed method and measured material properties. Tables showing the measured and predicted losses of each girder are given in Appendix K. The measured elastic prestress loss at transfer is influenced by the heat of hydration of the concrete, modulus of elasticity of the concrete, and the restraint of girder deformation by the steel forms. The measured long-term prestress losses were adjusted to reflect the losses at time infinity rather than those obtained at 385 to 490 days. This was done by dividing the measured long-term prestress losses by the time-development factor, k_{td}.

The measured total prestress losses for Nebraska girders G1 and G2 were 31.96 ksi and 35.65 ksi, which are 15.8% and 17.6% of the actual jacking stress, respectively. The measured total prestress losses for New Hampshire girders G3 and G4 were 43.51 ksi and 42.33 ksi, 21.5% and 20.9% of the actual jacking stress, respectively. The corresponding values for the Texas girder were 25.35 ksi (12.5%) and for the Washington girders were 42.06 ksi (20.8%) and 39.98 ksi (19.7%). The ratios of the total estimated-to-measured prestress losses ranged from 0.84 to 1.27 with an average of 1.00 and a standard deviation of 15%.

The purpose of Table 21 is to compare the total prestress losses estimated using the PCI-BDM method, the AASHTO-LRFD Refined method, the AASHTO-LRFD Lump-Sum method, the proposed approximate method, and the proposed detailed method with those obtained from the experimental results. Because various methods require different types of input data and because much of the creep and shrinkage properties are typically not available at the time of design, all prediction methods are applied using the specified concrete strength and the corresponding estimated material properties as would typically be done by designers. The last two columns of the table are the values listed in Table 20 for the estimated losses calculated using the proposed detailed method and measured properties. The table shows that the proposed detailed method gives a better correlation with test results than the AASHTO-LRFD Refined method and the PCI-BDM method. The proposed approximate method is almost as accurate as the detailed method and the PCI-BDM method, but is much sim-

TABLE 20 Measured versus estimated prestress losses

Girder	Elastic shortening		Elastic gain due to deck load		Elastic gain due to superimposed dead loads		Loss from transfer to deck		Loss after deck placement		Total long-term losses		Total prestress losses		
	M[1]	E[2]	M	E	M	E	M	E	M	E	M	E	M	E	Ratio of E/M
Nebraska G1	17.02	19.67	-4.52	-5.04	-1.85	-1.85	15.64	31.56	5.67	-3.67	21.31	27.90	31.96	40.68	1.27
Nebraska G2	16.50	19.67	-4.44	-5.04	-1.85	-1.85	19.35	31.56	6.08	-3.67	25.43	27.90	35.65	40.68	1.14
New Hampshire G3	25.17	17.94	-5.36	-3.99	-1.39	-1.39	21.46	22.22	3.63	1.73	35.08	23.95	43.51	36.51	0.84
New Hampshire G4	24.42	17.94	-5.18	-3.99	-1.39	-1.39	20.82	22.22	3.66	1.73	24.48	23.95	42.33	36.51	0.86
Texas G7	12.88	14.71	-5.91	-4.84	-1.56	-1.56	17.16	18.55	2.77	-1.41	19.94	17.14	25.35	25.46	1.00
Washington G18	27.62	20.87	-5.36	-4.06	-1.58	-1.58	13.16	23.51	8.21	-0.28	21.37	23.23	42.06	38.47	0.91
Washington G19	25.49	20.87	-5.33	-4.06	-1.58	-1.58	13.33	23.51	8.06	-0.28	21.40	23.23	39.98	38.47	0.96

[1]M = Measured
[2]E = Estimated
Measured material properties and prestress losses were modified for time infinity. Measured elastic gains due to superimposed dead loads were estimated.

TABLE 21 Measured versus estimated total prestress losses

Girder	Measured[1]	PCI-BDM		AASHTO-LRFD Specifications				Proposed approximate method		Proposed detailed method (using estimated properties)		Proposed detailed method (using measured properties)	
				Refined		Lump-sum							
	Loss	Loss	Ratio*	Loss	Ratio*	Loss	Ratio*	Loss	Ratio*	Loss	Ratio*	Loss	Ratio*
Nebraska G1	31.96	36.85	1.15	52.24	1.63	50.29	1.57	40.18	1.26	38.42	1.20	40.68	1.27
Nebraska G2	35.65	38.27	1.07	52.24	1.47	50.29	1.41	40.18	1.13	40.00	1.12	40.68	1.14
New Hampshire G3	43.51	39.84	0.92	54.26	1.25	50.51	1.16	41.50	0.95	41.39	0.95	36.51	0.84
New Hampshire G4	42.33	39.84	0.94	54.26	1.28	50.51	1.19	41.50	0.98	41.39	0.98	36.51	0.86
Texas G7	25.35	32.11	1.27	52.52	2.07	48.83	1.93	34.20	1.35	27.67	1.09	25.46	1.00
Washington G18	42.06	40.33	0.96	66.86	1.59	52.69	1.25	38.07	0.91	35.85	0.85	38.47	0.91
Washington G19	39.98	40.33	1.01	66.86	1.67	52.69	1.32	38.07	0.95	35.85	0.90	38.47	0.96
Average	---	---	1.05	---	1.57	---	1.41	---	1.07	---	1.01	---	1.00
Standard deviation	---	---	0.12	---	0.26	---	0.25	---	0.16	---	0.12	---	0.15

[1] Modified for time infinity.
* Ratio to measured losses.

pler. The PCI-BDM method gives good results as it accounts for the variability in creep and shrinkage properties. Both AASHTO methods significantly overestimate prestress loss for the instrumented bridges.

COMPARISON WITH PREVIOUSLY REPORTED EXPERIMENTAL RESULTS

Table 22 presents data on measured prestress losses reported in the literature. It also compares the measured total prestress losses with those estimated using the proposed detailed and approximate methods, the AASHTO-LRFD Refined, the AASHTO-LRFD Lump-Sum, and the PCI-BDM methods. Appendix J provides details of the bridge plans, girder cross-section properties, deck geometry, prestressing strands, loads and moments, and material properties for the bridges included in this comparison. All measured data were modified to reflect the losses at time infinity. The following observations can be made based on the data presented:

(a) The measured total prestress losses, including elastic shortening, for all the girders ranged from 25.18 ksi to 69.29 ksi.
(b) The total prestress losses in pretensioned high-strength bridge girders estimated with the proposed detailed method were the closest to the experimental values. The ratios of total prestress losses estimated with various prediction methods to those measured were consistent with the results obtained from the seven bridge girders instrumented in this project. The average ratios of estimated-to-measured total loss were 100%, 108%, 160%, 137% and 106%, using the proposed detailed method, the proposed approximate method, the AASHTO-LRFD Refined method, the AASHTO-LRFD Lump-Sum method, and the PCI-BDM method, respectively.
(c) Measured data from project 4 (presented in Table 22) were questionable because one girder showed total prestress losses that were double than that of an identical girder. Project 6 measurements consistently exceeded those predicted with the PCI-BDM and the proposed detailed methods and two beams showed higher measured prestress losses than those predicted by the AASHTO-LRFD Lump-Sum method despite the fact that the measured compressive strength of the beams involved was about 10 ksi.
(d) The total prestress losses estimated with the AASHTO-LRFD Refined method were consistently and substantially higher than the experimental values.
(e) The PCI-BDM method provided values closer to those measured than the AASHTO-LRFD methods.

NUMERICAL EXAMPLES: COMPARISON OF PROPOSED PRESTRESS LOSS PREDICTION METHODS WITH AASHTO-LRFD METHODS

The main purpose for calculating prestress loss is to determine concrete tensile stresses at the bottom fibers at the maximum positive moment section (mid-span in simply supported members) and to ensure that the concrete tensile stress limit is not exceeded at service conditions. As indicated earlier, it is proposed that transformed section properties be used in analysis. Therefore, elastic shortening losses and gains are automatically accounted for in the analysis and do not need to be

TABLE 22 Measured versus estimated total prestress losses for previously reported experiments

Project		Measured[1]	PCI-BDM	AASHTO-LRFD Specifications		Proposed approx.	Proposed detailed
				Refined	Lump-sum		
No.	Reference						
1	Greuel et al. (*37*)	37.74	34.16	46.31	32.03	35.81	37.83
2	Pessiki et al. (*38*)	36.46	42.48	47.45	50.15	34.69	33.74
		36.64	42.99	47.64	50.98	36.27	35.56
3	Mossiossian et al. (*39*)	32.54	34.07	45.87	52.05	36.72	35.20
		35.11	34.07	45.87	52.05	36.72	35.20
4	Kebraei et al. (*40*)	17.92	23.68	36.61	38.93	23.92	23.71
		36.77	23.68	36.61	38.93	23.92	23.71
5	Shenoy et al. (*41*)	25.18	37.32	31.66	32.92	32.25	36.67
6	Stanton et al. (*42*)	34.17	25.76	34.72	41.29	26.71	31.62
		34.00	27.52	34.72	41.29	26.71	31.62
		65.62	40.14	63.35	54.31	38.45	39.06
		55.06	40.14	63.35	54.31	38.45	39.06
		69.29	40.14	63.35	54.31	38.45	39.06
7	Seguirant et al. (*43*)	36.11	43.33	50.05	51.25	35.16	41.66
		41.65	44.00	50.28	51.69	37.05	46.63
		35.03	46.06	50.39	53.40	37.91	47.98
8	Gross et al. (*35*)	35.68	37.98	61.76	48.21	38.50	33.91
		30.30	40.24	65.73	49.91	39.50	30.03
		32.51	38.41	60.95	47.59	38.01	34.64
		26.02	34.00	55.57	46.35	35.89	30.52
9	Gross et al. (*35*)	43.69	48.63	92.35	58.42	53.29	43.60
		50.80	48.87	92.60	58.42	53.43	43.85
		43.99	49.29	95.13	57.94	57.10	45.51
		44.68	49.81	95.07	58.20	56.40	44.84
		49.93	41.68	80.53	53.46	49.51	39.25
		50.80	48.90	95.43	59.05	56.46	44.88
		48.46	50.45	96.94	59.11	57.47	46.16
10	Gross et al. (*35*)	28.24	34.18	48.92	47.50	38.81	31.24
		27.95	34.18	48.92	47.50	38.81	31.24
		26.25	34.18	48.92	47.50	38.81	31.24
		23.96	30.64	46.36	47.48	36.76	27.72
Ave. Estimated/Measured Ratio			1.06	1.60	1.37	1.08	1.00

[1]Modified for time infinity.

calculated separately. Since most designers currently use gross section properties, it is necessary for them to calculate and account for elastic losses and gains separately to accurately determine the concrete tensile stresses. The following series of examples demonstrate the two main issues being examined:

(1) It is necessary to accurately estimate prestress loss for accurate calculation of concrete tensile stresses.
(2) Whether gross or transformed section properties are used, the calculated concrete stresses are essentially the same if the proper components of the prestress loss are used. Either long-term losses due to creep, shrinkage, and relaxation in conjunction with transformed section properties, or total losses (including elastic losses and gains) in conjunction with gross section properties should be used.

An interior beam of the New Hampshire bridge used in the experimental program is used in these examples. All data used in these examples were those specified in the design documents.

Input Data

Girder type: New England NE1400BT, with an 8-in. thick cast-in-place composite deck slab
Effective slab width = 89 in.;
Ambient relative humidity at the bridge is estimated to be 70%;
Specified initial concrete compressive strength f'_{ci} = 5.7 ksi;
Specified ultimate compressive strength, f'_c, for the girder concrete = 8 ksi and that of the deck concrete = 5 ksi;
Precast girder properties are A_g = 857 in.^{2}, h = 55.12 in., I_g = 353,196 in.^{4}, y_b = 26.26 in.;
Prestressing immediately before transfer f_{pi} = 200 ksi introduced with 40-0.6 in. diameter, low-relaxation strands;
A_{ps} = 8.68 in.^{2};

Eccentricity of strands relative to the gross girder area centroid is 20.61 in.;
Initial tension just before transfer of prestress is 200 ksi;
Modulus of elasticity is E_P = 28,500 ksi;
Bending moments at mid-span:
Due to girder weight, M_g = 16,203 k-in.;
Due to deck weight, haunch, and diaphragms, M_d = 13,915 k-in.;
Due to SIDL due to the weight of barriers and wearing surface, M_s = 6,058 k-in.; and
Due to live load plus impact, M_l = 20,284 k-in.

The live load moment shown is for AASHTO-LRFD Service III stress calculation, that is, tensile stress limit check. In an earlier example, the modulus of elasticity, shrinkage, and creep of the girder and deck concretes were estimated using the proposed formulas. These properties will be used here as needed by the various methods of loss prediction.

Gross and Transformed Section Properties

E_c at transfer = 3,978 ksi and at service = 4,836 ksi;
Deck concrete modulus of elasticity E_{cd} = 3,707 ksi;
Transforming the prestressing steel area to precast concrete using $n_i = 28{,}500/3978 = 7.16$;
Transformed area is $(n_i - 1)A_{ps} = 6.16(8.68) = 53$ in.^{2};
Total transformed area of the section = 857 + 53 = 910 in.^{2}; and
Composite section properties are calculated by transforming the deck concrete to the girder with an area = $n_d A_d = 0.77\,(8)\,89 = 545$ in.^{2} and a corresponding total area of 857 + 548 = 1402 in.^{2}.

The other properties are similarly calculated as shown in Table 23.

Example 1—Approximate Loss Method and Transformed Section Properties

The elastic shortening loss of prestress due to introduction of prestress to the concrete member as well as any instantaneous gain due to the application of gravity loads are automatically accounted for if transformed section properties are used in the analysis. The long-term prestress loss may be calculated as follows:

$$\Delta f_{pLT} = 10.0\,\frac{f_{pi}A_{ps}}{A_g}\,\gamma_h\gamma_{st} + 12.0\,\gamma_h\gamma_{st} + 2.5$$

$$\gamma_h = 1.7 - 0.01H = 1.7 - 0.01(70) = 1.00$$

$$\gamma_{st} = 5/(1 + f'_{ci}) = 5/(1 + 5.7) = 0.75$$

$$\Delta f_{pLT} = (10.0)\left(\frac{200 \times 8.68}{857}\right)(1.00)(0.75) + (12.0)(1.00)(0.75) + 2.5$$

$$\Delta f_{pLT} = 15.19 + 9.00 + 2.50 = 26.69\ \text{ksi}$$

The long-term prestress losses are assumed to be equivalent to a negative prestress, $\Delta P = \Delta f_{pLT}A_{ps} = 26.69\ (8.68) = 232$ kip, applied at centroid of the steel area to the net concrete section, or more approximately to the transformed concrete section. Three loading stages are considered for computing concrete stresses:

(a) Prestress transfer.
(b) Placement of the deck and the occurrence of long-term loss.
(c) Superimposed dead and live loads.

For illustration, calculation of the bottom fiber concrete stress due to prestress transfer, using initial prestress force just before transfer, P_i, and transformed section properties:

$$f_{cb} = \frac{P_i}{A_{ti}} + \frac{P_i e_p y_b}{I_{ti}} + \frac{M_g y_b}{I_{ti}} = \frac{200(8.68)}{910} + \frac{200(8.68)\,19.4(25.05)}{374,534} - \frac{16,203(25.05)}{374,534}$$

$$= 1.91 + 2.25 - 1.08 = 3.08\ \text{ksi}$$

The bottom fiber stress due to deck plus haunch and diaphragms are calculated with precast section transformed

TABLE 23 Section properties

	Precast section			Composite section	
	Gross	Transformed at transfer	Transformed at service	Gross	Transformed
A, in.^{2}	857	910	899	1402	1445
y_b, in.	26.26	25.05	25.29	39.05	38.06
y_t, in.	28.86	30.07	29.83	16.07	17.06
I, in.^{4}	353,196	374,534	370,385	716,173	762,151
e_p, in.	20.61	19.40	19.64	33.39	32.41

properties at service. The SIDL and live load effects are calculated with composite section transformed properties. The various stress components are summarized in Table 24.

The AASHTO-LRFD concrete stress limit at service is $-0.19\sqrt{f'_c} = -0.19\sqrt{8.0} = -0.537$ ksi (i.e., tension). The bottom fiber stress shown in the table is compression and is thus below the limit.

Although not required in design, the elastic shortening loss of steel stress at transfer as well as the elastic changes in steel stress at the time of application of various loads can be determined by simply substituting y_b in the above stress formula for e_p and multiplying the resulting concrete stress at steel centroid by the steel modular ratio n_i or n, whichever is applicable.

The following is an example:

Concrete stress at transfer at steel centroid = 200(8.68)/910 + 200(8.68)19.40(19.40)/374,534 − 16,203(19.40)/374,534 = 1.91 + 1.74 − 0.84 = 2.81 ksi and
Elastic loss at transfer = 2.81(7.16) = 20.14 ksi.
Similarly, the elastic gain at deck placement is −4.34 ksi, that due to SIDL is −1.52 ksi and that due to live load is −5.08 ksi.

Example 2—Approximate Loss Method and Gross Section Properties

The common practice at present is to use gross concrete section properties for concrete stress calculation to check against code limits. Some commercial software packages give designers the option of using transformed section properties, which give the impression that considerable savings could result from this refinement. This stipulation is based on the assumption that long-term prestress losses given in the AASHTO-LRFD Specifications are valid regardless of whether gross or transformed section properties are used.

This example demonstrates that proper accounting for elastic prestress loss components produces accurate results regardless of whether gross or transformed section properties are used. It also shows that the use of gross section properties requires the extra steps of separately calculating elastic shortening loss at transfer and gain increments at various loading stages. Elastic loss may be calculated using transformed section properties as shown in Example 1 or using the approximate formula given in the AASHTO-LRFD Specifications. For clarity of comparison, the elastic loss value from Example 1 will be used. Elastic loss calculation according to the LRFD formula is given in Example 3.

Based on Example 1, the initial prestress, P_o, equals (200.00 − 20.14)40(0.217) = 1561 kip. The elastic gain due to deck weight = −4.34 ksi = −38 kip, that due to SIDL = −0.52 ksi = −13 kip and that due to live load = −5.08 ksi = 44 kip. All loads and prestress forces are applied to the gross precast section, except the SIDL and live load and the associated elastic prestress gains which are applied to the gross composite section. Table 24 shows that while the results are comparable to the more direct analysis of Example 1, the elastic loss/gain calculation is unnecessary.

TABLE 24 Comparisons of prestress losses and concrete bottom fiber stress

Loading stage	Loading	Prestress loss method* (ksi)					Concrete bottom fiber stress (ksi)				
		1	2	3	4	5	1	2	3	4	5
Prestress transfer	P_i	26.13	29.50	29.50	26.13	29.50	4.16	4.69	4.69	4.16	4.69
Girder self weight	M_g	-6.01	-6.80	-6.80	-6.01	-6.80	-1.08	-1.20	-1.20	-1.08	-1.20
	Elastic loss		-2.95	-2.95		-2.95		-0.47	-0.47		-0.47
Subtotal		**20.12**	**19.75**	**19.75**	**20.12**	**19.75**	**3.08**	**3.02**	**3.02**	**3.08**	**3.02**
Deck placement	M_d	-4.34	-4.77	-4.77	-4.34	-4.77	-0.95	-1.03	-1.03	-0.95	-1.03
	Elastic gain		0.52					0.10			
	Long-term loss				19.31		-0.57			-0.41	
Superimposed D.L.	M_s	-1.52	-1.65	-1.65	-1.52	-1.65	-0.30	-0.33	-0.33	-0.30	-0.33
	Elastic gain		0.17					0.03			
	Long-term loss	26.69	26.69	31.35	6.07	34.20		-0.53	-0.74	-0.12	-0.81
Live load + impact	M_l	-5.08	-5.57	-5.57	-5.08	-5.57	-1.01	-1.11	-1.11	-1.01	-1.11
	Elastic gain		0.61					0.11			
Total		**35.87**	**37.75**	**39.11**	**34.56**	**41.96**	**0.25**	**0.26**	**-0.19**	**0.29**	**-0.24**

* Method 1: proposed approximate method with transformed section properties.
Method 2: proposed approximate method with gross section properties.
Method 3: AASHTO LRFD Lump-Sum method with gross section properties.
Method 4: Proposed detailed method with transformed section properties.
Method 5: AASHTO-LRFD Refined method with gross section properties.

Example 3—AASHTO-LRFD Lump-Sum Method

The proposed approximate method demonstrated in Examples 1 and 2 is intended to be offered as a replacement of the AASHTO-LRFD Lump-Sum method. This example demonstrates the AASHTO-LRFD Lump-Sum method. According to the AASHTO-LRFD Specifications, the elastic shortening loss at prestress transfer may be calculated using the following formula:

$$\Delta f_{pES} = n_i f_{cgp}$$

where: f_{cgp} = concrete stress at the center of gravity of prestressing tendons due to the prestressing force at transfer and the self weight of the member. Exact calculation of f_{cgp} and Δf_{pES} requires knowledge of the prestress force immediately after transfer, which is a function of Δf_{pES} itself. The Specifications allow use of the approximate value of steel stress after transfer of 0.70 f_{pu} = 0.70(270) = 189 ksi for the calculation of f_{cgp}.

$$f_{cgp} = \frac{P_o}{A_g} + \frac{P_i e_p^2}{I_g} + \frac{M_g e_p}{I_g} = \frac{189(8.68)}{857} + \frac{1.89(8.68)(20.61)^2}{353,196} + \frac{16,203(20.61)}{353,196} = 2.94\,\text{ksi}$$

$$\Delta f_{pES} = 7.16(2.94) = 21.05\,\text{ksi}$$

Alternatively, a formula is given in the AASHTO-LRFD Commentary that implicitly employs the transformed section concept described above for the calculation of Δf_{pES}. In that case, the elastic loss would be 20.14 ksi as calculated in Example 1. For clarity of comparison, the 20.14 ksi value is used here. There is no mention in the AASHTO-LRFD of elastic stress changes in steel at stages of loading other than at transfer of prestress. These changes are thus implied to be included in the long-term loss formula.

The long-term loss according to Table 5.9.5.3-1 of the AASHTO-LRFD (*1*) is as follows:

$$33.0\left[1.00 - 0.15\left(\frac{f'_c - 6}{6}\right)\right] + 6.00\text{PPR} - 6.00 = 33\left[1 - 0.15\frac{8-6}{6}\right] + 6(1.0) - 6 = 31.35\,\text{ksi}$$

PPR = partial prestress ratio (1.0 for prestressed precast beams)

Example 4—Proposed Detailed Method

The detailed method of prestress loss calculation requires calculating creep and shrinkage material properties. The required values will be calculated as needed for determining the concrete bottom fiber stress. The bottom fiber stress and the stress at steel centroid will be determined at the various stages of construction.

Elastic shortening loss due to initial prestress force and girder self weight is automatically accounted for, as shown in Example 1, if transformed section properties are used. The concrete bottom fiber stress at transfer is 3.08 ksi, and the stress at steel centroid is 2.81 ksi.

Girder shrinkage strain from transfer to deck placement:
$\epsilon_{bid} = 217 \times 10^{-6}$

Girder creep coefficient from transfer to deck placement:
$\psi_{bid} = 0.86$

Girder creep coefficient from transfer to final time: $\psi_{bif} = 1.45$

Substituting the value of $\alpha_g = 1 + \frac{e_p^2 A_g}{I_g}$

$$= 1 + \frac{(20.61)^2 857}{353,196} = 2.03$$

Transformed section factors between transfer and deck placement:

$$K_{id} = \frac{1}{1 + n_i \alpha_g \frac{A_{ps}}{A_g}(1 + 0.7\psi_{bif})} = \frac{1}{1 + 7.16(2.03)\frac{8.68}{857}[1 + 0.7(1.45)]} = 0.77$$

Long-term prestress losses between transfer and deck placement:

Shrinkage loss: $\Delta f_{pSR} = \epsilon_{bid} E_p K_{id} = 217 \times 10^{-6}\,(28{,}500)0.77$
$= 4.76$ ksi

Creep loss: $\Delta f_{pCR} = \Delta f_{pES} \psi_{bid} K_{id} = 20.16(0.86)0.77$
$= 13.35$ ksi

Relaxation loss: $\Delta f_{pR2} = 1.20$ ksi

Total losses: $\Delta f_{pid} = \Delta f_{pSR} + \Delta f_{pCR} + \Delta f_{pR2}$
$= 4.76 + 13.35 + 1.20$
$= 19.31$ ksi

Therefore, the change in concrete stress at the level of prestressing strands, Δf_{pc}, is:

$$\Delta f_{cd} = \frac{\Delta f_{pid} A_{ps} \alpha}{A_g} = \frac{19.31(8.68)2.03}{857} = 0.40\,\text{ksi}$$

$$\Delta f_{pc} = f_{cgp} - \Delta f_{cd} = 2.81 - 0.40 = 2.41\,\text{ksi}$$

The concrete stresses just prior to deck placement are the sum of the stresses at transfer and the long-term losses between transfer and deck placement. The change in concrete stress at the bottom fiber due to long-term loss is:

$$\Delta P = \Delta f_{pid} A_{ps} = -19.31 \times 8.68 = -168\,\text{kip}$$

$$\Delta f_{cb} = \frac{-168}{899} + \frac{-168(19.64)(25.29)}{370,385} = -0.41\,\text{ksi}$$

Therefore, the concrete bottom stress just prior to deck placement is = 3.08 –0.41 = 2.67 ksi.

The concrete stress due to deck placement is computed using precast transformed section properties at service, while the concrete stress due to SIDL is calculated using composite transformed section properties. As shown in Example 1, the change in the concrete stress at the bottom fiber of the girder is = –0.95 –0.30 = –1.25 ksi. Therefore, the concrete bottom stress just after placement of the deck and SIDL is = 2.67 –1.25 = 1.42 ksi.

Shrinkage strain from deck placement to final:
$\epsilon_{bdf} = 150 \times 10^{-6}$

Deck shrinkage strain from deck placement to final:
$\epsilon_{ddf} = 451 \times 10^{-6}$

Girder creep coefficient from deck placement to final time:
$\psi_{bdf} = 0.90$

Deck creep coefficient from deck placement to final time:
$\psi_{ddf} = 1.79$

$$K_{df} = 1 \Big/ \left(1 + n_i \alpha_{gc} \frac{A_{ps}}{A_{gc}} (1 + 0.7\psi_{bif})\right)$$

$$= 1 \Big/ \left(1 + 7.16(3.12) \frac{8.68}{1402} [1 + 0.7(1.45)]\right) = 0.78$$

Shrinkage loss: $\Delta f_{pSD} = \epsilon_{bdf} E_p K_{df} = 150 \times 10^{-6}\,(28{,}500)0.78$
$= 3.33$ ksi

Creep loss due to initial loads:

$$\Delta f_{pCD1} = n_i f_{cgp} (\psi_{bif} - \psi_{bid}) K_{df}$$

$$= 7.16(2.81)(1.45 - 0.86)0.78 = 9.26\,\text{ksi}$$

Creep loss due to deck and SIDL: $\Delta f_{pCD2} = n \Delta f_{cdp} \psi_{bdf} K_{df}$

The long-term loss between transfer and deck placement produces a concrete stress change of –0.41 ksi. The change in concrete stress due to instantaneous application of deck weight and SIDL is –0.95 ksi and –0.30 ksi, respectively, as calculated in Example 1. Thus, Δf_{pCD2} = 5.89(–0.41 –0.95 –0.30)(0.90)(0.78) = –6.86 ksi.

Relaxation loss: $\Delta f_{pR3} = 1.20$ ksi
Prestress gain due to shrinkage of the deck: Δf_{pSS}:
Change in concrete stress at the level of prestressing strands due to shrinkage of the deck.

$$\Delta f_{ssp} = \left[\frac{\epsilon_{ddf} A_d E_{cd}}{1 + 0.7\psi_{ddf}}\right]\left[\frac{1}{A_{gc}} + \frac{e_{pc} e_{dc}}{I_{gc}}\right]$$

$$\Delta f_{ssp} = \left[\frac{451 \times 10^{-6}(712)(3,707)}{1 + 0.7(1.79)}\right]$$

$$\left[\frac{1}{1,402} + \frac{(33.39)(-16.07 - 4.00)}{716,173}\right] = -0.12\,\text{ksi}$$

$$\Delta f_{ssp} = \Delta f_{ssp} K_{df} n(1 + 0.7\psi_{bdf})$$

$$= -0.12(0.78)5.89[1 + 0.7(0.9)] = -0.90\,\text{ksi}$$

Total long-term stress change between deck placement and final time:

$$\Delta f_{pdf} = \Delta f_{pSD} + \Delta f_{pCD1} + \Delta f_{pCD2} + \Delta f_{pR2} + \Delta f_{pSS}$$

$$= 3.33 + 7.62 + (-6.82) + 1.20 + (-0.90) = 6.07\,\text{ksi}$$

The change in the concrete stress at the bottom fiber of the girder due to long-term losses is:

$$\Delta P = \Delta f_{pdf} A_{ps} = 6.07 \times 8.68 = 53\,\text{kip}$$

$$\Delta f_{cb} = -\frac{53}{1445} - \frac{53(32.41)38.06}{762,151} = -0.12\,\text{ksi}$$

The net concrete bottom fiber stress before live load application = 1.42 – 0.12 = 1.30 ksi.

Concrete Stresses Due to Live Load

The concrete stress due to live load was calculated in Example 1, using composite transformed section properties, to be –1.01 ksi. Therefore, the net concrete bottom stress at service = 1.30 – 1.01 = 0.29 ksi.

Example 5—AASHTO-LRFD Refined Method

The AASHTO-LRFD Specifications Refined method of loss calculation includes elastic loss at transfer as previously calculated in addition to long-term losses calculated separately for shrinkage, creep, and relaxation effects. Similar to the Lump-Sum method, the elastic gains due to external loads, other than member self weight, are implicitly included in the long-term estimate.

Shrinkage Loss: Δf_{pSR}

$$\Delta f_{pSR} = 17.0 - 0.15H = 17 - 0.15(70) = 6.51\,\text{ksi}$$

Creep Loss: Δf_{pCR}

$$\begin{aligned}\Delta f_{pCR} &= 12.0 f_{cgp} - 7.0 f_{cdp} \\ &= 12.0(2.81) - 7.0\left[\frac{13,915(20.61)}{353,196} + \frac{6,058(33.39)}{716,173}\right] \\ &= 33.72 - 7.0(0.81 + 0.28) = 33.72 - 7.65 \\ &= 26.07\,\text{ksi}\end{aligned}$$

Relaxation Loss: Δf_{pR2}

$$\begin{aligned}\Delta f_{pR2} &= 0.3\left[20.0 - 0.4\Delta f_{pES} - 0.2\left(\Delta f_{pSR} + \Delta f_{pCR}\right)\right] \\ &= 0.3[20.0 - 0.4(20.16) - 0.2(6.51 + 26.07)] \\ &= 0.3(20.0 - 8.06 - 6.51) = 1.63\,\text{ksi}\end{aligned}$$

Thus, total long-term loss = 6.51 + 26.07 + 1.63 = 34.20 ksi.

The concrete stress analysis is similar to that for Example 3, except that the concrete stress due to long-term loss changes from 0.74 ksi to (–0.74)(34.20/31.35) = –0.81 ksi, and the net final concrete stress changes from –0.19 ksi to –0.26 ksi.

CHAPTER **4**

CONCLUSIONS AND SUGGESTED RESEARCH

CONCLUSIONS

Observations, conclusions, and recommendations related to individual areas within this research are given in this chapter. Below is a summary of general conclusions:

(a) The prestress losses prediction formulas used by current AASHTO Specifications do not account for the variability in material properties.

(b) The modulus of elasticity of concrete has been shown to have a high degree of variability, attributed to such factors as properties and the proportion of the coarse aggregates used, moisture content and temperature of the constituents at time of mixing, methods of mixing and curing, method of testing, size and shape of specimens tested, and difference between compaction of concrete in the precast member and that in a test cylinder. A formula has been proposed for estimating modulus of elasticity that assumes a concrete unit weight relationship to concrete strength. The proposed formula has been shown to give more accurate estimates than those obtained by the current AASHTO-LRFD and ACI-363 formulas.

(c) This research has determined that concrete compressive strength, V/S ratio, curing methods, and time elapsed after the end of curing influence shrinkage. A proposed shrinkage formula produced results that averaged 105% of the measured values, compared to 174% when using the AASHTO-LRFD method and 155% when using the ACI-209 method.

(d) The creep coefficient is influenced by the same factors that influence the shrinkage coefficient in addition to the age of the concrete at the time of loading and the time elapsed after loading. A proposed creep formula produced results that averaged 98% of the experimental values, compared to 161% for AASHTO-LRFD and 179% for those estimated using ACI-209.

(e) Predictions of modulus of elasticity, shrinkage, and creep are influenced by local materials and practices. Therefore, data for local materials and mixture proportions should be used when available.

(f) Temperature rise in a precast member due to heat of hydration and steam curing initially restrains the member as concrete begins to set. However, when the member cools toward ambient temperature, concrete contraction leads to tensile stresses which may offset or exceed the internal compressive stresses developed during initial cement hydration. These effects should be carefully considered in interpreting the concrete strain data, especially in the first 48 hours after concrete placement.

(g) A detailed method for estimating prestress losses in pretensioned bridge girders has been proposed. The method is applicable for noncomposite members, composite precast girders with cast-in-place decks, and high-strength concrete.

(h) An approximate method has been proposed for estimating long-term prestress loss due to shrinkage and creep of concrete and relaxation of strands. The method proposes coefficients for typically encountered conditions in pretensioned girder bridge applications.

(i) Seven girders were instrumented in Nebraska, New Hampshire, Texas, and Washington, representing a range of geographic conditions and construction practices. The measured total prestress losses averaged 37.3 ksi.

(j) Measured elastic loss was higher than the average estimated loss by all prediction methods; it averaged 114% of the estimated value. The average measured total loss was very close to the average predicted total loss.

(k) Test results reported in the literature showed that the total prestress losses averaged 38.5 ksi; the initial elastic loss was 19.0% of the jacking stress of 202.5 ksi.

(l) The AASHTO-LRFD Refined method tends to overestimate creep effects because it does not consider the reduction in the creep coefficient associated with the increase in concrete strength.

(m) The AASHTO-LRFD Lump-Sum method results showed a better agreement with test results than the Refined method, because it accounts for the variability of the loss with concrete strength.

(n) The proposed approximate method produces better estimates of long-term prestress losses than those obtained by the AASHTO-LRFD Lump-Sum method because the Lump-Sum method does not account for the level of prestressing or ambient relative humidity.

SUGGESTED RESEARCH

This project focused on precast pretensioned girder bridges. Further research is needed to investigate prestress losses in post-tensioned high-strength concrete bridges. In particular, spliced girder bridges, reinforced with both pretensioning and post-tensioning should be considered because of the multi-stage nature of prestressing.

Further research is also needed to investigate initial and long-term girder camber. Data from field installations could be used to calibrate the analytical results obtained on the basis of the theory developed in this project.

SIGN CONVENTION AND NOTATION

SIGN CONVENTION

The following sign convention is used in this report. A positive moment is one which produces tension in the bottom fibers of a beam. Conversely, a negative moment is one which produces tension in the top fibers. Stress (or strain) is positive when tensile in steel or compressive in concrete. Downward distance from section centroid is positive. Conversely, an upward distance from section centroid is negative.

NOTATION

The symbols used in this report are defined when they first appear in the text. The symbols are as consistent as possible with those used in the AASHTO-LRFD Specifications. Previous relevant research on material properties and prestress loss sometimes use symbols that are inconsistent with those in AASHTO-LRFD. Symbols that are unique to that research are defined when they appear in the text and are not listed below.

SYMBOL	DESCRIPTION
AASHTO	American Association of State Highway and Transportation Officials
ACI	American Concrete Institute
ASTM	American Society for Testing and Materials
A_d	Area of deck (in.^{2})
A_g	gross cross section area (in.^{2})
A_{gc}	gross area of composite cross-section (in.^{2})
A_n	net cross section area of precast member (in.^{2})
A_{nc}	net area of composite cross section (in.^{2})
A_{ps}	area of prestressing steel (in.^{2})
A_{ti}	area of transformed cross section at transfer (in.^{2})
CR_C	loss of prestress due to creep of concrete (ksi)
E_c	modulus of elasticity of concrete (ksi)
E_{cd}	modulus of elasticity of cast-in-place deck (ksi)
E_{ci}	modulus of elasticity of girder concrete at transfer (ksi)
E'_{c1}, E'_{c2}, E'_{c3}	age-adjusted effective modulus of elasticity of concrete at times 1, 2, and 3 due to constant sustained stress (ksi)
E''_{c1}, E''_{c2}	age-adjusted effective modulus of elasticity of concrete at times 1 and 2 due to gradually developing stress (ksi)
E_p	modulus of elasticity of prestressing steel (ksi)
e_{dc}	eccentricity of deck with respect to gross composite section, always negative (in.)
e_{pc}	eccentricity of steel with respect to gross composite section, always positive (in.)
e_{pn}	eccentricity of steel with respect to net precast section, always positive (in.)
e_{pnc}	eccentricity of steel with respect to net composite section, always positive (in.)
e_{pti}	eccentricity of steel with respect to initial transformed section, always positive (in.)
f'_c	specified compressive strength of concrete at 28 days, unless another age at service is specified (ksi)
f_{cb}	concrete stress at the extreme bottom fiber of precast girder (ksi)
f_{cgp}	concrete stress at center of prestressing steel due to initial prestressing force and member weight at section of maximum moment (ksi)
f'_{ci}	specified compressive strength of concrete at time of initial loading or prestressing (ksi)
f_{pc}	concrete stress at center of prestressing steel (ksi)
f_{pe}	effective prestressing steel stress after losses (ksi)
f_{pi}	initial prestressing steel stress at the beginning of a relaxation loss period (ksi)
f_{pj}	prestressing steel stress at jacking (ksi)
f_{ps}	average prestressing steel stress at service (final) time (ksi)
f_{pt}	prestressing steel stress immediately after transfer (ksi)
f_{pu}	specified tensile strength of prestressing steel (ksi)
f_{py}	yield strength of prestressing steel (ksi)
f_y	specified yield strength of reinforcing bars (ksi)
H	average annual ambient mean relative humidity (percent)
h	overall thickness of member (in.)
I_g	moment of inertia of the gross precast cross section (in.^{4})
I_{gc}	moment of inertia of gross composite cross section (in.^{4})
I_n	moment of inertia of net precast cross section at transfer (in.^{4})
I_{nc}	moment of inertia of net composite cross section (in.^{4})
I_{tc}	moment of inertia of transformed composite section (in.^{4})
I_{td}	moment of inertia of transformed precast section (in.^{4})

I_{ti}	moment of inertia of transformed section at transfer (in.^{4})
K_1	correction factor for aggregate type in predicting average value
K_2	correction factor for aggregate type in predicting upper and lower bounds
K_{df}	transformed section age-adjusted effective modulus of elasticity factor, for adjustment between the time of deck placement and the final time
K_{id}	transformed section age-adjusted effective modulus of elasticity factor, for adjustment between the time of transfer and deck placement
k_c	volume-to-surface ratio correction factor
k_f	concrete strength creep correction factor
k_{hc}	humidity correction factor for creep
k_{hs}	humidity correction factor for shrinkage
k_h	humidity correction factor, used for both creep and shrinkage
k_{la}	loading age correction factor
k_s	volume-to-surface ratio shrinkage correction factor
k_{td}	time-development correction factor
L	span length (ft)
L_r	intrinsic relaxation loss, which is the loss of stress at constant strain (ksi)
L_i	intrinsic relaxation loss between transfer and deck placement (ksi)
L_d	intrinsic relaxation loss between deck placement and final time (ksi)
M_d	maximum moment due to deck weight (k-in.)
M_g	maximum moment due to self weight (k-in.)
M_l	maximum moment due to live loads with impact (k-in.)
M_s	maximum moment due to superimposed dead loads (k-in.)
n	steel modular ratio = E_p / E_c
n_d	deck concrete modular ratio = E_p / E_{cd}
n_i	initial steel modular ratio E_p / E_{ci}
P_e	effective prestressing force (kip)
P_i	initial prestressing force (kip)
P_{sd}	horizontal force in deck due to shrinkage of deck (kip)
PPR	partial prestressing ratio
SH	shrinkage
t	time (days)
t_d	age of concrete at deck placement (days)
t_f	age of concrete at final time (days)
t_i	age of concrete when load is initially applied (days)
V/S	volume-to-surface ratio of the member
w_c	unit weight of concrete (kcf)
y_b	distance from neutral axis to extreme bottom fibers of precast girder (in.)
y_t	distance from neutral axis to extreme top fibers of precast girder (in.)
y_{tb}	distance from neutral axis to extreme bottom fibers of transformed section at transfer (in.)
y_{bd}	distance from neutral axis to extreme bottom fiber of transformed section at deck placement (in.)
y_{bc}	distance from neutral axis to extreme bottom fiber of transformed composite section (in.)
y_p	distance from centroid of prestressing strands to extreme bottom fiber of precast girder (in.)
α_s	Coefficient of thermal expansion of steel (per °F)
α_g	gross precast section properties factor
α_{gc}	gross composite section properties factor
α_n	net precast section properties factor
α_{nc}	net composite section properties factor
Δf_{cd}	change in concrete stress at center of prestressing steel due to long-term losses between transfer and deck placement, deck weight, and superimposed load (ksi)
Δf_{cdf}	change in concrete stress at center of prestressing steel due to deck shrinkage (ksi)
Δf_{cdp}	change in concrete stress at center of prestressing steel due to deck and superimposed loads (ksi)
Δf_{pc}	change in concrete stress at center of prestressing steel (ksi)
Δf_{pCD1}	loss of steel stress due to creep, between deck placement and final time, of girder under initial loads (ksi)
Δf_{pCD2}	loss of steel stress due to creep, between deck placement and final time, of girder under deck and superimposed load (ksi)
Δf_{pCR}	loss of steel stress due to creep of girder concrete (ksi)
Δf_{pdf}	loss of steel stress between deck placement and final time (ksi)
Δf_{pED1}	elastic prestress gain due to deck placement (ksi)
Δf_{pED2}	elastic prestress gain due to superimposed dead load (ksi)
Δf_{pES}	loss of steel stress due to elastic shortening (ksi)
Δf_{pLT}	total long-term loss of steel stress (ksi)
Δf_{pLT1}	long-term loss of steel stress between transfer and deck placement (ksi)
Δf_{pLT2}	long-term loss of steel stress between deck placement and final time (ksi)
Δf_{pR}	loss of steel stress due to relaxation (ksi)
Δf_{pR1}	loss of steel stress due to relaxation before transfer (ksi)
Δf_{pR2}	loss of steel stress due to relaxation between transfer and deck placement (ksi)

Δf_{pR3}	loss of steel stress due to relaxation between deck placement and final time (ksi)
Δf_{pSD}	loss of steel stress due to shrinkage of girder between deck placement and final time (ksi)
Δf_{pSR}	loss of steel stress due to shrinkage of girder concrete (ksi)
Δf_{pSS}	loss of steel stress due to shrinkage of the deck (ksi)
Δf_{pSR}	loss of steel stress due to shrinkage (ksi)
Δf_{pT}	total loss of steel stress (ksi)
Δf_{pt}	loss of steel stress due to temperature variation (ksi)
ΔP_p	change in prestressing force (ksi)
ΔT	Change in temperature (°F)
ϵ_{bdf}	shrinkage of girder between deck placement and final time (in./in.)
ϵ_{bid}	shrinkage of girder between transfer and deck placement (in./in.)
ϵ_{bif}	shrinkage of girder between transfer and final time (in./in.)
ϵ_{ddf}	shrinkage of deck between deck placement and final time (in./in.)
ϵ_{sh}	shrinkage strain at a given time, t, (in./in.)
$\epsilon_{sh\ u}$	ultimate shrinkage (in./in.)
γ_h	correction factor for humidity
γ_{st}	correction factor for concrete compressive strength
ρ_n	tensile reinforcement ratio for initial net section
ρ_{nc}	tensile reinforcement ratio for net composite section
χ	aging coefficient to account for concrete stress variability with time, taken as a constant 0.7
$\psi(t, t_i)$	creep coefficient minus the ratio of the strain that exists t days after casting to the elastic strain caused when load is applied t_i days after casting
ψ_{bdf}	girder creep coefficient minus the ratio of the strain that exists at final time to the elastic strain caused when load is applied at the time of deck placement
ψ_{bid}	girder creep coefficient minus the ratio of the strain that exists at the time of deck placement to the elastic strain caused when load is applied at the time of transfer
ψ_{bif}	girder creep coefficient minus the ratio of the strain that exists at final time to the elastic strain caused when load is applied at the time of transfer
ψ_{ddf}	deck creep coefficient minus the ratio of the strain that exists at final time to the elastic strain caused when load is applied at the time of deck loading
ψ_u	ultimate creep coefficient

REFERENCES

1. American Association of State Highway and Transportation Officials, "AASHTO-LRFD Bridge Design Specifications," Second Edition, Washington, DC (1998).
2. American Association of State Highway and Transportation Officials, "AASHTO Standard Specifications for Highway Bridges," Fifteenth Edition, Washington, DC (1993).
3. ACI Committee 318, "Building Code Requirements for Reinforced Concrete," ACI 318-98/318R-99, American Concrete Institute, Detroit, MI (1999).
4. Precast/Prestressed Concrete Institute, "Precast/Prestressed Concrete Bridge Design Manual," Chicago, IL (1997).
5. ACI Committee 363, "State of the Art Report on High-Strength Concrete," American Concrete Institute, Detroit, MI (1992) p. 3.
6. Myers, J. J. and Carrasquillo, R. L., "Production and Quality Control of High Performance Concrete in Texas Bridge Structures," Research Report 580/589-1, Center for Transportation Research, University of Texas, Austin, TX (1999) 176 pp.
7. Comité Euro-International du Beton-Fédération Internationale de la Précontrainte, "CEB-FIP Model Code 1990 (CEB-FIP MC90)," Buletin D'Information No. 213/214, Lausanne, Switzerland, May 1993.
8. FHWA, "Compilation and Evaluation of Results from High Performance Concrete Bridge Projects," Contract No. DTFH61-00-C-00009, Federal Highway Administration, Washington, DC (2002).
9. Ahlborn, T. M., French, C. E., and Shield, C. K., "High-Performance Concrete Prestressed Bridge Girders: Long Term and Flexural Behavior," Report 2000-32, Minnesota Department of Transportation, St. Paul, MN (2000) p. 91.
10. Huo, X. S., "Time-Dependent Analysis and Application of High Performance Concrete in Bridges," Ph.D. Dissertation, Department of Civil Engineering, University of Nebraska, Lincoln, NE (August 1997) p. 211.
11. Huo, X. S., Al-Omaishi, N., and Tadros, M. K., "Creep, Shrinkage and Modulus of Elasticity of High Performance Concrete," *ACI Materials Journal*, Vol. 98, No. 6, Detroit, MI (2001) pp. 440–449.
12. ACI Committee 209, "Prediction of Creep, Shrinkage, and Temperature Effects in Concrete Structures," Committee Report, American Concrete Institute, Detroit, MI (1992).
13. Hansen, T. C. and Mattock, A. H., "Influence of Size and Shape of Member on the Shrinkage and Creep of Concrete." *ACI Materials Journal*, Vol. 63, No. 2, Detroit, MI (1966) pp. 267–289.
14. Trost, H. "Auswirkungen des Superprositionspringzips auf Kriech-und Relaxations-probleme bei Beton and Apannbeton," Beton und Stahlbetonbau, V. 62, No. 10, 1967, pp. 230–238; No. 11, Germany (1967) pp. 261–269.
15. Bazant, Z. P., "Prediction of Concrete Creep Effects Using Age-Adjusted Effective Modulus Method," *ACI Journal*, Vol. 69, No. 4 (April 1972) Detroit, MI, pp. 212–217.
16. Dilger, W. H., "Creep Analysis of Prestressed Concrete Structures Using Creep Transformed Section Properties," *PCI Journal*, Vol. 27, No. 1, Chicago, IL (January–February 1982) pp. 89–117.
17. Tadros, M. K., Ghali, A. and Dilger, W. H., "Time-Dependent Prestress Loss and Deflection in Prestressed Concrete Members," *PCI Journal*, Vol. 20, No. 3, Chicago, IL (May–June 1975) pp. 86–98.
18. Tadros, M. K., Ghali, A., and Meyer, A. W., "Prestress Loss and Deflection of Precast Concrete Members," *PCI Journal*, Vol. 30, No. 1, Chicago, IL (January–February 1985) pp. 114–141.
19. Tadros, M. K., Ghali, A. and Dilger, W. H., "Time-Dependent Analysis of Composite Frames," *ASCE Journal of Structural Engineering*, New York, NY (April 1977) pp. 871–884.
20. Abdel Karim, A. and Tadros, M. K., "Computer Analysis of Spliced Girder Bridges," *ACI Structural Journal*, Vol. 90, No. 1, Detroit, MI (January–February 1993), pp. 21–31.
21. AASHO, "Standard Specifications for Highway Bridges," Eleventh Edition, Washington, DC (1973).
22. AASHTO, "Standard Specifications for Highway Bridges," Twelfth Edition, Washington, DC (1977).
23. PCI Committee on Prestress Losses, "Recommendations for Estimating Prestress Losses," *PCI Journal*, Vol. 20, No. 4, Chicago, IL (July–August 1975) pp. 43–75.
24. American Association of State Highway and Transportation Officials, "AASHTO-LRFD Bridge Design Specifications." First Edition, Washington, DC (1994).
25. Comité Euro-International du Beton-Fédération Internationale de la Précontrainte, "Practical Design of Structural Concrete," London, UK (1999) p. 25.
26. Ontario Ministry of Transportation, "Ontario Design Highway Code-Bridge," Toronto, Ontario, Canada (1983).
27. ACI-ASCE Joint Committee 423, "Tentative Recommendations for Prestressed Concrete," *Journal of the ACI*, Vol. 54, Detroit, MI (1958) pp. 545–1299.
28. Concrete Technology Associates, "Prestress Losses," Technical Bulletin 73-B7, Concrete Technology Associates, Tacoma, WA (July 1973).
29. Lwin, M. M., Khaleghi, B., and Hsieh, J, C., "Prestressed I-Girder Design Using High Performance Concrete and the New AASHTO LRFD Specifications," PCI/FHWA International Symposium on High Performance Concrete New Orleans, LA (October 1997) pp. 406–418.
30. Al-Omaishi, N., "Prestress Losses in Pretensioned High-Strength Concrete Bridge Girders," Ph.D. Dissertation, Department of Civil Engineering, University of Nebraska, Lincoln, NE (2001).
31. ASTM C192/C192M-00, "Standard Practice for Making and Curing Concrete Test Specimens in the Laboratory," American Society for Testing and Materials, Annual Book, Philadelphia, PA (1992) pp. 113–119.
32. ASTM C469-94, "Standard Test Method for Static Modulus of Elasticity and Poisson's Ratio of Concrete in Compression," American Society for Testing and Materials, Annual Book, Philadelphia, PA (1994) pp. 238–241.
33. ASTM C 512, "Standard Test Method for Creep of Concrete in Compression," Philadelphia, PA, pp. 267–270.
34. Mokhtarzadeh, A., "Mechanical Properties of High Strength Concrete," Ph.D. Dissertation, Department of Civil Engineering, University of Minnesota, Minneapolis, MN (1996).
35. Gross, S. P. and Burns, N. H., "Field Performance of Prestressed High Performance Concrete Bridges in Texas," Research Report

580/589-2, Center for Transportation Research, University of Texas at Austin, Austin, TX (1999).
36. Magura, D. D., Sozen, M. A., and Siess, C. P., "A Study of Stress Relaxation in Prestressing Reinforcement," *PCI Journal*, Vol. 9, No. 2, Chicago, IL (April 1964) pp. 13–57.
37. Greuel, A., Rogers, B. T., Miller, R. A., Shahrooz, B. M., and Baseheart, T. M., "Evaluation of a High Performance Concrete Box Girder Bridge," Research Report, University of Cincinnati, Cincinnati, OH (2000).
38. Pessiki, S., Kaczinski, M., and Wescott, H. H., "Evaluation of Effective Prestress Forces in 28-Year-Old Prestressed Concrete Bridge Beams," *PCI Journal*, Vol. 41, No. 5, Chicago, IL (November–December 1996) pp. 78–89.
39. Mossiossian, V. and Gamble, W. L., "Time-dependent Behavior of Non-composite and Composite Prestressed Concrete," Federal Highway Administration, Illinois State Division of Highways, Urbana, IL (1972).
40. Kebraei, M., Luedke, J. and Azizinamini, A. A., "High Performance Concrete in 120th and Giles Bridge, Sarpy County, Nebraska," University of Nebraska, Lincoln, NE (1997).
41. Shenoy, C. V. and Frantz, G. C. "Structural Test of 27-Year-Old Prestressed Concrete Bridge Beams," *PCI Journal*, September–October, Chicago, IL (1991) pp 80–90.
42. Stanton, J. F., Barr, P. and Eberhard, M. O., "Behavior of High-Strength HPC Bridge Girders," Research Report, University of Washington, Seattle, WA (2000).
43. Seguirant, Stephen J., "New Deep WSDOT Standard Sections Extend Spans of Prestressed Concrete Girders," *PCI Journal*, Vol. 43, No. 4, Chicago, IL (July–August 1998) pp. 92–119.

APPENDIXES A THROUGH M

UNPUBLISHED MATERIAL

Appendixes A through M as submitted by the research agency on CD-ROM are not published herein. For a limited time, they are available from the NCHRP on a loan basis. Please send requests to Cooperative Research Programs; 500 Fifth St., NW; Washington, DC 20001. The appendix titles are as follows:

APPENDIX A	Other Methods of Shrinkage Strain Prediction
APPENDIX B	Other Methods of Creep Coefficient Prediction
APPENDIX C	Other Methods of Prestress Losses Prediction
APPENDIX D	Material Testing
APPENDIX E	Modulus of Elasticity Data
APPENDIX F	Shrinkage Data
APPENDIX G	Creep Data
APPENDIX H	Temperature Readings
APPENDIX I	Strain Readings
APPENDIX J	Specific Details of the Previous Measured Prestress Losses Experimental Data
APPENDIX K	Prestress Loss Data
APPENDIX L	Detailed Method Spreadsheet
APPENDIX M	Proposed AASHTO-LRFD Revisions

Abbreviations used without definitions in TRB publications:

AASHO	American Association of State Highway Officials
AASHTO	American Association of State Highway and Transportation Officials
APTA	American Public Transportation Association
ASCE	American Society of Civil Engineers
ASME	American Society of Mechanical Engineers
ASTM	American Society for Testing and Materials
ATA	American Trucking Associations
CTAA	Community Transportation Association of America
CTBSSP	Commercial Truck and Bus Safety Synthesis Program
FAA	Federal Aviation Administration
FHWA	Federal Highway Administration
FMCSA	Federal Motor Carrier Safety Administration
FRA	Federal Railroad Administration
FTA	Federal Transit Administration
IEEE	Institute of Electrical and Electronics Engineers
ITE	Institute of Transportation Engineers
NCHRP	National Cooperative Highway Research Program
NCTRP	National Cooperative Transit Research and Development Program
NHTSA	National Highway Traffic Safety Administration
NTSB	National Transportation Safety Board
SAE	Society of Automotive Engineers
TCRP	Transit Cooperative Research Program
TRB	Transportation Research Board
U.S.DOT	United States Department of Transportation